Science
AAAS

Supplementary Materials for

Bacterial spore germination receptors are nutrient-gated ion channels

Yongqiang Gao *et al*.

Corresponding author: David Z. Rudner, rudner@hms.harvard.edu

Science **380**, 387 (2023)
DOI: 10.1126/science.adg9829

The PDF file includes:

Other Supplementary Material for this manuscript includes the following:

Materials and Methods

General methods

All strains were derived from *Bacillus subtilis 168* (*39*) or *Bacillus cereus ATCC 10876* (*27*). Sporulation was induced by nutrient exhaustion in complete Difco Sporulation Medium (DSM) (Fisher Scientific, cat#BD234000) (*40*) at 37 ˚C for 30h. Sporulation efficiency was determined by comparing the heat-resistant (80 ˚C for 20min) colony forming units (CFUs) of mutants to wild-type. All in-frame deletion mutants were derived from the *Bacillus* knock-out collection (BKE) (*41*), or generated by direct transformation of isothermal assembly products into *B. subtilis* 168. The antibiotic cassettes in the deletion mutants were excised using a temperature-sensitive plasmid that constitutively expresses Cre recombinase (*42*). All non-deletion mutants were generated by direct transformation of linearized plasmids or genomic DNA. Site-directed mutants were generated using a modified QuickChange protocol. All strains, plasmids and primers used in this study can be found in Supplemental Tables S1, S2, and S3. The strains used in each figure are indicated in Table S1. Strain and plasmid constructions are described in Supplemental Methods. All experiments presented in the text figures were from one of three biological replicates. All experiments presented in the supplemental figures were from one of at least two biological replicates.

Spore purification

To generate spores for germination assays and immunoblot analyses, cells were grown in liquid DSM at 37 ˚C to an OD_{600} of 0.2-0.3, and then spread on DSM agar plates and incubated for 96h at 37 ˚C. Spores from each agar plate were scraped, washed 3 times with ddH_2O and then resuspended in 350 µL 20% histodenz (Sigma-Aldrich, cat#D2158). The suspension was layered on top of 1 mL 50% histodenz in a microfuge tube and the step-gradient was centrifuged at 16,000 x*g* for 30min at room temperature. The pellet containing mature, phase-bright spores was collected and washed 4 times with ddH_2O. The purified spores were used on the same day in germination assays. If spores were only used for immunoblot analyses or to determine total DPA content, they were scraped from DSM agar plates and resuspended in PBS with 1.5 mg/mL lysozyme, and incubated at 37 ˚C for 1h. SDS was then added to a final concentration of 2% (w/v), incubated for 30 min followed by 5 washes with ddH_2O.

DPA quantification

Purified spores were normalized to an OD_{600} of 1 in 1 mL ddH_2O, and the spore suspension was incubated at 100 ˚C for 30m to release DPA. After 16,000 x*g* centrifugation for 5 min, 300 µL of the supernatant was collected and mixed with 300 µL 100 µM $TbCl_3$. 150µL of the mixture was transferred to a black, flat-bottom, 96-well plate and the fluorescence signal was measured at 545 nm with excitation at 272 nm using an Infinite M Plex plate reader (Tecan). Each sample was analyzed in technical triplicate and compared to a standard curve generated using purified DPA (Sigma-Aldrich, cat#P63808).

DPA release assay

Histodenz-purified phase-bright spores were normalized to OD_{600} of 1 in 25 mM HEPES pH 7.4, and heat-activated at 70 ˚C for 30min, followed by incubation on ice for 15m. 75 µL of the spore suspension was transferred to a black, flat-bottom, 96-well plate and an equal volume of 25 mM HEPES pH 7.4 (buffer), 2 or 20 mM L-alanine, 20 mM AGFK (20 mM of L-asparagine, D-glucose, fructose, and KCl), 20 mM GLPK (20 mM of D-glucose, L-leucine, L-proline and KBr) resuspended

in 25 mM HEPES pH 7.4 was added to the spores. All nutrients and buffer contained 100 μM $TbCl_3$ resulting in a final concentration of 50 μM. The fluorescence was monitored at 545 nm with excitation at 272 nm every 2min for 2h in an Infinite M Plex plate reader (Tecan). The 96-well plate was maintained at 30 ˚C and agitated between measurements. All spore samples and conditions were tested in technical triplicate and compared to a standard curve.

Reduction in optical density (OD_{600}) assay

Histodenz-purified phase-bright spores were normalized to OD_{600} of 1.2 in 25 mM HEPES pH 7.4, and heat-activated at 70 ˚C for 30min, followed by incubation on ice for 15min. 100 μL of spore suspension was then transferred to a clear, flat-bottom, 96-well plate. An equal volume of nutrients or buffer as described above was added to the spore suspension for a final OD_{600} of 0.6. The OD_{600} was monitored every 2min for 4h using an Infinite M Plex plate reader (Tecan). The plate was maintained at 37 ˚C with agitation between measurements. All samples were analyzed in technical triplicate.

Cation release assay using Inductively Coupled Plasma Mass Spectrometry (ICP-MS)

Histodenz-purified phase-bright spores were normalized to OD_{600} of 5 in 20 mL ddH_2O, heat-activated at 70 ˚C for 30min followed by incubation on ice for 15min. 1 mL of the spore suspension was mixed with 1 mL ddH_2O and boiled for 30m to release all DPA and ions from the spore core. The supernatant was collected and stored on ice. The remaining 19 mL spore suspension was pre-warmed at 37 ˚C for 20min, followed by the addition of an equal volume of 20 mM L-alanine. The mixture was vortexed and incubated at 37 ˚C. At the indicated time points, 2 mL of the spore suspension were collected and the germination exudate (the supernatant) was collected by centrifugation (at 16,000 x*g* for 30s). 1.8 mL of the supernatant was transferred to a fresh microfuge tube avoiding the spore pellet and was stored on ice until all samples were collected. In all cases, the spore suspension was collected 20s prior to the indicated time point.

Upon completion of the time course, the germination exudates were separately passed through 0.2 μm syringe filters to remove all particulates. 150 μL of the filtrate was used for DPA quantification by mixing with equal volume of 100 μM $TbCl_3$ and analyzed as described above. The remaining 1.6 mL of filtered germination exudate was mixed with 400 μL 10% nitric acid. The concentrations of K^+, Mg^{2+} and Ca^{2+} in these samples were quantified using an Agilent 7900 Inductively Coupled Plasma Mass Spectrometer in the Center for Environmental Health Sciences Bioanalytical Core Facility at MIT. The instrument was operated in helium mode. All samples were analyzed in biological triplicate. A standard curve for each cation was generated prior to analyzing the germination exudates for each ICP-MS experiment using ultrapure stocks of KCl, $MgCl_2$, $CaCl_2$ (Avantor, cat#BDH82026-000, cat#BDH82026-008, cat#BDH82025-960). The concentration of ions present prior to L-alanine addition was subtracted from the concentrations at all time points after addition. The data were plotted as a percent ion released based on the concentration released at 60min after L-alanine addition.

***gerAA* library construction**

The *gerAA* gene in pLA29 was PCR-amplified using oJA178 and oJA179 and an error-prone Pfu polymerase containing the D473G mutation. The mutagenized PCR product was then restriction digested and ligated into the SpeI-BamHI fragment of pJA060. The plasmid library was transformed into *E. coli* and ~20,000 colonies were scraped, pooled, and stored at -76 ˚C. To

validate the library, individual clones were isolated and the *gerAA* gene was subjected to Sanger sequencing using oJA178. ~15 kb was sequenced and 10 mutations were found for an average of approximately one mutation per 1.4 kb (*gerAA* size = 1449 bp). The plasmid library was isolated with a miniprep kit (Zymo Research, cat#D4212), linearized by digestion with ScaI and then transformed into BJA186a. ~23,000 transformants were scraped, pooled, and stored at -76 ˚C in 15% glycerol.

Screen for constitutively active GerAA mutants

Aliquots of BJA186a containing the native *gerA* locus and the mutagenized library of *gerAA* expressed at a neutral ectopic locus were thawed and plated on LB for single colonies. Individual colonies were picked and patched to confirm the presence of the correct antibiotic markers, and then used to inoculate individual wells in deep 96-well plates with 0.5 mL DSM. 96-well plates were covered with a breathable membrane and incubated at 37 ˚C with agitation for 24-30h. DSM cultures were then diluted 1:5 in water and the OD_{600} of individual wells was compared to the OD_{600} of BJA186a and BJA177a harboring *gerAA*(P326S) sporulated in triplicate. The reference patches of sporulated cultures with low optical densities were then used to inoculate 3 mL DSM. These cultures were re-screened for OD_{600} relative to BJA186a (parental control), BJA277 (*yhdG::gerAA* control), and BJA230 (*yhdG::gerAA*[P326S] control) and additionally tested for low spore viability based on resistance to heat treatment (CFUs after 80 ˚C for 20min) and for the presence of phase-dark spores under phase-contrast illumination. Strains with low OD_{600}, low spore viability, and phase-dark spores were streaked for singles and genomic DNA was isolated. Genomic DNA was used to backcross mutants into wild-type (BDR2413) that were retested to confirm linkage. Genomic DNA was also used for PCR of the *yhdG* locus containing the mutagenized *gerAA* gene using oJA176 and oJA177. Amplicons were then analyzed by Sanger sequencing using oJA117 and oJA148.

Structural modeling with AlphaFold-multimer

Protein structures were modeled using AlphaFold-multimer-v2 and ColabFold (*17-19*) run locally on the Harvard Medical School O2 computing cluster (https://github.com/YoshitakaMo/localcolabfold for more details. General parameters for all runs were as follows: The multiple sequence alignment (MSA) was built using mmseqs2. Sequences from the same operon were paired in the MSA, and both paired and unpaired sequences were used to generate models. Five models were generated. Models were relaxed using AMBER and ranked by pTM score; homologous templates found in the PDB were used. Specific parameters for individual runs were as follows: GerAA pentamer – maximum number of model recycling was set to 12. The model (pTM = 0.892, pLDDT = 85.3) is used throughout the text. GerAA-GerAB-GerAC trimer – maximum number of model recycling was set to 3. The top ranked model (pTM = 0.853, pLDDT = 87.9) is used throughout the text. GerAA-GerAB-GerAC dimer of trimers – maximum number of recycling was set to 12. The top ranked model (pTM = 0.771, pLDDT = 81) is used throughout the text. GerAC pentamer – maximum number of model recycling was set to 12. The top ranked model (pTM = 0.78, pLDDT = 88.5) is used throughout the text. The maximum number of recycling for modeling the GerQA pentamer was set to 12 and the top ranked model (pTM = 0.89, pLDDT = 84.1) is presented. Structural alignments were performed in PyMOL. Pore visualization was created with MOLEonline (*43*). Predicted alignment error plots were created using AlphaPickle (https://github.com/mattarnoldbio/alphapickle/tree/v1.4.0).

Evolutionary co-variation analysis

EVcouplings software (https://github.com/debbiemarkslab/EVcouplings) (*20, 44, 45*) version 0.0.5 was used on multiple sequence alignments generated for GerAA, GerAB, and GerAC. Alignments were generated using the jackhmmer software (*46*) with 5 iterations against the uniref100 dataset downloaded January 2020[61] across a range of normalized bitscores. The GerAB alignment consisted of 20,525 sequences with 95.6% coverage, at least 70% non-gap characters with fragments filtered at a threshold of 70%. The GerAA, alignment consisted of 23,876 sequences with 95.9% coverage. The GerAC alignment consisted of 21,695 sequences and 96.2% coverage. Evolutionary couplings were then calculated for these alignments using pseudolikelihood maximization to infer parameters used to calculate evolutionary couplings scores. Pairs of alignments were then concatenated using the EVcouplings complex pipeline (*20*). The resulting concatenated alignment, with the column coverage threshold changed to 50% and the theta parameter set to 0.9, contained 2,011 sequences and had 96.7% of residue positions across all three protein sequences meet our coverage threshold. This software was then used to infer parameters used to calculate evolutionary couplings scores for all possible pairs of residues, both for intra-monomer and inter-monomer possible contacts. Long-range (separated by at least 5 amino acids in sequence) residue pairs with Evolutionary Coupling scores >90% were then displayed in the contact maps shown in Figure 2D and S8.

Microscopy

30h sporulation cultures, purified phase-bright spores, and exponentially growing cells were concentrated by centrifuge at 8 Krpm, and then immobilized on 1.5% agarose pads. Phase-contrast and fluorescence microcopy were performed using a Nikon TE2000 inverted microscope equipped with Plan Apo 100x/1.4 Oil Ph3 DM objective lens and CoolSNAP HQ2 monochrome CCD camera (Photometrics). For the sporulation cultures or purified spores, the exposure times for phase-contrast and GerAA-GFP fluorescence were 250 and 800 ms, respectively. For the exponentially growing cells, the exposure times for GerAA-GFP and GerAA-mYpet were 500 ms. Image analysis and processing were performed using Fiji or MetaMorph software (Molecular Devices; version 7.7).

Analysis of membrane potential and membrane permeability

To monitor the membrane potential and membrane permeability of exponentially growing cells after induction of GerAA or GerAA(V362A), the indicated strains were grown in 30 mL LB medium at 37 ˚C to an OD_{600} of 0.2-0.3 and IPTG was added to a final concentration of 50 μM. 1 mL culture was collected at the indicated time points and 200 μL were stained with the potentiometric fluorescent dye 3,3′-Dipropylthiadicarbocyanine iodide [$DiSC_3(5)$] (Invitrogen, cat#D306) by the addition of 2 μL of a 100 μM stock (1 μM final), and 600 μL of culture were stained with propidium iodide (PI) (Sigma-Aldrich, cat#P4864) (0.5 μM final). After concentration by centrifugation at 8 Krpm, the cells were immobilized on 1.5% agarose pads and analyzed by fluorescence microscopy using the RFP/mCherry filter set on a Nikon TE2000 inverted microscope equipped with Plan Apo 100x/1.4 Oil Ph3 DM objective lens and CoolSNAP HQ2 monochrome CCD camera (Photometrics). Exposure times for phase-contrast, $DiSC_3(5)$, PI, GFP and BFP, were 250, 200, 200, 400, and 400 ms, respectively. $DiSC_3(5)$ fluorescence was always imaged prior to imaging GFP and BFP. Image analysis and processing were performed using Fiji or GraphPad Prism [(version 9.4.1(458)]. Strains expressing GerAA or GerAA(V362A) lacking GerAB and GerAC were back-diluted to an OD_{600} of 0.05 when they reached an OD_{600} of 1.0 to maintain exponential growth throughout the time course.

Membrane potential and membrane permeability in exponentially growing cells after L-alanine addition was monitored as follows: the indicated strains were grown in 30 mL LB medium at 37 ˚C

in the presence of 50 μM IPTG for 1.5 hours until the OD_{600} reached 0.2. L-alanine was then added to a final concentration of 50 mM. 1 mL of culture was collected before and at the indicated timepoints after L-alanine addition and stained with $DiSC_3(5)$ (1 μM final) or propidium iodide (PI) (0.5 μM final) and analyzed by fluorescence microscopy as described above.

For the experiments in Supplemental Figures S18 and S19, cells expressing the wild-type *gerA* complex harboring P*veg-gfp*, and those expressing *gerAA*(V362L), *gerAB*, *gerAC* or *gerAA*, *gerAB*(G25A), *gerAC* harboring P*veg-bfp* were grown separately in LB medium at 37 ˚C until an OD_{600} of 0.5. The cultures were then diluted to OD_{600} of 0.05 and mixed. At OD_{600} of 0.2, L-alanine was added (50 mM final) and 60min later membrane potential was analyzed using $DiSC_3(5)$. The two cell types were identified by imaging GFP and BFP fluorescence as described above.

Quantification of $DiSC_3(5)$ fluorescence and GerAA-mYpet foci

The fluorescence intensity of both $DiSC_3(5)$-stained cells and the discrete fluorescent foci formed by co-expression of GerAA-mYpet, GerAB and GerAC-Hi6 were quantified using an Image J plugin in MicrobeJ (*47*). Superplots were generated using GraphPad Prism 9 (version 9.3.1). For comparisons of two strains (Figure S19 and S20), P-values were determined using a two-tailed, unpaired t-test for variance analysis. For the comparisons of more than two strains (Figure 3E and S18), P-values were determined by one-way analysis of variance (ANOVA), using Tukey's multiple comparisons tests for selected pairwise comparisons. All P-values were based on the median values of three biological replicates.

For $DiSC_3(5)$ fluorescence quantification, all single cells in the phase contrast channel were detected based on cell area >1.1 μm^2, cell length >1 μm, cell width between 0.5-2 μm, cell angularity < 0.5 rad. The fluorescence signals in the $DiSC_3(5)$ channel were then quantified within each cell and a median value as the fluorescence intensity.

For quantification of GerAA-mYpet foci, all single cells in the phase contrast channel were detected based on the parameters above. All GerAA-mYpet foci in YFP channel, were detected in each single cell, by setting the fluorescent tolerance value in "Maxima" to 200. Both the foci intensity (mean value) and the average fluorescence intensity (mean value) per cell, were quantified. In a subset of cells, the expression level of GerAA-mYpet was too high leading to crowded foci. It was not possible to accurately detect and quantify individual GerAA-mYpet foci in these cells. To enable analysis, cells with average fluorescence intensity greater than 800, were removed, and only foci in cells with an average fluorescence intensity less than 800, were used for further analysis in GraphPad Prism.

Co-expression and co-purification of GerAA-ProC, GerAA-FLAG, GerAB and GerAC-His6

B. subtilis strains (BYG1161, BYG1212, BYG1211) harboring IPTG- and xylose-regulated alleles of *gerAA*, *gerAB* and *gerAC*, were pre-cultured in LB medium at 37 ˚C to an OD_{600} of 0.6, and then diluted into 1 L LB medium supplemented with 1 mM IPTG and 3.3 mM xylose at an OD_{600} of 0.01. The cells were grown at 37 ˚C for ~4h and harvested at an OD_{600} of 0.8-1 by centrifugation at 8 Krpm for 15min. The cell pellets were washed twice with 200 mL 1X SMM (0.5M sucrose, 20mM maleic acid, 20mM $MgCl_2$, adjusted to pH 6.5) and then resuspended in 40 mL 1X SMM with 0.5 mg/mL lysozyme, and gently agitated at room temperature for ~60min until >95% of the cells were converted to protoplasts as monitored by phase-contrast microscopy.

The protoplasts were pelleted by centrifugation, resuspended in 40 mL cold Lysis Buffer (50 mM HEPES pH 7.6, 150 mM NaCl, 20 mM $MgCl_2$, 1 mM DTT) supplemented with 5 units/mL of benzonase (Sigma-Aldrich, cat#E1014) and 1X complete protease inhibitor (Roche, cat#05056489001), and incubate on ice for 60min. The membrane fraction was collected by ultracentrifugation a 35 Krpm at 4 ˚C for 1h, and then dispersed in 45 mL homogenization buffer (20 mM HEPES pH 7.6, 150 mM NaCl and 20% glycerol) supplemented with 1% n-Dodecyl-β-D-maltopyranoside (DDM) (Anatrace, cat#D310S) using a glass homogenizer. The suspension was rotated at 4 ˚C for 1h followed by ultracentrifugation 35 Krpm at 4 ˚C for 1h, The soluble material (Load) was supplemented with $CaCl_2$ (2 mM final) and loaded onto 1-1.5 mL of homemade anti-ProC antibody resin, , generated with mouse monoclonal anti-Protein C antibody, harvested from in-house hybridoma culture with clone ID of HPC-4, purified following patent US5202253A and CNBr-activated Sepharose 4B (Cytiva, cat#GE17-0430-01). The resin was washed with 25 column volumes (CVs) of Wash Buffer (20 mM HEPES pH 7.6, 150 mM NaCl, 20% glycerol, 2 mM $CaCl_2$, 0.1% DDM), and the bound proteins were eluted with 5 CVs of Elution Buffer (20 mM HEPES pH 7.6, 150 mM NaCl, 10% glycerol, 0.1% DDM, 5 mM EDTA pH 8.0, and 0.4 mg/mL ProC peptide (Genscript, Fast peptide synthesis, EDQVDPRLIDGK). 6 µL of Load and Eluate (from 5 mL) were resolved by SDS-PAGE and analyzed by immunoblot as described below.

Lysates and Immunoblot analysis

Spore lysates were generated from spores purified by Histodenz step-gradient or with lysozyme and SDS. Spores were concentrated to an OD_{600} of ~10 in 500 µL cold PBS with 1 mM phenylmethylsulfonyl fluoride (PMSF) (Sigma-Aldrich, cat#52332) and transferred to 2 mL tubes containing lysis matrix B (MP Biomedicals, cat#116911050). The spores were incubated on ice for 15 min, and then lysed using a FastPrep (MP Biomedicals) with 6.5 m/s for 60s. An equal volume of 2X sample buffer (4% SDS, 250 mM Tris pH 6.8, 20% glycerol, 10 mM EDTA, and Bromophenol blue) containing 10% β-mercaptoethanol was immediately added to the lysate. After centrifugation (15 Krpm for 5m), the supernatant was collected and total protein was determined by a noninterfering protein assay (G-Biosciences, cat#786-005). Protein concentrations were normalized and ~20 µg of total protein was resolved by SDS-PAGE on 17.5% polyacrylamide gels and transferred to an Immobilon-P membrane (Millipore, cat#IPVH00010).

Lysates from vegetative cells were generated from *B. subtilis* cultures grown in LB medium at 37 ˚C. Cells were harvested at OD_{600} 0.5-0.8 and 1 mL of culture was normalized to an OD_{600} of 0.5 and centrifuged. The cell pellet was resuspended in 50 µL lysis buffer (20 mM Tris pH 7.5, 10 mM EDTA, 1 mg/mL lysozyme (Sigma-Aldrich, cat#L6876), 1 mM PMSF, 10 µg/mL DNase I (NEB, cat#M0303S), 100 µg/mL RNase A (NEB, cat#T3018L), 10 µg/mL leupeptin (Fisher Scientific, cat#78435), and 10 µg/mL pepstatin (Fisher Scientific, cat#78436), and rotated at 37 ˚C for 10min followed by the addition of 50 µL 2X sample buffer containing 10% β-mercaptoethanol. The lysates were resolved by SDS-PAGE on 17.5% acrylamide gels and transferred to an Immobilon-P membrane (Millipore, cat#IPVH00010).

Membranes were blocked in 5% non-fat milk in 1XPBS with 0.5% Tween-20 (PBST), and probed with anti-GerAA (1:5000) (*48*), anti-His (1:4,000) (GenScript, cat#A00186), anti-GerBC (1:5,000) (*49*), anti-SpoVAD (1:10,000) (*50*), anti-GFP (1:5,000) (*51*), anti-FLAG (1:5,000) (Sigma-Aldrich, cat#F7425), anti-ProC (1:1,000) (home-made mouse monoclonal anti-Protein C antibody,

harvested from in-house hybridoma culture with clone ID of HPC-4, purified following patent US5202253A), anti-SigA (1:10,000) (*52*), anti-ScpB (1:10,000) (*53*), anti-WalI (*54*) (1:5000), anti-SleB (1:5,000) (*55*), or anti-EzrA (1:10,000) (*56*) diluted in 3% BSA in PBST. The primary antibodies were detected with anti-mouse (1:20,000) or anti-rabbit (1:3,000) secondary antibodies coupled to horseradish peroxidase (Bio-Rad, cat#1706516 and cat#1706515), and detected by Western Lightning ECL reagent (PerkinElmer, cat#50-904-9323).

Analysis of cysteine-substituted GerAA in vegetatively growing *B. subtilis*

B. subtilis lysates were derived from exponentially growing cells expressing *gerAA* under the control of IPTG-regulated Phyperspank promoter, and *gerAB* and *gerAC* constitutively expressed under the control of the P*veg* promoter. All strains contained the functional GerAA variant C100S with or without substitutions V359C and/or G361C. Single colonies of the indicated strains were grown in 3 mL LB medium at 37 ˚C to an OD_{600} of 0.5. The cultures were back-diluted into 25 mL LB supplemented with 10 µM IPTG and grown at 37 ˚C. At OD_{600} and 0.5, 10 mL of each culture were centrifuged (10,000 xg, 2min). The pellets were washed once in 1X PBS + 0.1% glycerol (PBSG) pH 7.4. Each pellet was resuspended in 1 ml of PBSG, and 200 µL of each culture was used for further analysis. Cells from 200 µL were pelleted and resuspended in 50 µL lysis buffer (20 mM Tris pH 7.5, 1 mM EDTA, 1 mg/mL lysozyme, 1 mM PMSF, 10 mM $MgCl_2$, 12.5 units of Benzonase (Sigma-Aldrich, cat#E1014) for 10 min at 37 ˚C followed by the addition of 50 µL of 2X sample buffer (0.25 M Tris pH 6.8, 4% SDS, 20% glycerol, 10 mM EDTA) supplemented with 5% β-Mercaptoethanol. Proteins were resolved by SDS-PAGE on 17.5% acrylamide gels followed by immunoblot as described above.

Analysis of cysteine-substituted GerAA in *B. subtilis* spores

Immunoblots were performed with lysates from *B. subtilis* spores lacking all native germinant receptors and complemented with *gerAA*, *gerAB*, and *gerAC*, under the control of P*gerA*. The strains contained the functional GerAA variant C100S with or without V359C and G361C substitutions. Both strains (BLA438 and BLA463) lacked CotE and GerE (*57*) to enable efficient spore lysis using lysozyme. Spores were prepared from DSM agar plates as described above and were resuspended in PBS at an OD_{600} of 10. 400 µl of each spore preparation was pelleted, and resuspended in 50 µL lysis buffer for 10min at 37˚C. 50 µL of 2X sample buffer supplemented with 5% β-Mercaptoethanol was added to each and the lysates were analyzed by immunoblot. For the immunoblots in Figure S25, 800 µl of each spore preparation was pelleted, resuspended in 100 µL lysis buffer for 10min at 37˚C, and then 50 µL of the lysate was mixed with 50 µL 2X sample buffer containing 5% β-Mercaptoethanol and 50 µL was mixed with 50 µL of 2X sample buffer containing 0.5 mM Tributylphosphine (Sigma-Aldrich, cat#90827).

Strain Constructions:

BDR4445 [*gerQA*(I363A) (erm)] was generated by transforming *B. cereus* ATCC 10876 with pFR69 via electroporation and selecting on LB(erm) at 30 ˚C. A single transformant was grown at 30˚C for 8h and then serially dilated and plated on LB(erm) plates and incubated overnight at 42˚C. Integration of the plasmid at the *gerQA* locus and the I363A mutation were confirmed by PCR and Sanger sequencing.

BLA438, BLA463 Δ*cotE::phleo* Δ*gerE::kan* were generated by direct transformation of isothermal assembly products generated from three PCR products. For Δ*cotE::phleo* the pieces were (1) a 1 kb PCR product upstream of *cotE* amplified with oLA412 and oLA414 and *B. subtilis* 168 genomic DNA as template; (2) a 1 kb PCR product downstream of *cotE* amplified with oLA415 and oLA413 and *B. subtilis* 168 genomic DNA as template; (3) *phleo* cassette amplified with oJM028 and oJM029 from pWX468 plasmid (*loxP-phleo*, laboratory stock). For Δ*gerE::kan* the pieces were (1) a 1 kb PCR product upstream of *gerE* amplified with oLA416 and oLA418; (2) a 1 kb PCR product downstreem of *gerE* amplified with oLA419 and oLA417; (3) *kan* cassette amplified with oJM028, oJM029 from pWX470 plasmid (*loxP-kan*, laboratory stock).

BJA498, BJA500, and BJA501 were generated by random PCR mutagenesis of *gerAA* followed by subsequent screening and backcross (see materials and methods for screen details).

Plasmid Constructions:

pYG63[*yhdG::PsspB-spoVA(Bs)(spec) (amp)*] was constructed in a 3-way ligation with 2 PCR products and pCB033 cut with EcoRI and XhoI. One PCR product containing promoter region of *sspB* (primers oYG117 and oYG118 and *B. subtilis* 168 gDNA) was cut with EcoRI and SpeI, and another PCR product containing *spoVA* operon (primers oYG148 and oYG149 and *B. subtilis* 168 gDNA) was cut with SpeI and XhoI. pCB033 is a double crossover integration vector at the *yhdG* locus with a *spec* cassette (laboratory stock).

pYG53[*yhdG::PsspB-spoVA1(Bc) (spec) (amp)*] was constructed in a 3-way ligation with 2 PCR products and pCB033 cut with EcoRI and XhoI. One PCR product containing promoter region of *sspB* (primers oYG117 and oYG118 and *B. subtilis* 168 gDNA) was cut with EcoRI and SpeI, and another PCR product containing *spoVA1* operon of *B. cereus ATCC 14579* (primers oCB59 and oYG119 and *B. cereus ATCC 14579* gDNA) was cut with SpeI and XhoI. pCB033 is a double crossover integration vector at the *yhdG* locus with a *spec* cassette (laboratory stock).

pYG56[*ycgO::PsspB-spoVA2(Bc) (kan) (amp)*] was constructed in a 3-way ligation with 2 PCR products and pCB041 cut with EcoRI and XhoI. One PCR product containing promoter region of *sspB* (primers oYG117 and oYG118 and *B. subtilis* 168 gDNA) was cut with EcoRI and SpeI, and another PCR product containing *spoVA2* operon of *B. cereus ATCC 14579*(primers oYG120 and oYG122 and *B. cereus ATCC 14579* gDNA) was cut with SpeI and XhoI. pCB041 is a double crossover integration vector at the *ycgO* locus with a *kan* cassette (laboratory stock).

pYG95[*ycgO::PsspB-spoVA(Cdif)(kan) (amp)*] was constructed in a 3-way ligation with 2 PCR products and pCB041 cut with EcoRI and XhoI. One PCR product containing promoter region of *sspB* (primers oYG117 and oYG118 and *B. subtilis* 168 gDNA) was cut with EcoRI and SpeI, and another PCR product containing *spoVA* operon of *C. difficile 630* (primers oYG255 and oYG266 and *C. difficile 630* gDNA) was cut with SpeI and XhoI. pCB041 is a double crossover integration vector at the *ycgO* locus with a *kan* cassette (laboratory stock).

pYG129[*yhdG::PsspB-gerUA-gerUC-gerUB-gerVB(spec) (amp)*] was constructed in a 2-way isothermal assembly reaction with a PCR product containing gerUA operon amplified with primers

oYG324 and oYG341 using gDNA of *Bacillus megaterium*, and pYG53 amplified with primers oYG259 and oYG260.

pYG275 [*yhdG::PgerA-gerAA(V362A)(tet) (amp)*] was constructed by site-directed mutagenesis using primers oYG596 and oYG597, and pLA39 as template.

pYG243 [*yhdG::PgerA-gerAA(V362L)(tet) (amp)*] was constructed by site-directed mutagenesis using primers oYG569 and oYG570, and pLA39 as template.

pYG244 [*yhdG::PgerA-gerAA(Q366L)(tet) (amp)*] was constructed by site-directed mutagenesis using primers oYG571 and oYG572, and pLA39 as template.

pYG245 [*yhdG::PgerA-gerAA(Q354L)(tet) (amp)*] was constructed by site-directed mutagenesis using primers oYG573 and oYG574, and pLA39 as template.

pYG248 [*yhdG::PgerA-gerAA(L358A)(tet) (amp)*] was constructed by site-directed mutagenesis using primers oYG579 and oYG580, and pLA39 as template.

pYG262[*yhdG::PgerA-gerAA-gfp(tet) (amp)*] was constructed in a 2-way isothermal assembly reaction with a PCR product containing gfp amplified with primers oYG110 and oYG590 using plasmid pHCL132 (laboratory stock), and pLA39 amplified with primers oYG589 and oYG352.

pYG253[*yhdG::PgerA-gerAA(V362L)-gfp(tet) (amp)*] was constructed by site-directed mutagenesis using primers oYG569 and oYG570, and pYG262 as template.

pYG254[*yhdG::PgerA-gerAA(Q366L)-gfp(tet) (amp)*] was constructed by site-directed mutagenesis using primers oYG571 and oYG572, and pYG262 as template.

pYG255[*yhdG::PgerA-gerAA(Q354L)-gfp(tet) (amp)*] was constructed by site-directed mutagenesis using primers oYG573 and oYG574, and pYG262 as template.

pYG263[*yhdG::Pspank-gerAA(erm) (amp)*] was constructed in a 2-way isothermal assembly reaction with a PCR product containing *gerAA* with primers oYG600 and oYG601 using plasmid pLA39, and pCB057 cut with HindIII and SpeI. pCB057 is a double crossover integration vector at the *yhdG* locus with a *erm* cassette and IPTG-inducible promoter Pspank (laboratory stock).

pYG264[*yhdG::Pspank-gerAA(V362A)(erm) (amp)*] was constructed by site-directed mutagenesis using primers oYG596 and oYG597, and pYG263 as template.

pYG265[*yhdG::Phy-gerAA(erm) (amp)*] was constructed in a 2-way isothermal assembly reaction with a PCR product containing *gerAA* with primers oYG600 and oYG601 using plasmid pLA39, and pCB100 cut with HindIII and SpeI. pCB100 is a double crossover integration vector at the *yhdG* locus with a *erm* cassette and IPTG-inducible promoter Phyperspank (laboratory stock).

pYG266[*yhdG::Phy-gerAA(V362A)(erm) (amp)*] was constructed by site-directed mutagenesis using primers oYG596 and oYG597, and pYG265 as template.

pYG268[*yhdG::Phy-gerAA(V362L)(erm) (amp)*] was constructed by site-directed mutagenesis using primers oYG569 and oYG570, and pYG265 as template.

pYG304[*ycgO::Phy-gerAB(spec) (amp)*] was constructed in a 2-way isothermal assembly reaction with a PCR product containing *gerAB* with primers oYG650 and oYG651 using plasmid pLA13, and plasmid pCB090 cut with HindIII and SpeI. pCB090 is a double crossover integration vector at the *ycgO* locus with a *spec* cassette and IPTG-inducible promoter Phyperspank (laboratory stock).

pYG442[*ycgO::Phy-gerAB(G25A)(spec) (amp)*] was constructed by site-directed mutagenesis using primer oLA197, and pYG304 as template.

pYG305[*yvbJ::Phy-gerAC-His6(Cm) (amp)*] was constructed in a 2-way isothermal assembly reaction with a PCR product containing *gerAC-His6* with primers oYG652 and oYG653 using plasmid pLA131, and plasmid pCB124 cut with HindIII and SpeI. pCB124 is a double crossover integration vector at the *yvbJ* locus with a *cat* cassette and IPTG-inducible promoter Phyperspank (laboratory stock).

pYG276[*yhdG::Phy-gerAA-gfp(erm) (amp)*] was constructed in a 2-way isothermal assembly reaction with a PCR product containing *gerAA-gfp* with primers oYG600 and oYG614 using pYG262, and plasmid pCB100 cut with HindIII and SpeI. pCB100 is a double crossover integration vector at the *yhdG* locus with a *erm* cassette and IPTG-inducible promoter Phyperspank (laboratory stock).

pYG278[*yhdG::Phy-gerAA-proC(erm) (amp)*] was constructed in a 2-way isothermal assembly reaction with a PCR product containing *gerAA-proC* and plasmid pCB100 cut with HindIII and SpeI. The PCR product was first amplified with primers oYG619 and oYG617 using plasmid pCB276, and subsequently the PCR product was used as a template with primers oYG619 and oYG618 to generate *gerAA-proC*. pCB100 is a double crossover integration vector at the *yhdG* locus with a *erm* cassette and IPTG-inducible promoter Phyperspank (laboratory stock).

pYG316[*yhdG::Pxyl-gerAA-proC(phleo) (amp)*] was constructed in a 2-way isothermal assembly reaction with a PCR product containing *gerAA-proC* with primers oYG659 and oYG667 using plasmid pYG278, and plasmid pCB109 cut with HindIII and XhoI. pCB109 is a double crossover integration vector at the *yhdG* locus with a *phleo* cassette and xylose-inducible promoter P*xylA* (laboratory stock).

pYG383[*lacA::Pxyl-gerAA-FLAG(erm) (amp)*] was constructed in a 2-way isothermal assembly reaction with a PCR product containing Pxyl-gerAA-FLAG with primers oYG685 and oYG534 using plasmid pYG316, and plasmid backbone amplified with primers oYG684 and oYG721 using plasmid pDR183. pDR183 is a double crossover integration vector at the *lacA* locus with an *erm* cassette (laboratory stock).

pYG372[*yhdG::Pxyl-gerAA(phleo) (amp)*] was constructed in a 2-way isothermal assembly reaction with a PCR product containing *Pxyl-gerAA* with primers oYG659 and oYG745 using plasmid pYG316, and plasmid pCB109 cut with HindIII and XhoI. pCB109 is a double crossover integration vector at the *yhdG* locus with a *phleo* cassette and xylose-inducible promoter P*xylA* (laboratory stock).

pYG313[*yhdG::Pxyl-gerAA-gfp(phleo) (amp)*] was constructed in a 2-way isothermal assembly reaction with a PCR product containing *Pxyl-gerAA-gfp* with primers oYG658 and oYG659 using plasmid pYG276, and plasmid pCB109 cut with HindIII and XhoI. pCB109 is a double crossover integration vector at the *yhdG* locus with a *phleo* cassette and xylose-inducible promoter P*xylA* (laboratory stock).

pYG440[*yhdG::Pxyl-gerAA(V362L)-gfp(phleo) (amp)*] was constructed by site-directed mutagenesis using primers oYG569 and oYG570, and pYG313 as template.

pYG359[*yhdG::Pxyl-gerAA-mYpet(phleo) (amp)*] was constructed in a 2-way isothermal assembly reaction with a PCR product containing *mYpet* with primers pYG738 and pYG739 using plasmid pWX318(laboratory stock), and plasmid backbone amplified with primers oYG737 and oYG352 using plasmid pYG313.

pYG441[*yhdG::Pxyl-gerAA(V362L)-mYpet(phleo) (amp)*] was constructed by site-directed mutagenesis using primers oYG569 and oYG570 and pYG359 as template.

pYG344[*yhdG::Phy-gerAA(L348A)(erm) (amp)*] was constructed by site-directed mutagenesis using primers oYG699 and oYG700, and pYG265 as template.

pYG345[*yhdG::Phy-gerAA(T355M)(erm) (amp)*] was constructed by site-directed mutagenesis using primers oYG701 and oYG702, and pYG265 as template.

pYG282[*yhdG::Phy-gerAA(L358A)(erm) (amp)*] was constructed by site-directed mutagenesis using primers oYG579 and oYG580, and pYG265 as template.

pYG365[*ycgO::Pveg-gerAB(G25A)(spec) (amp)*] was constructed by site-directed mutagenesis using primer oLA197, and pLA155 as template.

pYG298[*yhdG::Phy-gerAA(V362A)-proC(erm) (amp)*] was constructed by site-directed mutagenesis using primers oYG596 and oYG597, and pLA155 as template.

pYG427[*yhdG::Phy-gerAA-FLAG(erm) (amp)*] was constructed in a 2-way isothermal assembly reaction with a PCR product containing *gerAA-FLAG* with primers oYG619 and oYG821 using plasmid pYG383, and plasmid pCB100 cut with HindIII and SpeI. pCB100 is a double crossover integration vector at the *yhdG* locus with a *erm* cassette and IPTG-inducible promoter Phyperspank (laboratory stock).

pYG428[*yhdG::Phy-gerAA(V362A)-FLAG(erm) (amp)*] was constructed by site-directed mutagenesis using primers oYG596 and oYG597, and pYG427 as template.

pYG366[*yhdG::Phy-gerAA(V362A)-gfp(erm) (amp)*] was constructed by site-directed mutagenesis using primers oYG596 and oYG597, and pYG276 as template.

pYG363[*yvbJ::PgerA-gerAA(V362L)(cat) (amp)*] was constructed in a 2-way ligation with a PCR product containing PgerA-gerAA(V362L) with primers oLA112 and oLA41 using plasmid pYG243, and plasmid pCB006. Both were cut with EcoRI and BamHI. pCB006 (*yvbJ::cat*) is a double crossover integration vector at the *yvbJ* locus with a *cat* cassette (laboratory stock).

pYG409[*yhdG::PgerA-(weakRBS)-gerAA(tet) (amp)*] was constructed by site-directed mutagenesis using primers oYG788 and oYG789, and pLA39 as template. The native *gerAA* RBS (AGAGGTGAA) was mutated to **T**GAGGTGAA resulting in an ~8-fold reduction in GerAA levels in purified spores.

pYG422[*yvbJ::Pveg-BFP(kan) (amp)*] was constructed in a 2-way isothermal assembly reaction with a PCR product containing Pveg-BFP with primers oYG812 and oYG813 using plasmid pER083(laboratory stock), and plasmid backbone amplified with primers oYG292 and oYG293 using plasmid pCB047. pCB047 (*yvbJ::kan*) is a double crossover integration vector at the *yvbJ* locus with a *kan* cassette (laboratory stock).

pYG423[*yvbJ::Pveg-gfp(kan) (amp)*] was constructed in a 2-way isothermal assembly reaction with a PCR product containing Pveg-gfp with primers oYG812 and oYG814 using plasmid pER117(laboratory stock), and plasmid backbone amplified with primers oYG292 and oYG293 using plasmid pCB047. pCB047 (*yvbJ::kan*) is a double crossover integration vector at the *yvbJ* locus with a *kan* cassette (laboratory stock).

pYG460[*yhdG::Pspank-gerAA-mYpet(erm) (amp)*] was constructed in a 2-way isothermal assembly reaction with a PCR product containing gerAA-mYpet with primers oYG868 and oYG832 using plasmid pYG359, and the plasmid pCB057 cut with HindIII and SpeI.

pYG469[*ycgO::Pxyl-gerAB(spec) (amp)*] was constructed in a 2-way isothermal assembly reaction with a PCR product containing *gerAB* with primers oYG885 and oYG886 using plasmid pYG304, and plasmid pCB096 cut with HindIII and XhoI. pCB096 [*ycgO::Pxyl (spec)*] is a double crossover integration vector at the *ycgO* locus with a *spec* cassette and the xylose-inducible promoter P*xylA* (laboratory stock).

pYG470[*yvbJ::Pxyl-gerAC(cat) (amp)*] was constructed in a 2-way isothermal assembly reaction with a PCR product containing *gerAC* with primers oYG883 and oYG887 using *B. subtilis* 168 gDNA, and plasmid pCB130 cut with HindIII and XhoI. pCB130 [*yvbJ::Pxyl (cat)*] is a double crossover integration vector at the *yvbJ* locus with a *cat* cassette and the xylose-inducible promoter P*xylA* (laboratory stock).

pFR69 [pMiniMAD-P*veg-mCherry-gerQA*(I363A) *(erm) (amp)*] was constructed by isothermal assembly of three pieces: 1) plasmid pFR50 cut with SalI and BamHI, 2) a PCR product containing ~1.36 kb upstream of GerQA(I363), and 3) a PCR product containing ~1.37 kb downstream of GerQA(I363). Both PCR products were amplified using gDNA from *B. cereus* ATCC 10876 as

template and oligonucleotides primers oFR399/oFR400 and oFR401/oFR402, respectively. pFR50 is a pMiniMAD-derived vector for looping-in and out in Gram (+) bacteria that contains *mCherry* under control of the *B. subtilis* 168 *veg* promoter (Ramírez-Guadiana and Rudner, unpublished).

pLA178 [*yhdG::Phy-RBSgerAB-gerAA*(C100S)*(erm) (amp)*] was constructed by site-directed mutagenesis using the primer oLA323 and pYG265 as template.

pLA191 [*yhdG::PgerA-RBSgerAB-gerAA*(C100S, V359C, G361C)*(tet) (amp)*] was constructed by site-directed mutagenesis using the primer oLA384 and pLA137 as template.

pLA201 [*yhdG::Phy-RBSgerAB-gerAA*(C100S, V359C, G361C)*(erm) (amp)*] was constructed in a 2-way isothermal assembly reaction with a PCR product containing *gerAA*(C100S, V359C, G361C) with primers oYG600 and oYG601 using plasmid pLA191, and the plasmid pCB100 restricted with HindIII and SpeI. pCB100 (*yhdG::erm*) is a double crossover integration vector at the *yhdG* locus with an erm cassette (laboratory stock).

pLA202 [*yhdG::Phy-RBSgerAB-gerAA*(C100S, V359C*)(erm) (amp)*] was constructed in a 2-way isothermal assembly reaction with a PCR product containing *gerAA*(C100S, V359C) with primers oYG600 and oYG601 using plasmid pLA192, and the plasmid backbone of pCB100 restricted with HindIII and SpeI. pCB100 is a double crossover integration vector at the *yhdG* locus with an *erm* cassette (laboratory stock). pLA192 [*yhdG::PgerA-RBSgerAB-gerAA*(C100S, V359C) (*tet) (amp)*] was constructed by site-directed mutagenesis using the primer oLA408 and pLA137 as a template.

pLA203 [*yhdG::Phy-RBSgerAB-gerAA*(C100S, G361*)(erm) (amp)*] was constructed in a 2-way isothermal assembly reaction with a PCR product containing *gerAA*(C100S, G361C) with primers oYG600 and oYG601 using plasmid pLA193, and the plasmid backbone of pCB100 restricted HindIII and SpeI. pCB100 is a double crossover integration vector at the *yhdG* locus with an *erm* cassette (laboratory stock). pLA193 [*yhdG::PgerA-RBSgerAB-gerAA*(C100S, G361C)(*tet) (amp)*] was constructed by site-directed mutagenesis using the primer oLA409 and pLA137 as a template.

pJA047 [*yhdG::gerAA(P326S) (tet)(amp)]* was constructed by site-directed mutagenesis of pLA39 [*yhdG::*P_{gerA}*-(RBSgerAB)-gerAA (tet)]* using oJA105 and oJA106

pJA060 [*yhdG::*P_{gerA} *(spec*)(*amp*)] was constructed by ligation of the EcoRI-SpeI fragment of pLA39 [*yhdG::*P_{gerA}*-(RBSgerAB)-gerAA (tet)]* into pCB033. pCB033 [*yhdG::spec*] is a double crossover integration vector at the *yhdG* locus with an erm cassette (laboratory stock).

The sequence of all plasmids was confirmed by Sanger sequencing.

Figure S1. Comparison of sequence identity between SpoVA homologs and germination receptor proteins. (A) Schematics of the *spoVA* locus. *B. subtilis spoVA* contains seven genes but only *spoVAC* (AC), *spoVAD* (AD), and *spoVAEb* (AEb) (shown in blue) are required for DPA import into spores during sporulation and DPA release during germination (*6*). *B. cereus* contains two *spoVA* loci. The *spoVA1* operon is similar to the *B. subtilis spoVA* operon. The *spoVA2* locus encodes AC, AD, and AEb homologs and four unrelated proteins. The *C. difficile* locus only encodes AC, AD, and AEb homologs. The percent identities relative to the *B. subtilis* homologs are indicated below each gene. The lighter the blue the lower the percent identity. The *B. cereus* loci are from the ATCC 14579 strain. The *C. difficile spoVA* locus is from strain 630. **(B)** The *B. megaterium gerUV* locus encodes two B subunits, GerUB and GerVB. The percent identity of each subunit is compared to the five germinant receptor loci in *B. subtilis*. Although the *yfk* and *ynd* operons encode GerA-family proteins, the germinants these factor respond to have not been identified. The percent identities relative to the *B. megaterium* homologs are indicated below each gene. The lighter the red the lower the identity. The *B. megaterium gerUV* locus is from strain QM B1551.

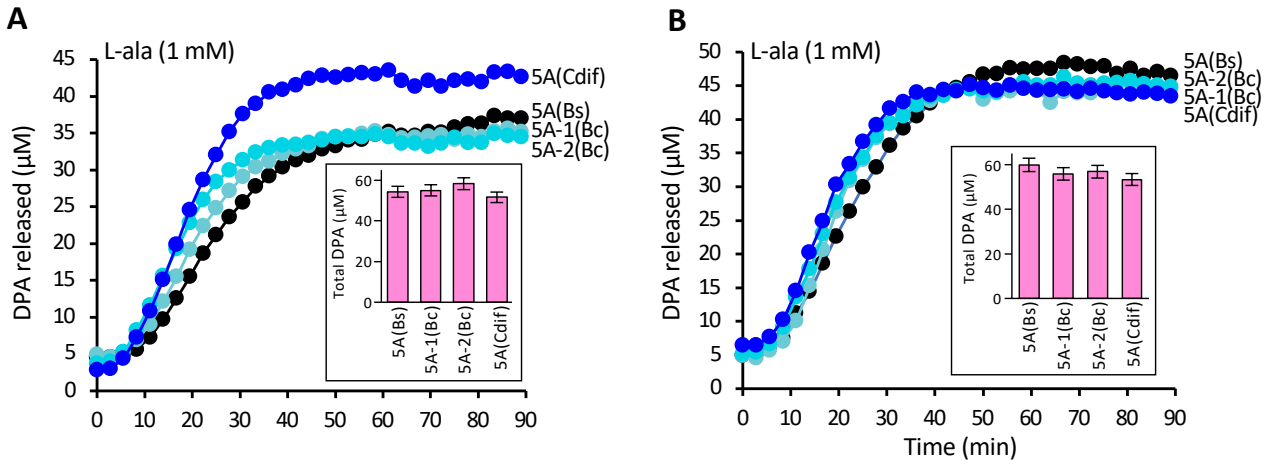

Figure S2. Biological replicates of the cross-species complementation of the SpoVA transporter. (A,B) *spoVA* loci from *B. cereus* and *C. difficile* support DPA release from *B. subtilis* spores in response to L-alanine. Purified spores of Δ*spoVA* mutant strains harboring an ectopic copy of the indicated *spoVA* (5A) locus from *B. subtilis* (Bs), *B. cereus* (Bc), or *C. difficile* (Cdif). Spores were mixed with 1 mM L-alanine and DPA release was monitored over time. The inserts show total DPA content in the purified spores.

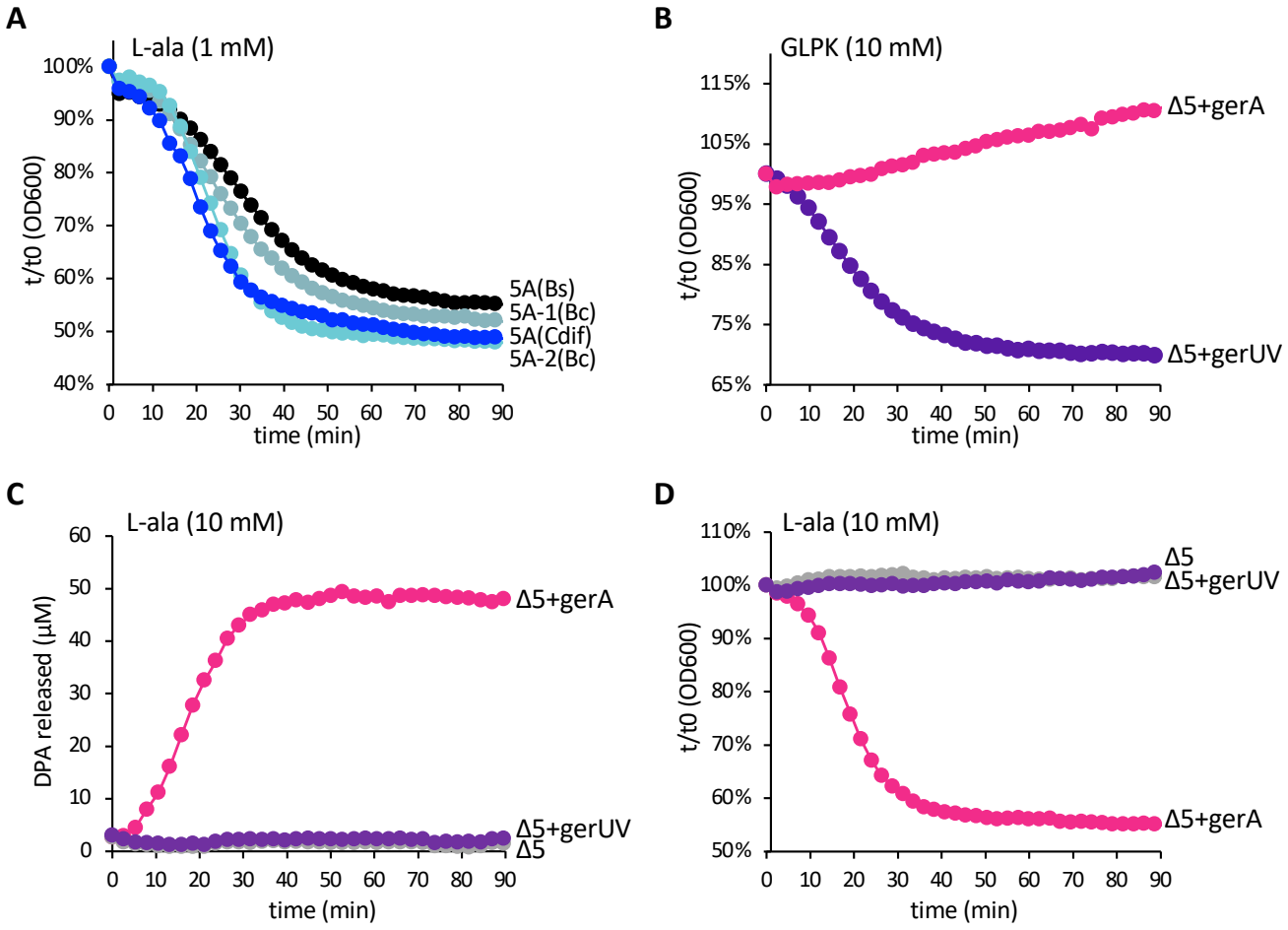

Figure S3. Cross-species complementation of key germination factors. (A) The *spoVA* loci from *B. cereus* and *C. difficile* support *B. subtilis* germination in response to L-alanine. Purified spores of Δ*spoVA* mutant strains harboring an ectopic copy of the indicated *spoVA* (5A) locus from *B. subtilis* (Bs), *B. cereus* (Bc), or *C. difficile* (Cdif) were mixed with 1 mM L-alanine and the optical density was monitored over time. **(B)** *B. subtilis* spores lacking native germinant receptors (Δ5) and harboring the *gerUV* locus from *B. megaterium* support germination in response to a mixture of 10 mM D-glucose, L-leucine, L-proline and K^+ (GLPK) as assayed by a drop in optical density. Spores harboring GerA (red circles) are unable to respond to GLPK. **(C,D)** *B. subtilis* spores lacking native germinant receptors (Δ5) and harboring the *gerUV* locus from *B. megaterium* are unable to germinate in response to L-alanine as assayed by DPA release **(C)** and a drop in optical density **(D)**. Spores harboring the *gerA* locus efficiently release DPA and drop in optical density in response to L-alanine. Representative data from one of three biological replicates are shown in each panel.

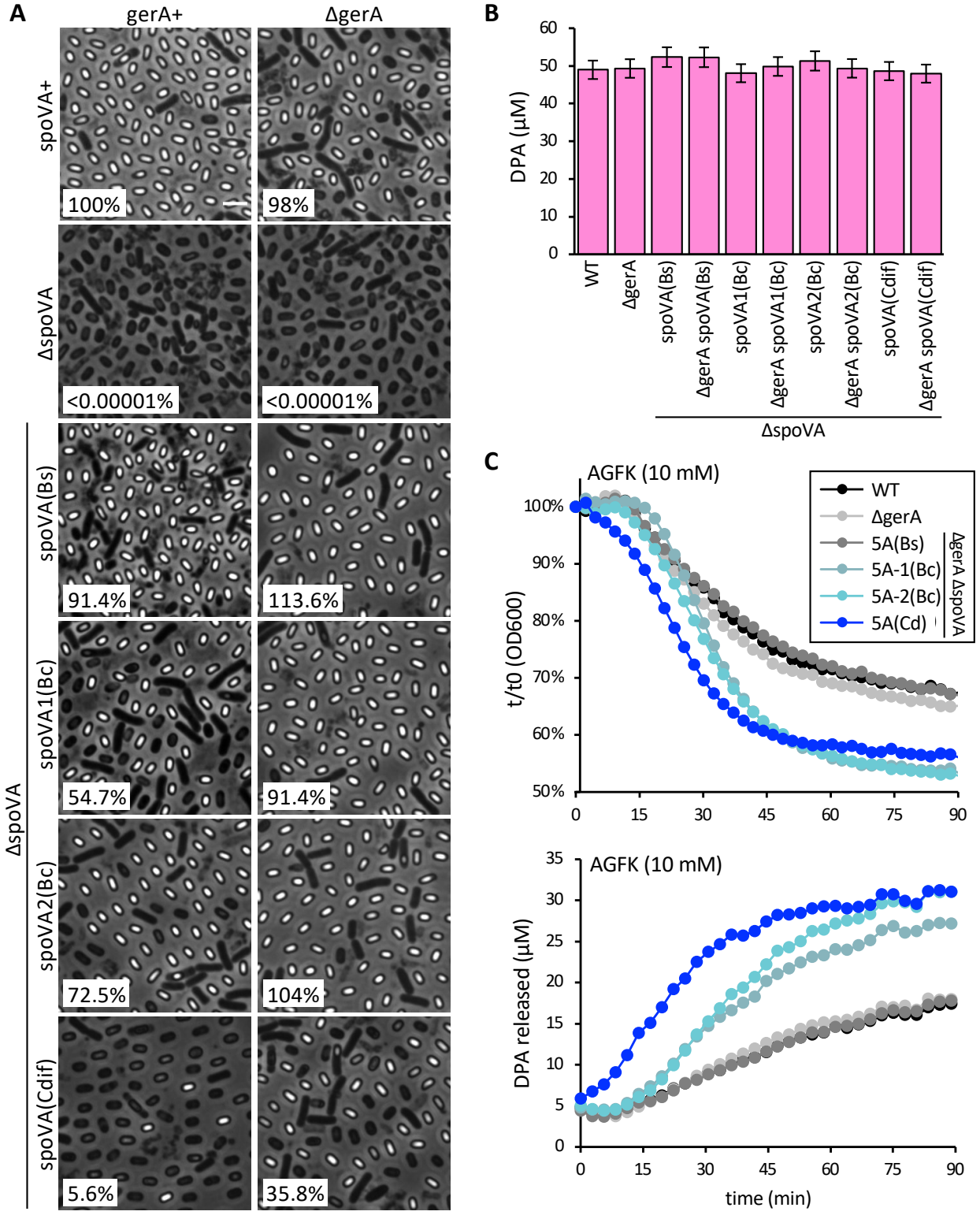

Figure S4. Heat-resistant spore formation is reduced in strains with non-native *spoVA* loci due to GerA-dependent premature germination. (A) Representative phase-contrast images of sporulating cultures of the indicated strains in the presence and absence of *gerA*. Scale bar, 2 μm. Sporulation efficiencies, as assayed by heat-resistance (80 ˚C for 20m) CFU, are shown in the lower left corner of each image. Strains with less homologous SpoVA proteins have fewer mature (phase-bright) spores and reduced sporulation efficiency. The suppression in the Δ*gerA* background indicates that these defects are due, in part, to premature activation of GerA. We have previously shown that GerA-dependent premature germination often results from impaired or slowed DPA accumulation in the spore core (*6*). **(B)** Purified phase-bright spores from all strains from (A) have similar levels of DPA, indicating that spores that successfully complete spore formation accumulate wild-type levels of DPA. **(C)** Analysis of spore germination as assayed by DPA release and drop in optical density using a mixtures of 10 mM L-asparagine, D-glucose, D-fructose, and K^+ (AGFK) that activates the GerB/GerK receptors. The phase-bright spores produced from strains with non-native *spoVA* loci and lacking GerA germinate as well as or better than wild-type *B. subtilis* spores. The more rapid initiation of germination of spores with non-native *spoVA* loci is likely due to the more rapid unplugging of the non-native SpoVA channels (*6*). Representative data from one of at least three biological replicates are shown in each panel.

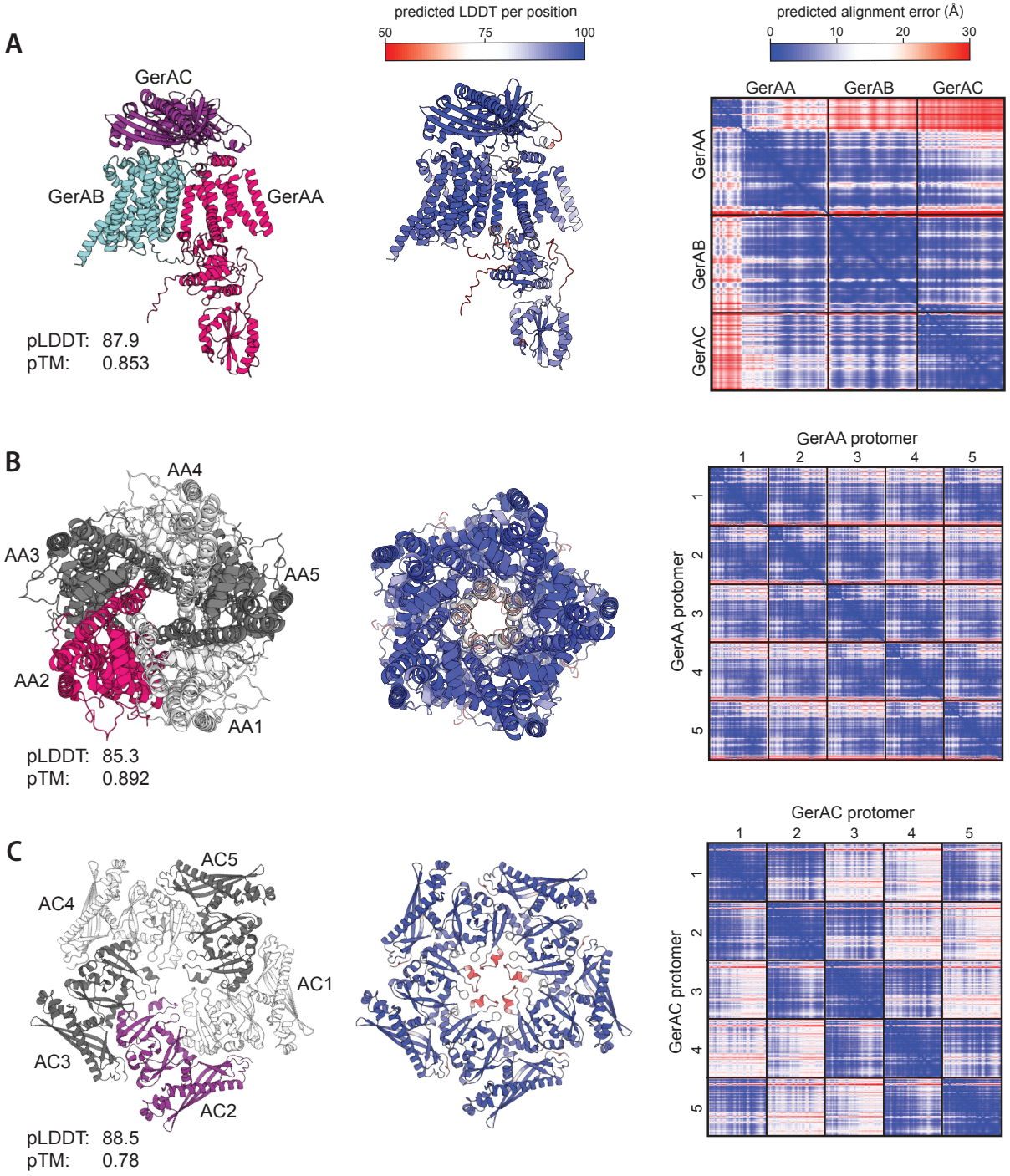

Figure S5. Predicted local distance difference tests and alignment error for the AlphaFold-predicted trimer and pentamers. (A) Structural model of the GerA trimer (left). Predicted local distance difference tests (pLDDT) per position mapped onto the GerA trimer model (middle). Higher pLDDT (blue) corresponds to a more confident prediction. Predicted alignment error in Å of all residues against all residues for the top-ranked model (right). Low error (blue) corresponds to well-defined relative domain positions. **(B,C)** Structural models of the GerAA and GerAC pentamers (left); predicted local distance difference tests (pLDDT) per position mapped onto the pentamer models (middle); predicted alignment error in Å of all residues against all residues for the top-ranked models (right). The per-residue accuracy of the structure (pLDDT) and the estimate of the template modeling score (pTM) for each model is shown below the predicted structures on the left.

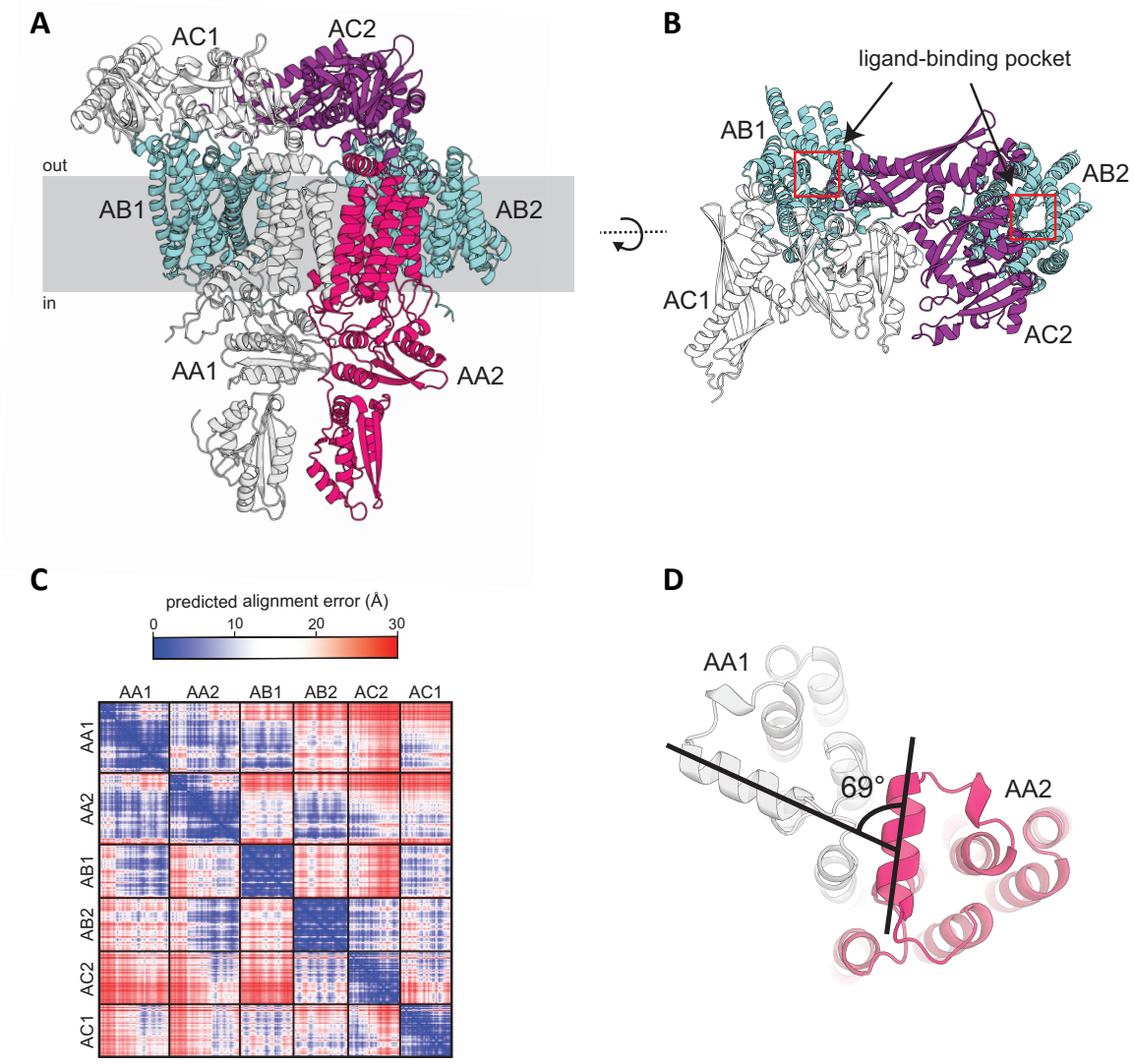

Figure S6. AlphaFold model of a dimer of GerAA-GerAB-GerAC trimers. (A) Structural prediction of a dimer of GerA trimers as viewed from the membrane. GerAA protomers are shown in red and light gray; GerAC protomers are shown in purple and light gray; and both GerAB protomers are displayed in cyan. **(B)** Viewed from above, the L-alanine-binding pockets in each GerAB protomer are visible. **(C)** Predicted alignment error (in Å) of all residues against all residues for the top-ranked dimer of trimers. Low error (blue) corresponds to well-defined relative domain positions. **(D)** Angle between GerAA protomers in the dimer of trimer model. Top-down view of the transmembrane domains of the GerAA protomers. The angle between each protomer (~69˚) is consistent with a pentamer of GerAA-GerAB-GerAC trimers.

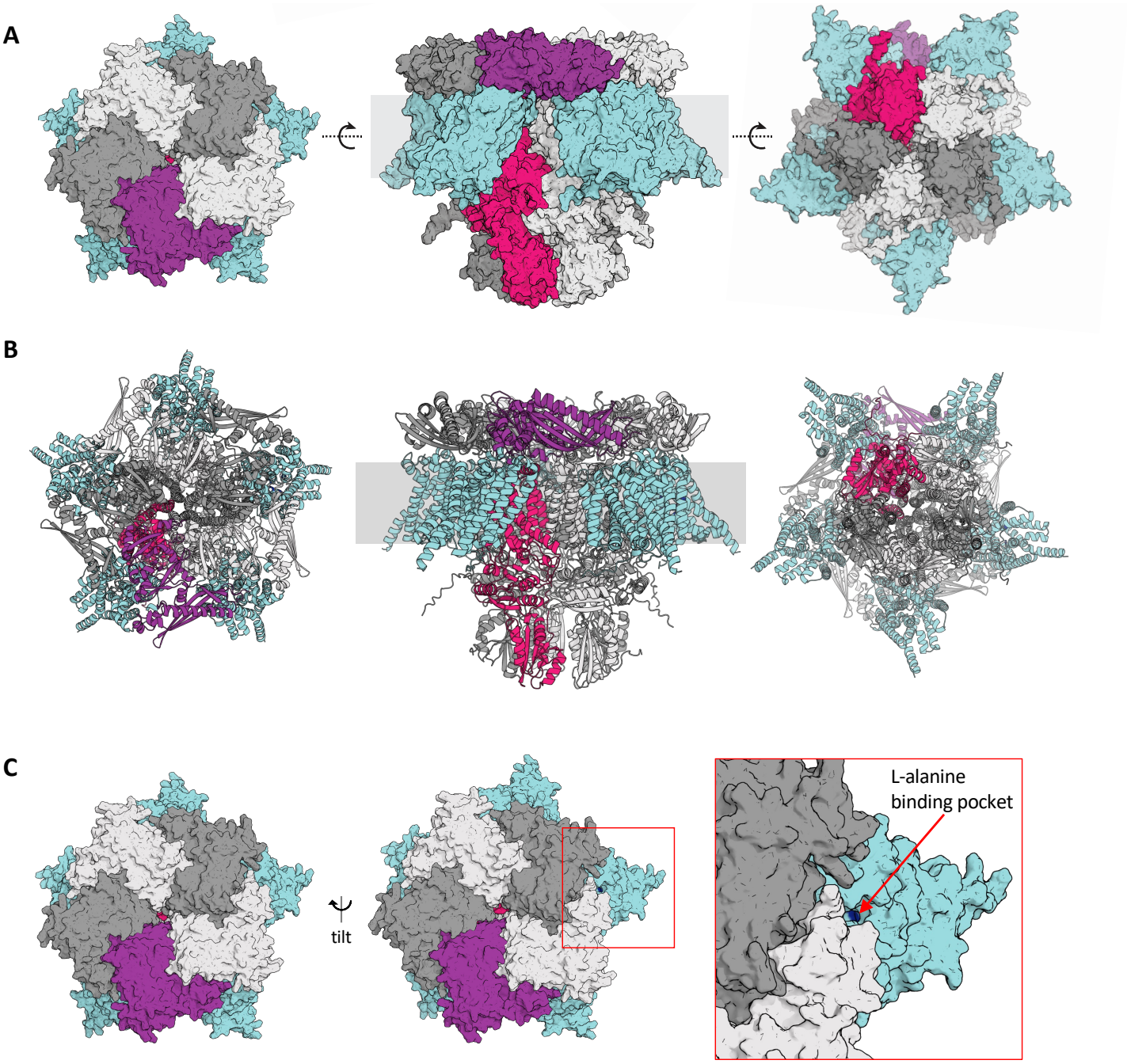

Figure S7. AlphaFold-predicted structure of the GerA complex and accessibility of the L-alanine binding pocket. (A) Space filling models of the predicted pentamer of trimers shown from outside looking in (left), within the membrane (middle), and inside looking out (right). GerAA protomers are shown in red, light and dark gray; GerAC protomers are shown in purple and light and dark gray; GerAB protomers are shown in cyan. **(B)** Ribbon models as in (A). **(C)** Spacing-filling model of the GerA complex from outside the spore looking in. A slight tilt of the complex reveals the L-alanine binding pocket (*10*). Characterized residues that line the pocket are colored dark blue.

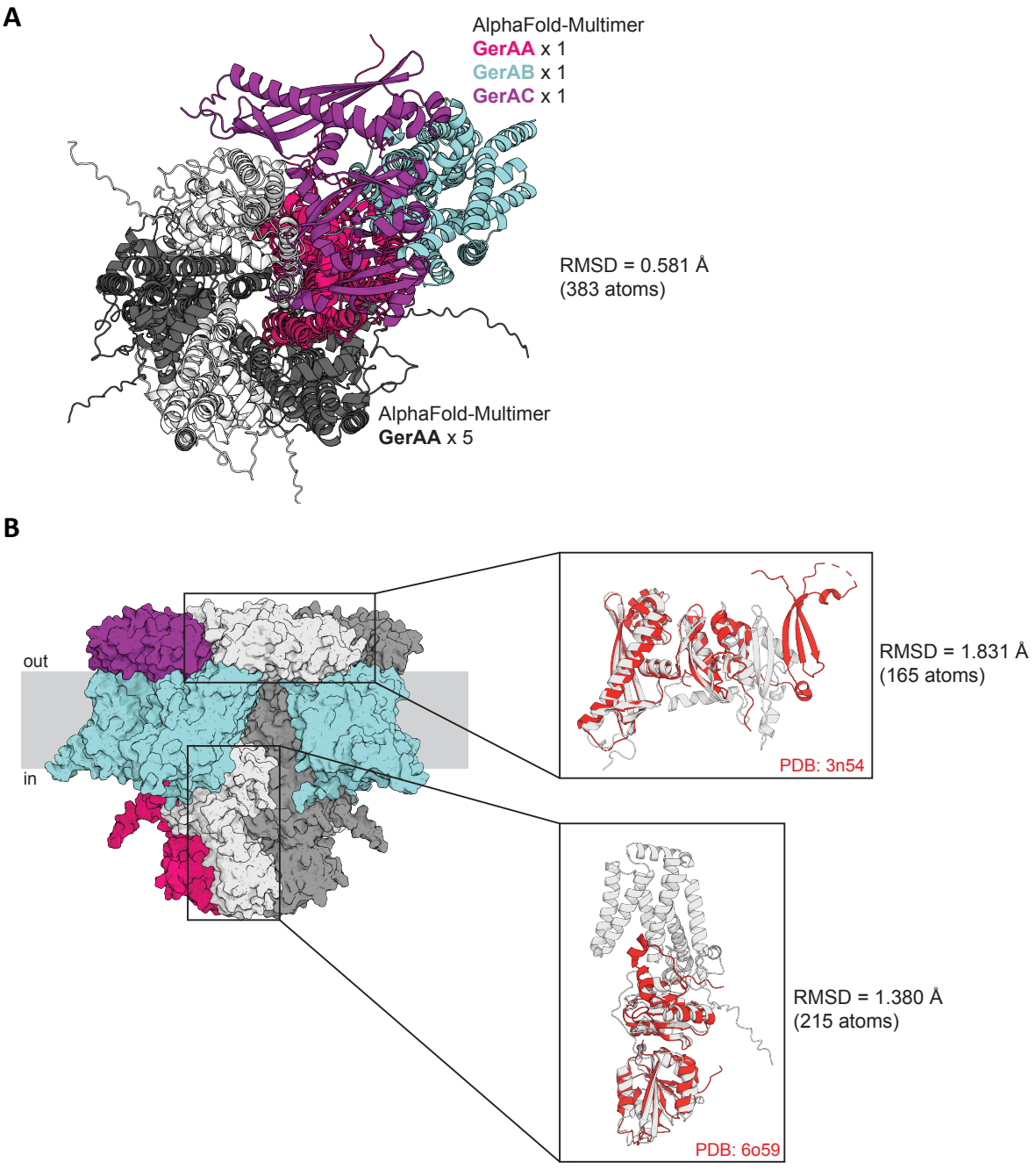

Figure S8. Alignment of GerAA in the GerA trimer model with a GerAA protomer in the independently predicted pentamer. (A) Top-down view of the GerA complex. An AlphaFold model of the GerAA-GerAB-GerAC trimer was aligned to an AlphaFold model of the GerAA pentamer using a shared GerAA protomer. The root-mean-square deviation (RMSD) between the predictions for GerAA in the two models is 0.581 Å over 308 atoms. This process was repeated four more times to arrive at the full 15-mer complex presented throughout the paper. **(B)** Alignment of the GerAC model (light gray) and the experimentally determined crystal structure of GerBC from *B. subtilis* (red) (PDB: 3n54) (*58*) is shown on the top. The RMSD between the model and crystal structure is 1.831 Å over 165 atoms. Alignment of the soluble cytoplasmic domain of GerAA (light gray) and the experimentally determined crystal structure of the cytoplasmic domain of the A subunit of $GerK_3$ from *B. megaterium* (red) (PDB: 6o59) (*59*) is shown below. The RMSD between the model and crystal structure is 1.38 Å over 215 atoms.

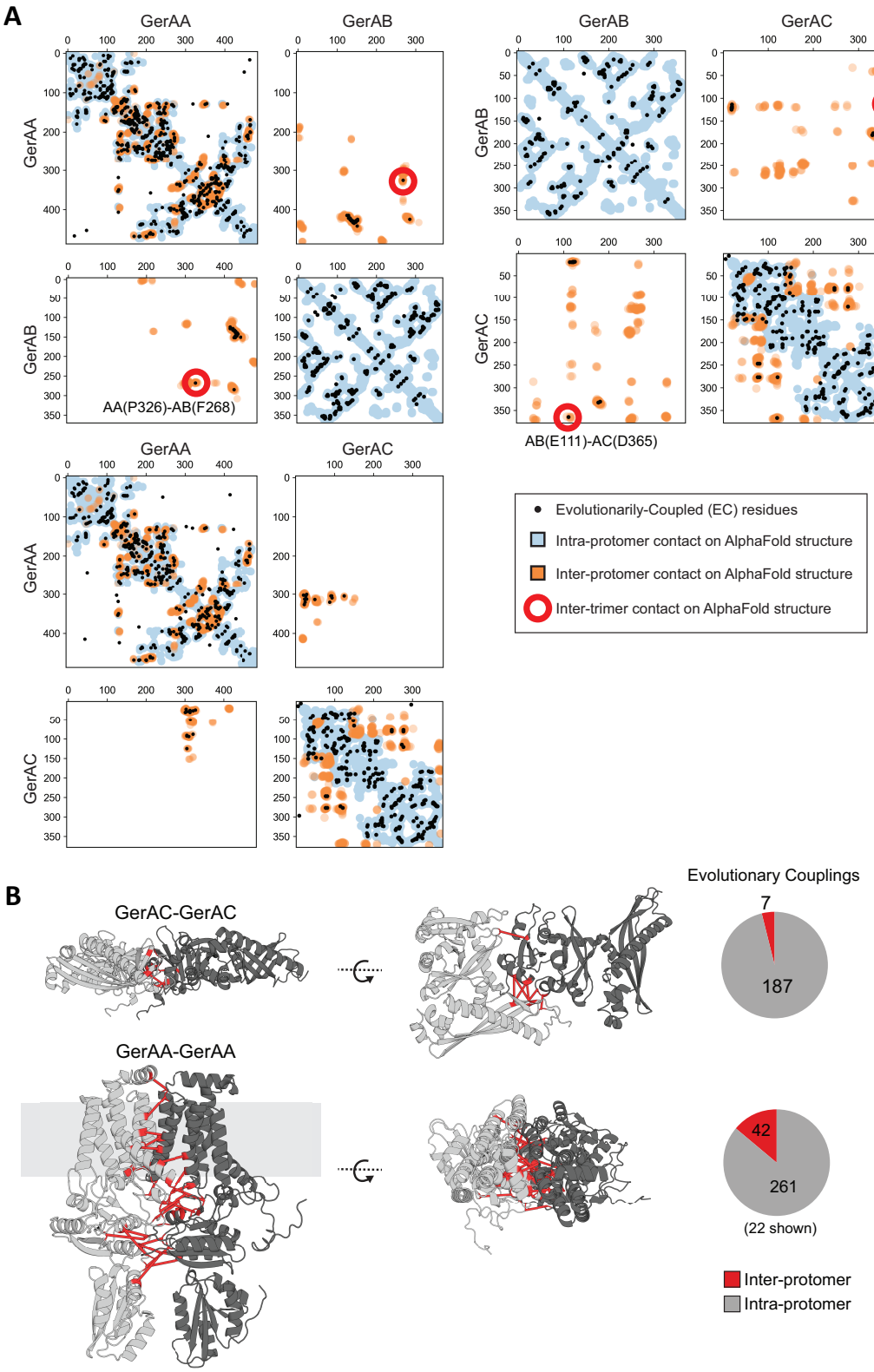

Figure S9. Evolutionary co-variation analyses of GerAA, GerAB and GerAC. (A) Evolutionarily-coupled (EC) residue pairs with probabilities ≥0.99 within GerAA, GerAB, and GerAC and between subunits are plotted as black circles. Residue pairs that are ≤8 Å apart in the AlphaFold-predicted dimer of trimers structure are shown as light blue (intra-protomer) and orange (inter-protomer) circles. Red circles highlight EC residue pairs in GerAA and GerAB subunits and GerAB and GerAC subunits in distinct GerAA-GerAB-GerAC trimers. **(B)** Intra-protomer EC residue pairs mapped onto AlphaFold-predicted structures. All high-confidence EC residue pairs present in adjacent GerAC subunits (top) and 22 of the 42 high-confidence EC residue pairs present in adjacent GerAA subunits (bottom) are shown with red lines connecting them.

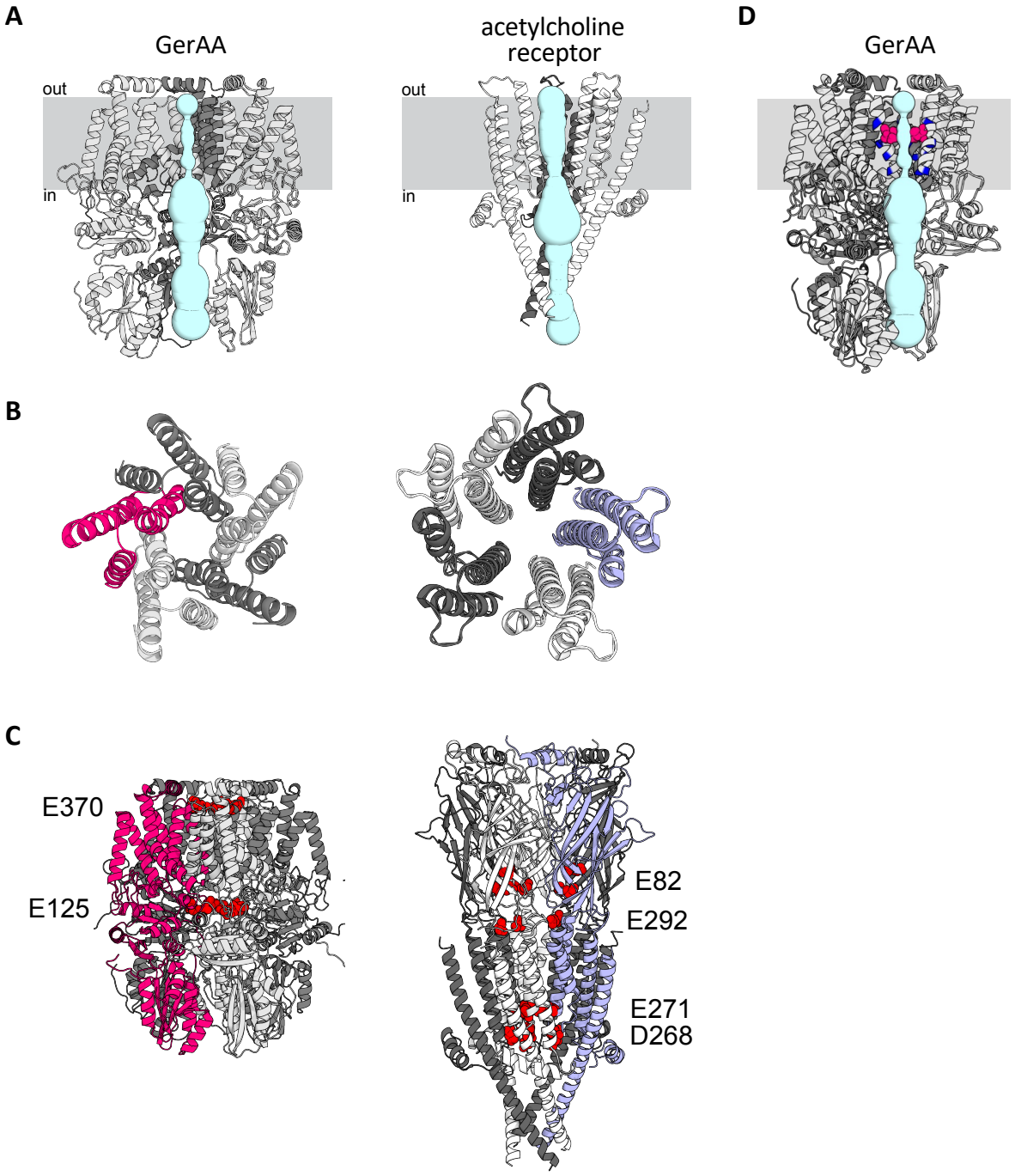

Figure S10. Comparative structural analysis of the GerA complex and the human nicotinic acetylcholine receptor complex. **(A)** Predicted pores (in light blue) of the GerAA pentamer (left, as in Figure 2E) and the human nicotinic acetylcholine receptor (right, PDB: 6pv7) (*60*). Three protomers of each pentamer are shown and the extracellular domains of the acetylcholine receptor have been omitted for clarity. **(B)** Top-down view of both channels showing the concentric helices surrounding the pore. **(C)** Side view of both channels highlighting acidic residues (red) on either side of the membrane-spanning pore region. **(D)** Predicted pore of the GerAA pentamer with V362 (red) and glycine patch (blue) in TM3 highlighted. The model has been rotated relative to (A) for clarity.

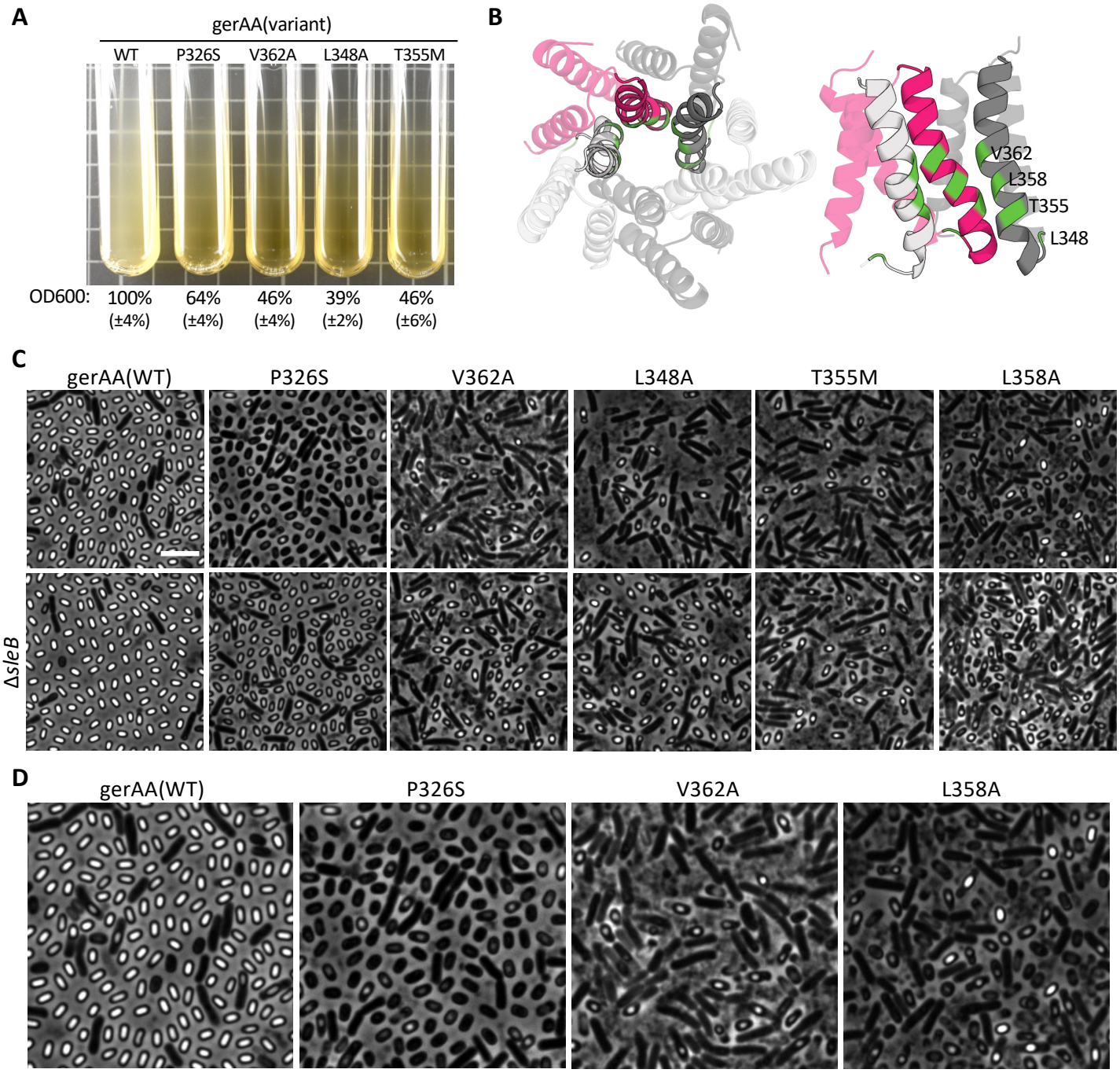

Figure S11. A genetic screen for constitutively active *gerAA* alleles. (A) Photograph of cultures of sporulating cells harboring an ectopic copy of the indicated *gerAA* variant. The optical density (OD_{600}) of the cultures relative to wild-type are shown below the image. Constitutively active mutants cause lysis during sporulation resulting in reduced optical density. The previously characterized *gerAA*(P326S) mutant served as the positive control. The three mutants with the greatest reduction in OD_{600} are shown. **(B)** Top-down and cutaway side view of the GerAA pentameric channel. Residues that were hit in the screen are highlighted in green. L358 was not identified in the screen but was tested afterwards. **(C)** Representative phase-contrast images of sporulating cultures of the indicated strains in the presence and absence *sleB.* The GerAA(P326S) mutant displays the characteristic premature germination phenotype with phase-dark spores. The other four mutants display significant lysis and teardrop-shaped spores. *sleB* encodes a cell wall hydrolase that degrades spore peptidoglycan during germination and during premature germination. In the absence of *sleB* (Δ*sleB*) the newly identified mutants have less lysis and more teardrop-shaped spores. Scale bar, 5 µm. **(D)** Increased magnification of images in (C) highlighting the lysis and morphologically distinct spores. Representative data from one of four biological replicates are shown.

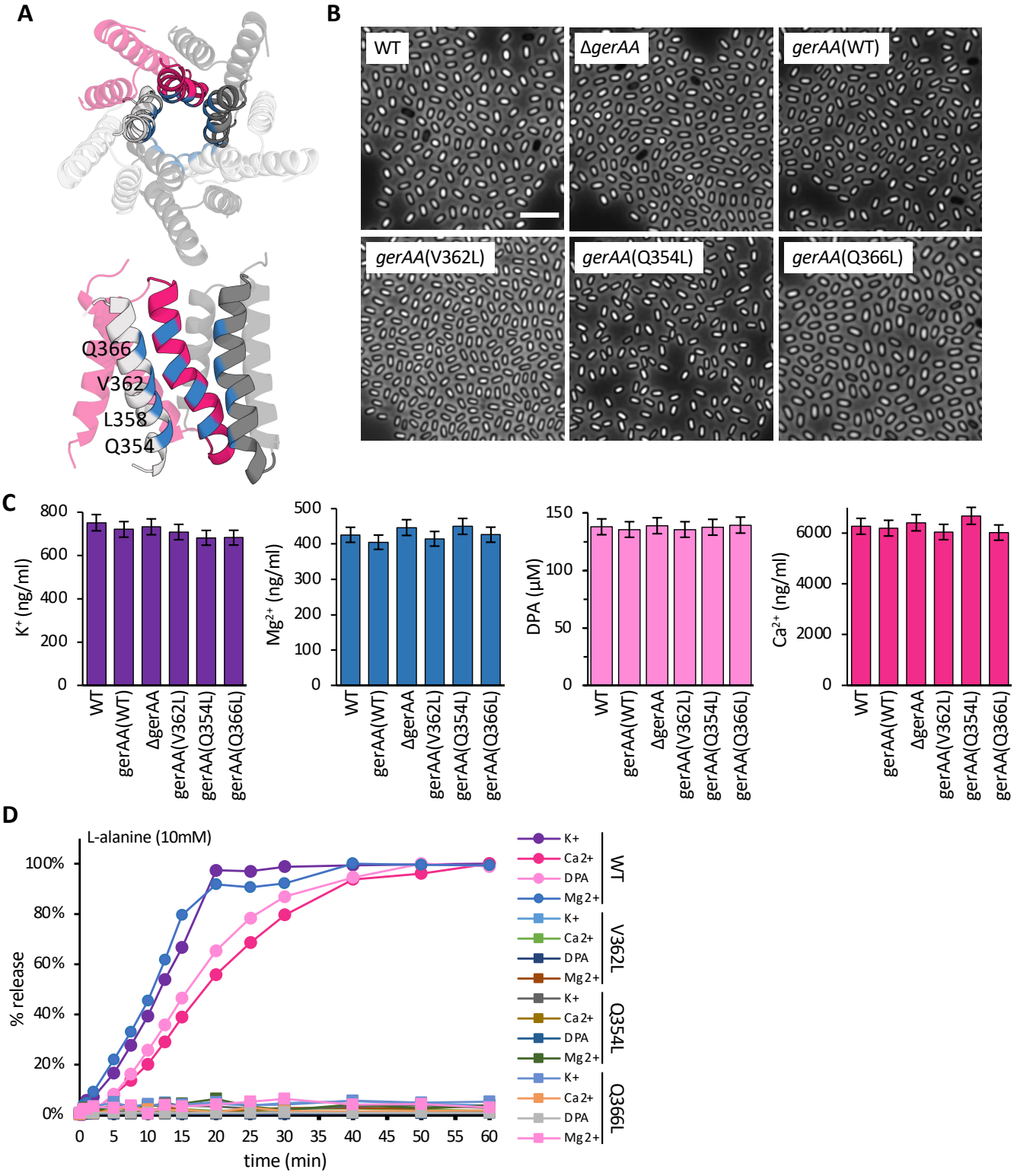

Figure S12. Amino acid substitutions of residues in the GerAA channel predicted to reduce the pore size fail to germinate in response to L-alanine. (A) Top-down and cutaway side view of the predicted GerAA pentameric channel. Residues that line the lumen of the channel are shown in blue. **(B)** Phase-contrast images of purified spores from the indicated strains. The *gerAA* alleles are the sole copy of *gerAA* in these strains. Scale bar, 5 μm. **(C)** Bar graphs showing the total K^+, Mg^{2+}, Ca^{2+}, and DPA content in the spores from (B). 1 mL of spores at an OD_{600} of 5 was analyzed for each strain. **(D)** Purified spores that have GerAA(WT) (circles) or the indicated mutants (squares) as the only copy of the GerAA subunit were mixed with 10 mM L-alanine and the germination exudates were collected at the indicated timepoints and analyzed for K^+, Mg^{2+}, Ca^{2+}, and DPA. The percent release at each time point, relative to the amount released at 60 min, is shown. Representative data from one of three biological replicates are shown in each panel.

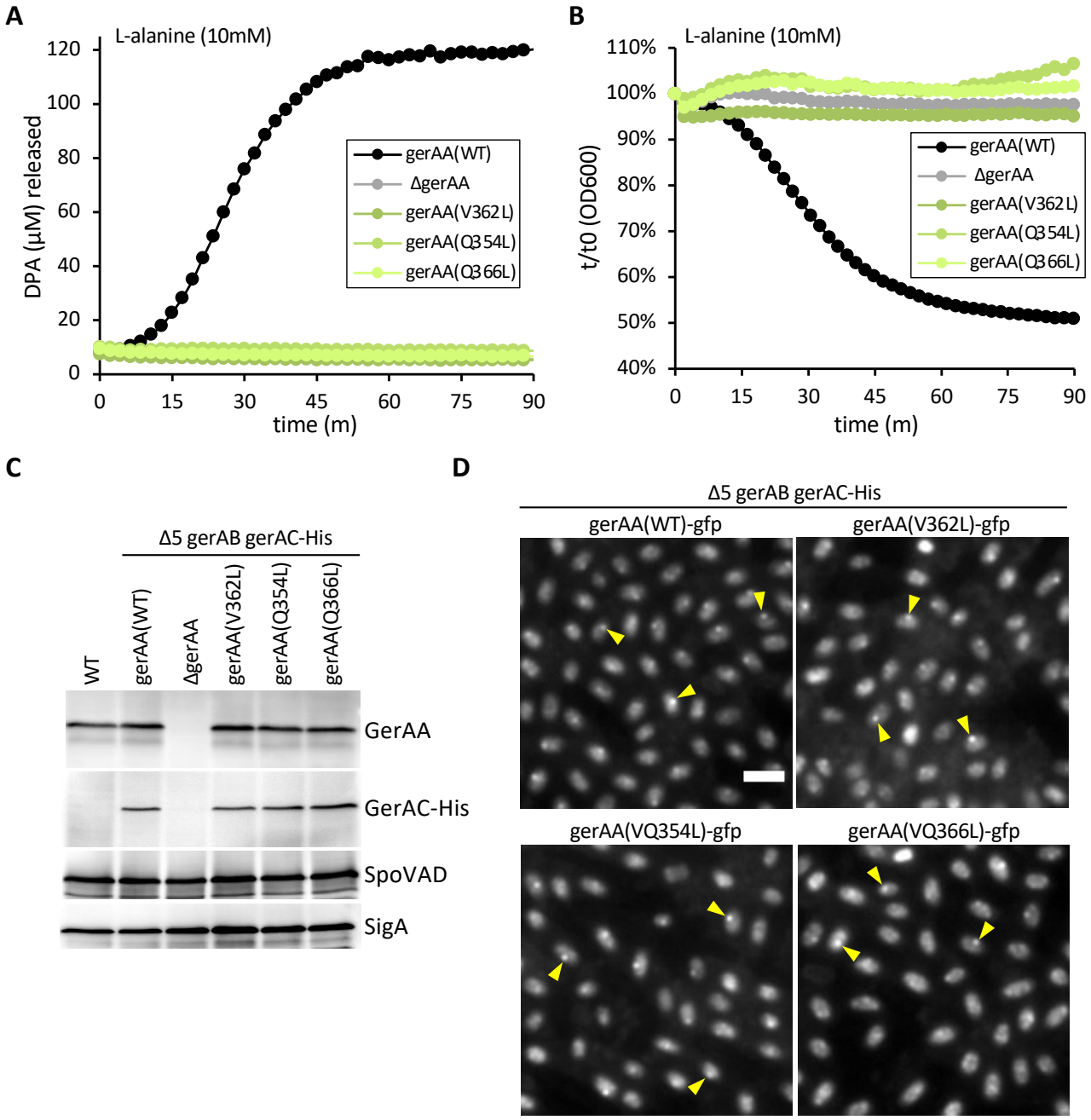

Figure S13. GerAA mutants predicted to reduce the pore size of the membrane channel fail to germinate in response to L-alanine but are stable and stabilize GerAC. (A,B) Plate reader-based germination assays using the same spores as those used in Figure S12. **(A)** DPA release after L-alanine addition over time. **(B)** OD600 was monitored over time after addition of L-alanine. **(C)** Representative immunoblots from lysates of the purified spores in Figure S12. GerAA(WT) and GerAA variants are stable and stabilize GerAC-His. GerAC-His is unstable in spores lacking GerAA (ΔgerAA). SpoVAD and SigA control for loading. **(D)** Representative fluorescence images of GerAA(WT)-GFP and indicated GerAA variants in spores. Scale bar, 2μm. GerAA localizes in germinosome foci (yellow carets). Representative data from one of three biological replicates are shown for (A), (B) and (D), and one of two biological replicates for (C).

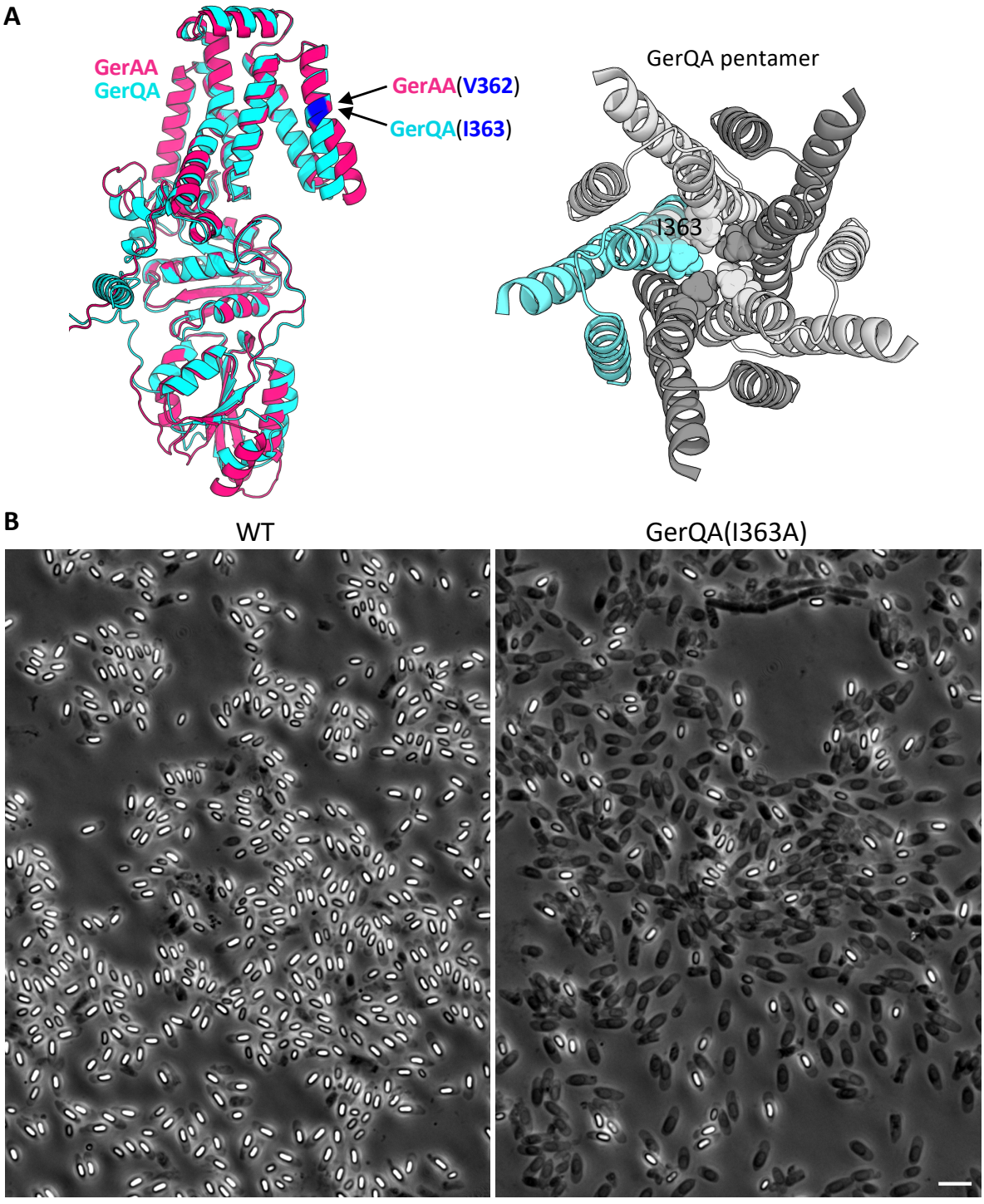

Figure S14. A *Bacillus cereus* GerQA mutant predicted to widen the membrane channel causes premature germination. (A) Alignment of the AlphaFold-predicted structures of *B. subtilis* GerAA (red) and *B. cereus* GerQA (aquamarine). The position of GerAA(V362) and GerQA(I363) are shown in dark blue (Left). Top-down view of the AlphaFold-predicted GerQA pentamer. The three TM segments from each GerQA protomer that make up the concentric rings that surround the membrane channel are shown. I363 is highlighted (Right). **(B)** Representative phase-contrast images of sporulated cultures of wild-type *B. cereus* and a merodiploid strain harboring *gerQA*(I363A). The majority of spores in the *gerQA*(I363A) mutant culture have undergone premature germination. Scale bar, 10 µm. Representative data from one of three biological replicates are shown.

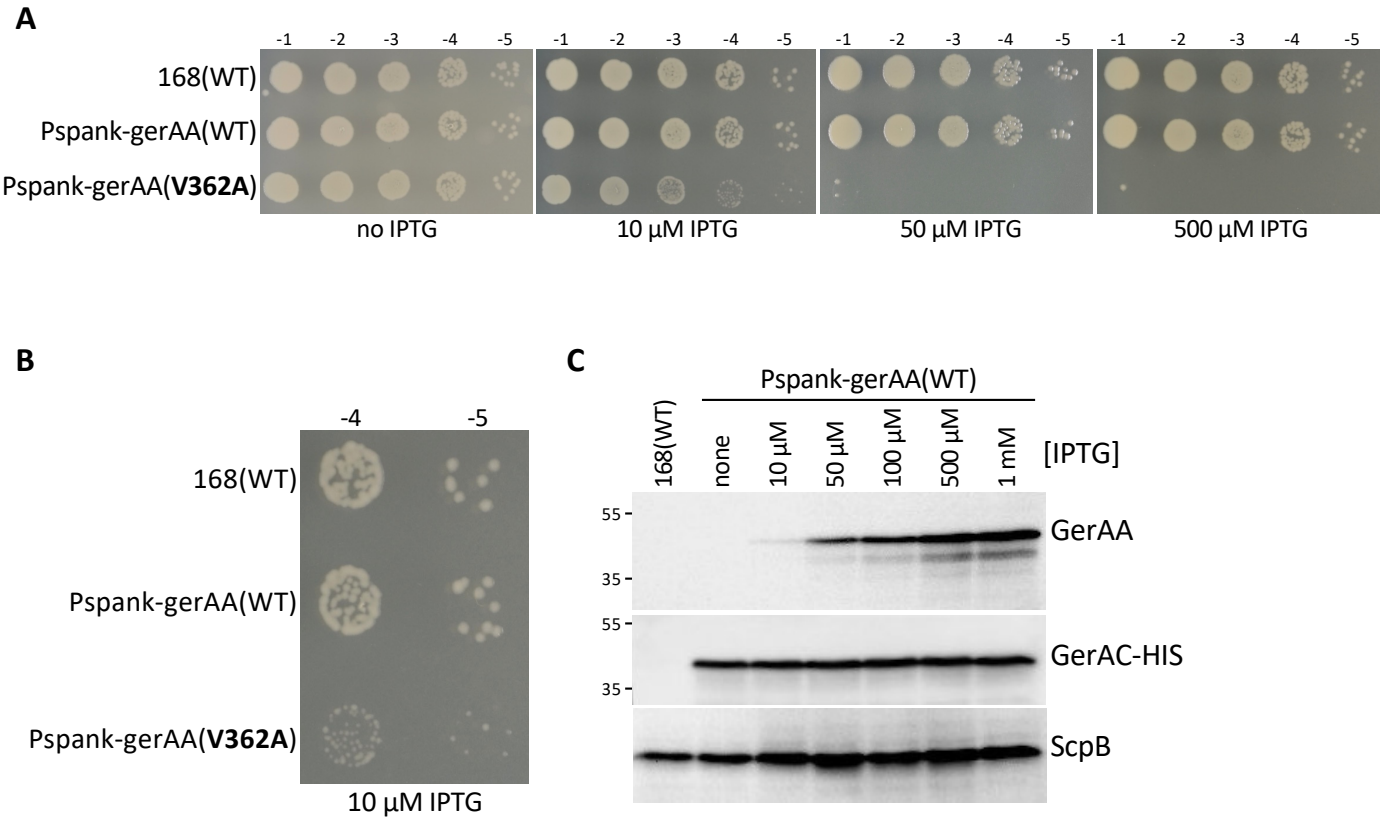

Figure S15. Low level expression of GerAA(V362A) impairs growth. (A) Serial dilutions of wild-type *B. subtilis* 168 and strains harboring IPTG-regulated alleles of *gerAA*(WT) and *gerAA*(V362A) with constitutively expressed (P_{veg}) *gerAB* and *gerAC-His*. The IPTG-inducible promoter (P_{spank}) is ~7-fold weaker than $P_{hyperspank}$ used in all other figures. **(B)** Zoom-in showing the impaired growth caused by *gerAA*(V362A) expression in the presence of 10 µM IPTG. **(C)** Representative immunoblots of the P_{spank}-*gerAA*(WT) strain in (A) grown in LB medium with the indicated concentrations of IPTG. GerAA(WT) was used instead of GerAA(V362A) due to impaired growth and lysis of the mutant allele. GerAA levels were almost undetectable at 10 µM IPTG yet were sufficient to impair growth. Constitutively expressed GerAC-His was analyzed for comparison. ScpB controlled for loading. Unlike during sporulation, GerAA, GerAB, and GerAC do not depend on each other for stability when expressed during vegetative growth. Representative data from one of three biological replicates are shown for (A) and (B) and one of two biological replicates for (C).

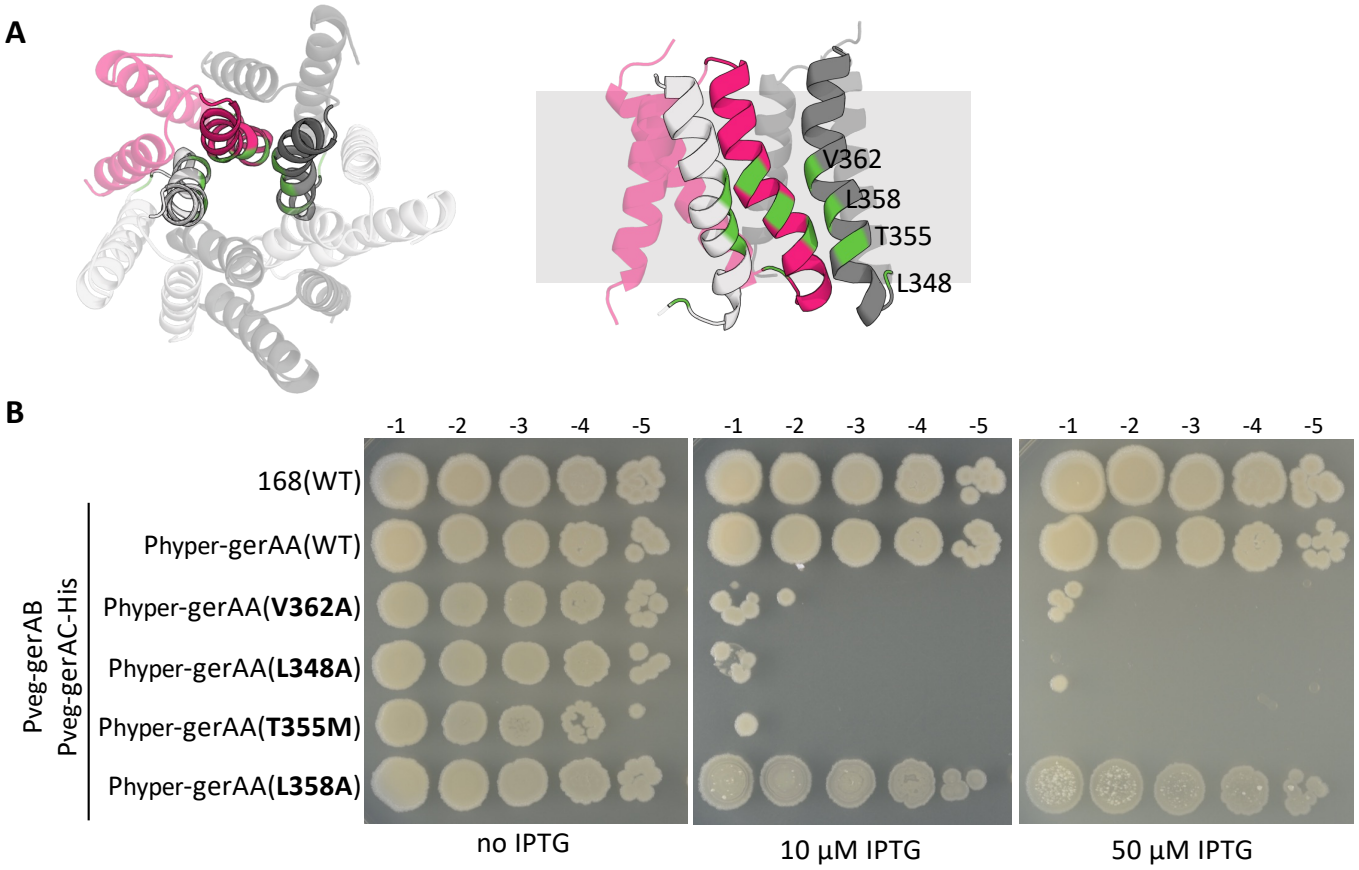

Figure S16. GerAA mutants that trigger premature germination during sporulation cause cell death when expressed during vegetative growth. (A) Top-down and cutaway side views of the GerAA pentameric channel. Residues that were hit in the screen for constitutively active alleles described in Figure S11 are highlighted in green. L358 was not identified in the screen but was tested afterwards. **(B)** Serial dilutions of the indicated strains with IPTG-regulated *gerAA* alleles and constitutively expressed *gerAB* and *gerAC-His*. The IPTG-regulated promoter $P_{hyperspank}$ (P_{hyper}) is ~7-fold stronger that P_{spank} used in Figure S15. Cells with P_{hyper}-*gerAA*(V362A), (L348A), or (T355M) die in the presence of IPTG. Cells expressing *gerAA*(L358A) lyse in stationary phase. Representative data from one of four biological replicates are shown.

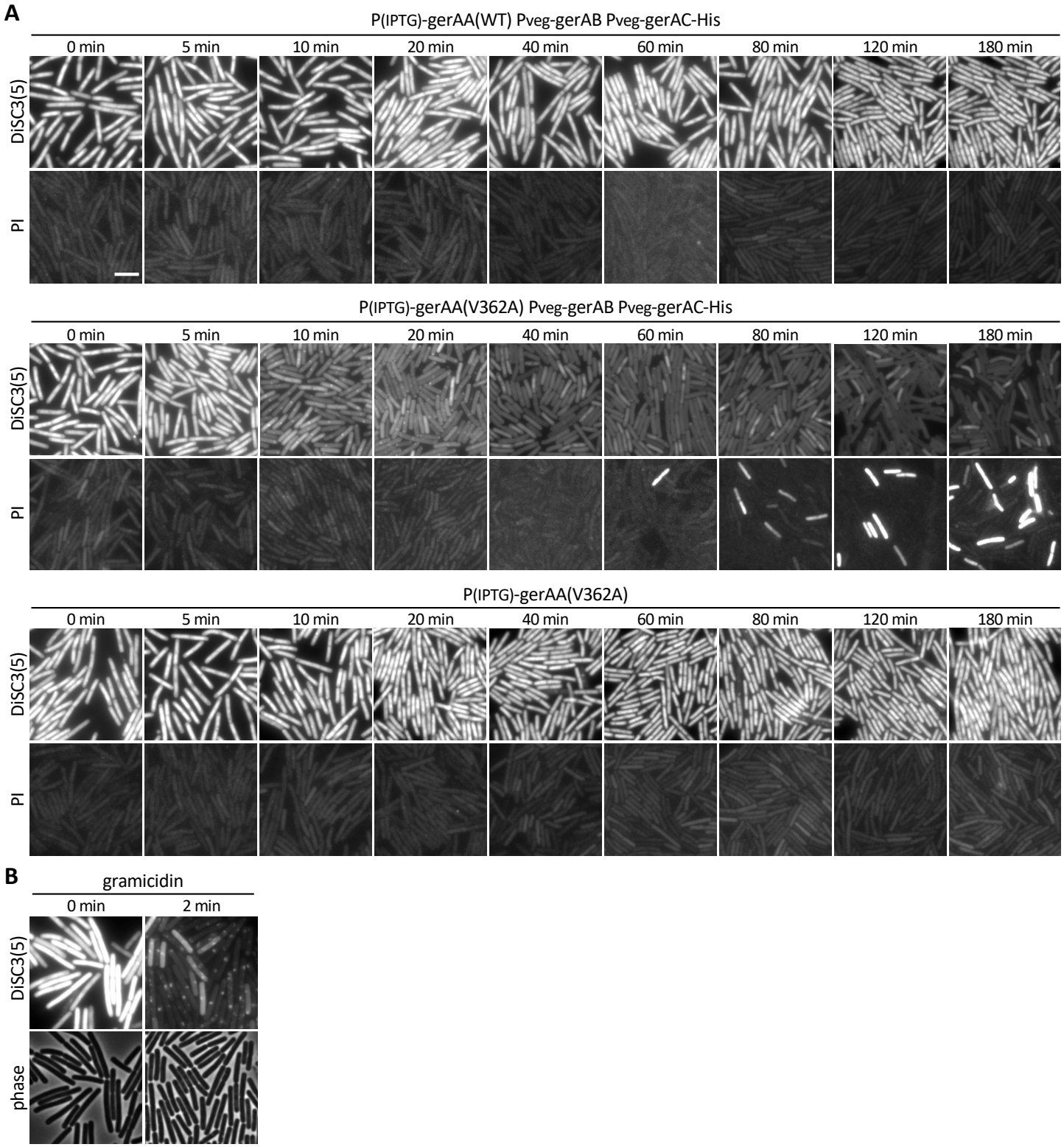

Figure S17. The GerA complex behaves like an ion channel when expressed in vegetatively growing cells. (A) Representative fluorescence images of exponentially growing cultures of the indicated strains. Time (in min) after IPTG addition (50 µM final) is indicated above each pair of images. The upper panels show fluorescence of the potentiometric dye $DiSC_3(5)$; the lower panels show propidium iodide (PI) staining. The two fields are from the same culture and timepoint but were stained and imaged separately. The loss of membrane potential in cells expressing GerAA(V362A), GerAB, and GerAC can explain the pervasive lysis and teardrop-shaped spores observed during sporulation. Scale bar, 5 µm. **(B)** Positive control for $DiSC_3(5)$. Representative phase-contrast and fluorescence images of wild-type *B. subtilis* stained with $DiSC_3(5)$ before and 2 min after addition of gramicidin, which generates membrane pores and dissipates membrane potential. Representative data from one of at least three biological replicates are shown in each panel.

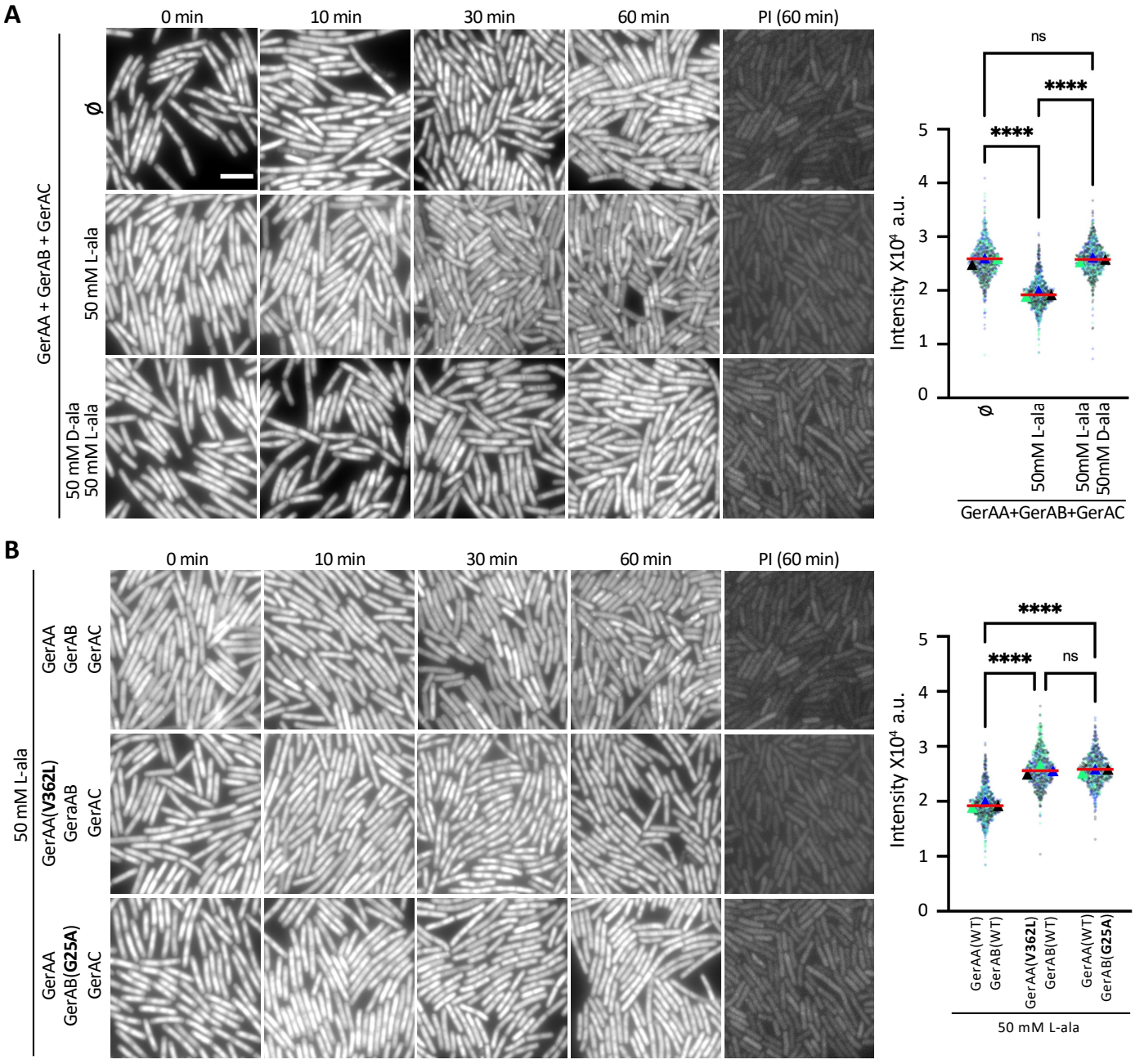

Figure S18. L-alanine triggers a drop in membrane potential in vegetative cells expressing the wild-type GerA complex. (A) Representative $DiSC_3(5)$ and propidium iodide (PI) fluorescence images from exponentially growing cultures expressing GerAA, GerAB, and GerAC before and after L-alanine (L-ala) addition or a mixture of L- and D-alanine. **(B)** Exponentially growing cultures of strains expressing GerAA, GerAB, GerAC or the indicated variants. Time in minutes after addition are indicated above the images. PI staining is only shown for the 60 min timepoint. The two images at 60 min are from the same cultures but were stained and imaged separately. Scale bar, 5 µm. The DiSC3(5) fluorescence intensities 30 min after L-alanine addition were quantified from three biological replicates (>500 cells for each) and plotted in different colors. Triangles indicate the median fluorescence intensity for each replicate, red lines show the median values for all cells per strain. P-value <0.0001 (****) and not significant (ns) are indicated.

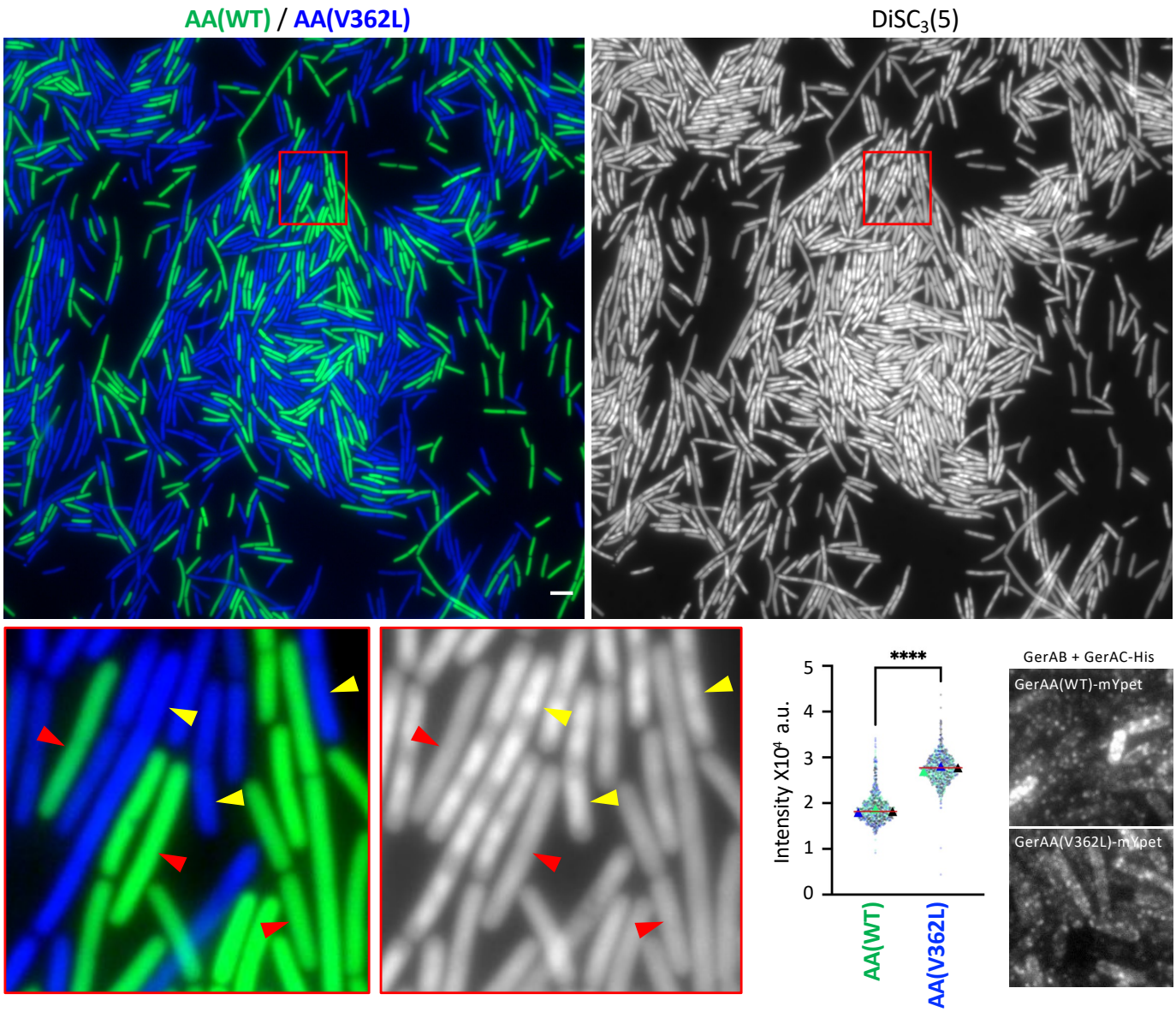

Figure S19. L-alanine triggers a drop in membrane potential in vegetative cells expressing the wild-type GerA complex compared to cells expressing a complex containing GerAB(V362L). A co-culturing experiment was performed to more rigorously control for intracellular $DiSC_3(5)$ accumulation and fluorescence imaging. A strain expressing GerAA(WT), GerAB, GerAC-His, and GFP was co-cultured with a strain expressing GerAA(V362L), GerAB, GerAC, and BFP. L-alanine (50 mM final) was added to the exponentially growing co-culture and 60 min later the cells were stained with $DiSC_3(5)$ and analyzed by fluorescence microscopy. GFP and BFP fluorescence identifies the two cell types in the field and $DiSC_3(5)$ reports on their membrane potential. Scale bar is 5 µm. A field of cells is shown at the top and a zoom in of the boxed region (red) is shown below. Red carets highlight individual cells expressing GerAA(WT) with reduced membrane potential and yellow carets highlight individual cells expressing GerAA(V362L) with higher negative membrane potential. $DiSC_3(5)$ fluorescence was quantified from sparser fields of cells from three biological replicates (>500 cells per replicate) and plotted together each with a different color. Triangles indicate the median fluorescence intensity for each replicate and red lines show the median values for all cells per strain. The difference in fluorescence intensity between cells expressing GerAA(WT) and GerAA(V362L) was significant ($P < 0.0001$). GerAA(WT)-mYpet and GerAA(V362L)-mYpet form similar fluorescent foci in the presence of GerAB and GerAC, indicating both assembled into similar complexes.

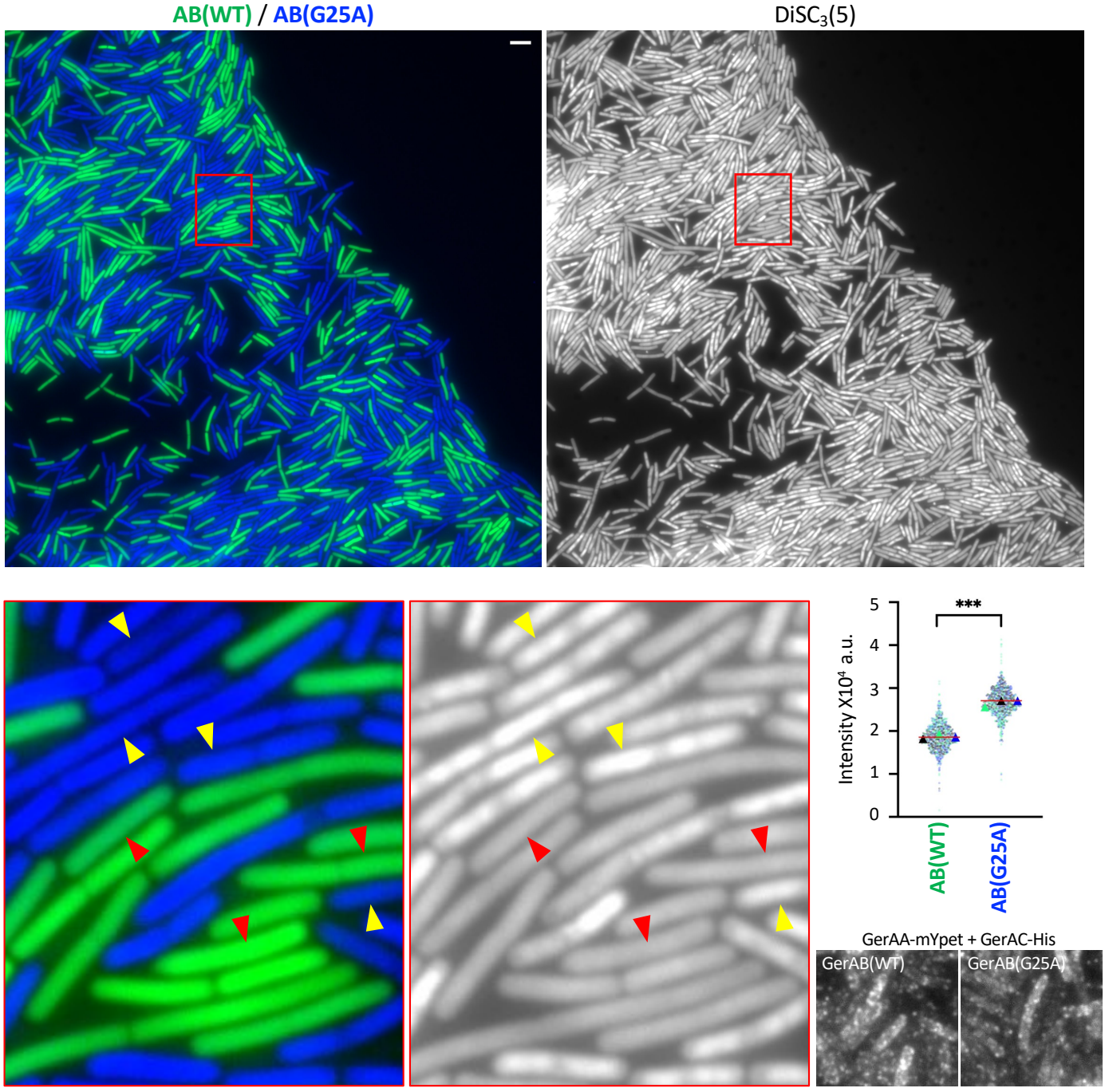

Figure S20. L-alanine triggers a drop in membrane potential in vegetative cells expressing the wild-type GerA complex compared to cells expressing a GerA complex containing GerAB(G25A). A co-culturing experiment was performed to more rigorously control for intracellular $DiSC_3(5)$ accumulation and fluorescence imaging. A strain expressing GerAA, GerAB(WT), GerAC-His, and GFP was co-cultured with a strain expressing GerAA, GerAB(G25A), GerAC, and BFP. L-alanine (50 mM final) was added to the exponentially growing co-culture and 60 min later the cells were stained with $DiSC_3(5)$ and analyzed by fluorescence microscopy. GFP and BFP fluorescence identifies the two cell types in the field and $DiSC_3(5)$ reports on their membrane potential. Scale bar is 5 µm. A field of cells is shown at the top and a zoom in of the boxed region (red) is shown below. Red carets highlight individual cells expressing GerAB(WT) with reduced membrane potential and yellow carets highlight individual cells expressing GerAB(G25A) with higher negative membrane potential potential. $DiSC_3(5)$ fluorescence was quantified from sparser fields of cells from three biological replicates (>500 cells per replicate) and plotted together each with a different color. Triangles indicate the median fluorescence intensity for each replicate and red lines show the median values for all cells per strain. The difference in fluorescence intensity between cells expressing GerAB(WT) and GerAB(G25A) was significant (P = 0.0002). GerAA-mYpet formed similar fluorescent foci in the presence of GerAC and either GerAB(WT) or GerAB(G25A), indicating both assembled into similar complexes.

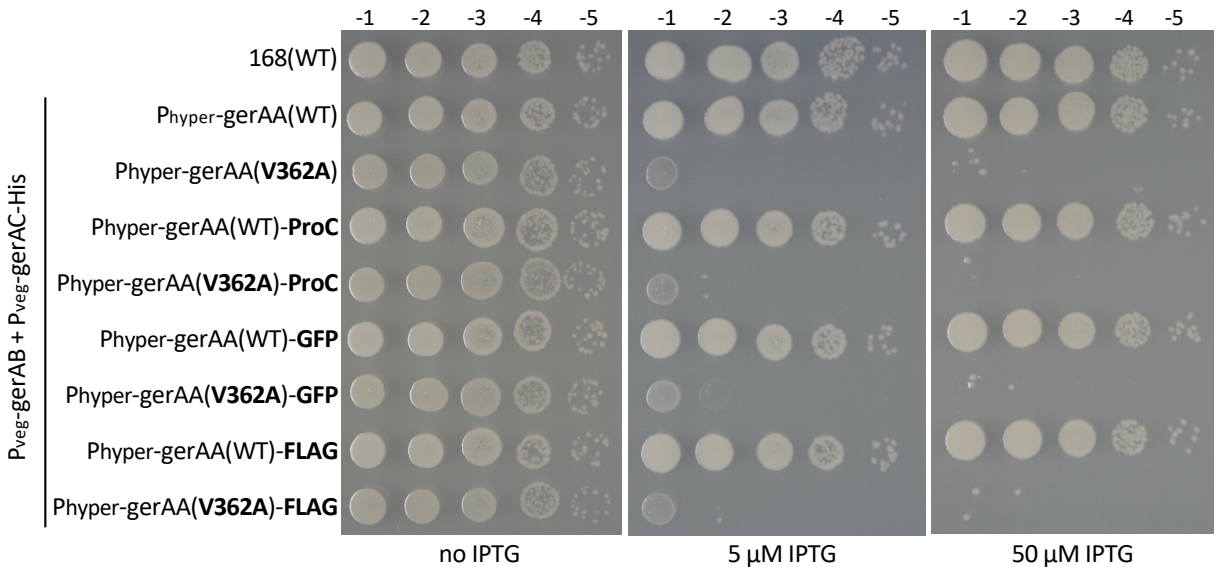

Figure S21. Fusing ProC, GFP, or FLAG to GerAA does not impact function as assayed by GerAA(V362A) killing. Serial dilutions of strains harboring IPTG-regulated *gerAA*(WT) and *gerAA*(V362A) fusions to Protein C (ProC), GFP, or FLAG and constitutively expressed *gerAB* and *gerAC-His*. The IPTG-regulated promoter (P_{hyper}) is ~7-fold stronger that P_{spank} used in Figure S15. Cells harboring Phyper-*gerAA*(V362A) and ProC, GFP, and FLAG fusions are not viable in the presence of IPTG. Representative data from one of three biological replicates are shown.

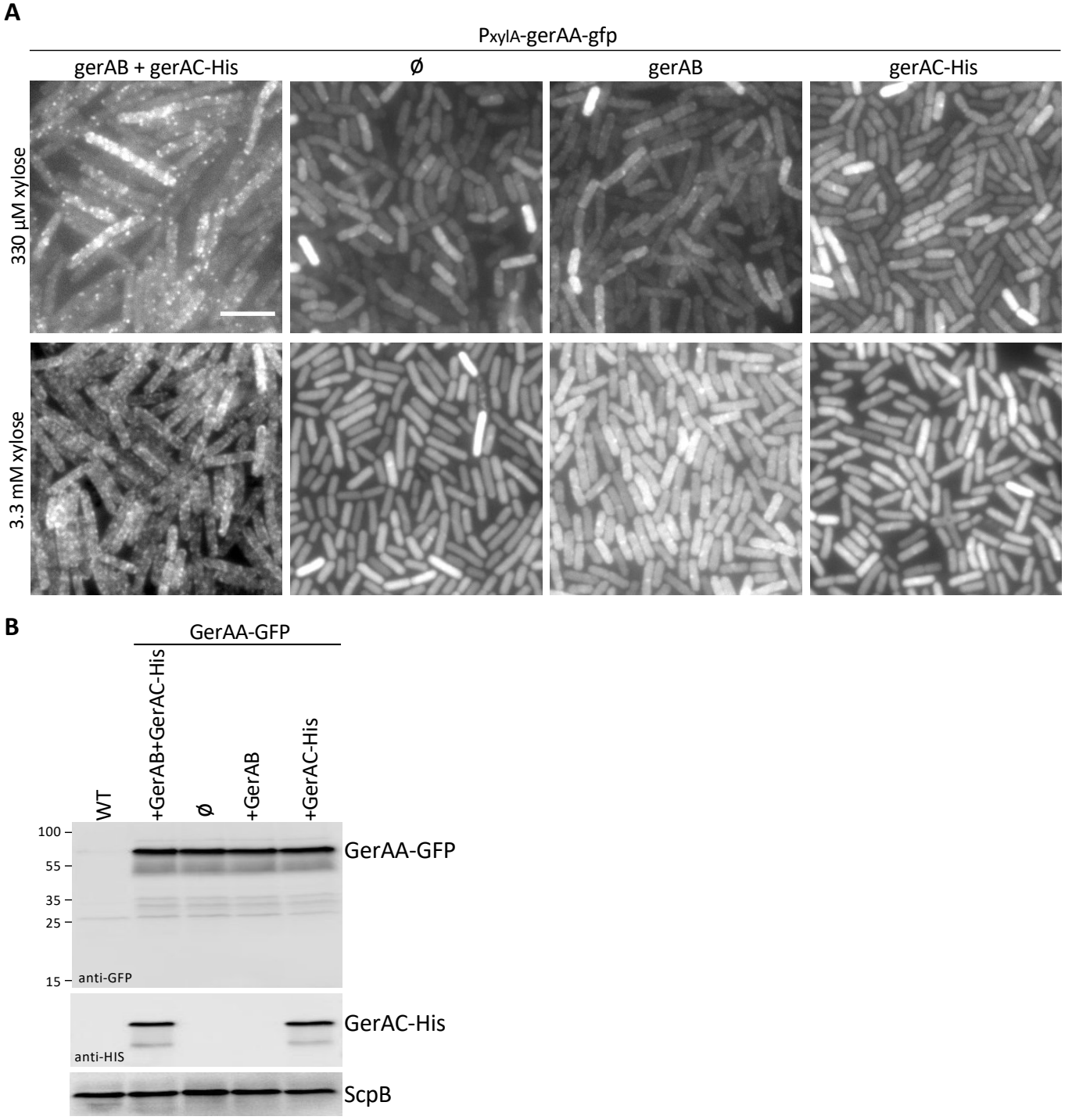

Figure S22. GerAA-GFP fluorescent foci require expression of GerAB and GerAC. (A) Representative fluorescence images of vegetative cells expressing GerAA-GFP in the presence and absence of GerAB and GerAC-His. The GerAA-GFP fusion was expressed under the control of a xylose-regulated promoter (P_{xylA}) at the indicated concentrations. GerAB and GerAC-His were expressed under the control of the IPTG-regulated promoter $P_{hyperspank}$ with 1 mM IPTG. Scale bar, 5 µm. **(B)** Immunoblots using lysates from the same strains in (A) grown in the presence of 1 mM IPTG and 3.3 mM xylose. Full-length GerAA-GFP and the minor degradation products were similar in all four strains. GerAC-His was analyzed as a control and ScpB controls for loading. Representative data from one of three biological replicates are shown for (A) and one of two biological replicates for (B).

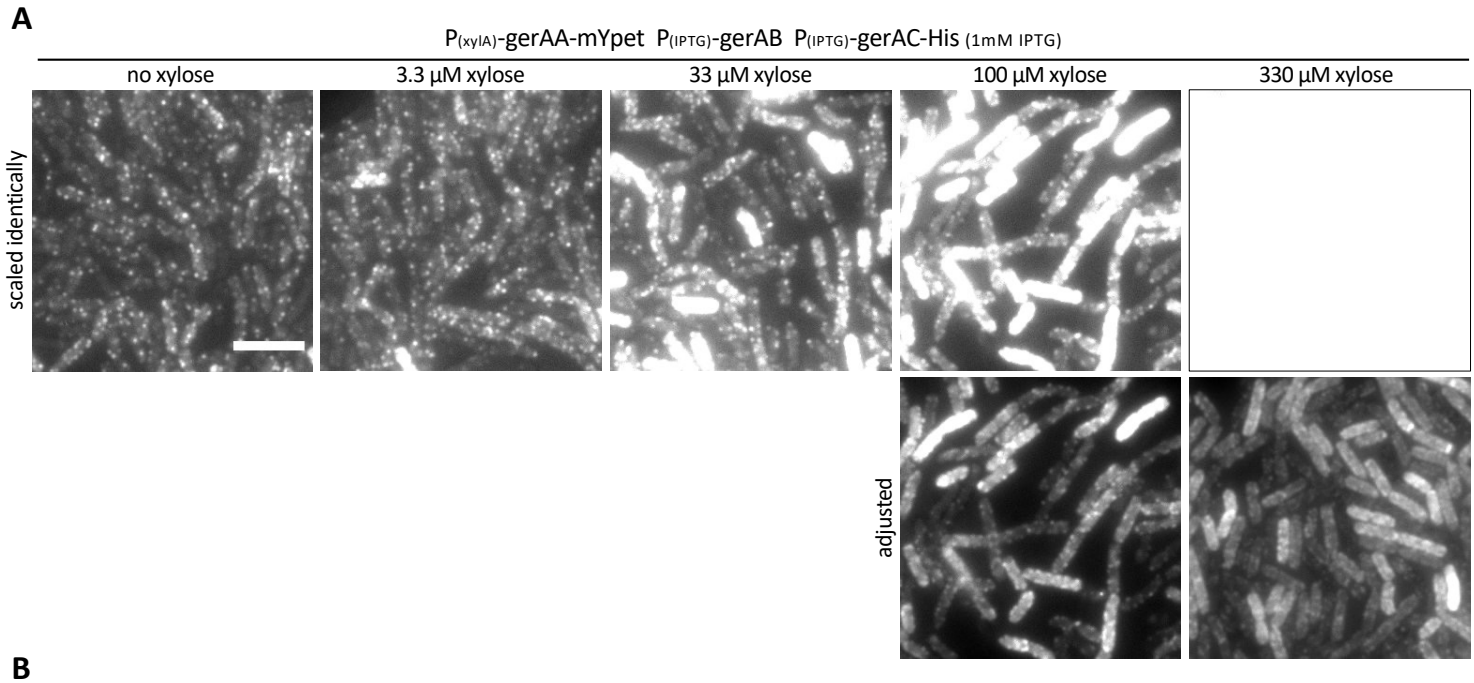

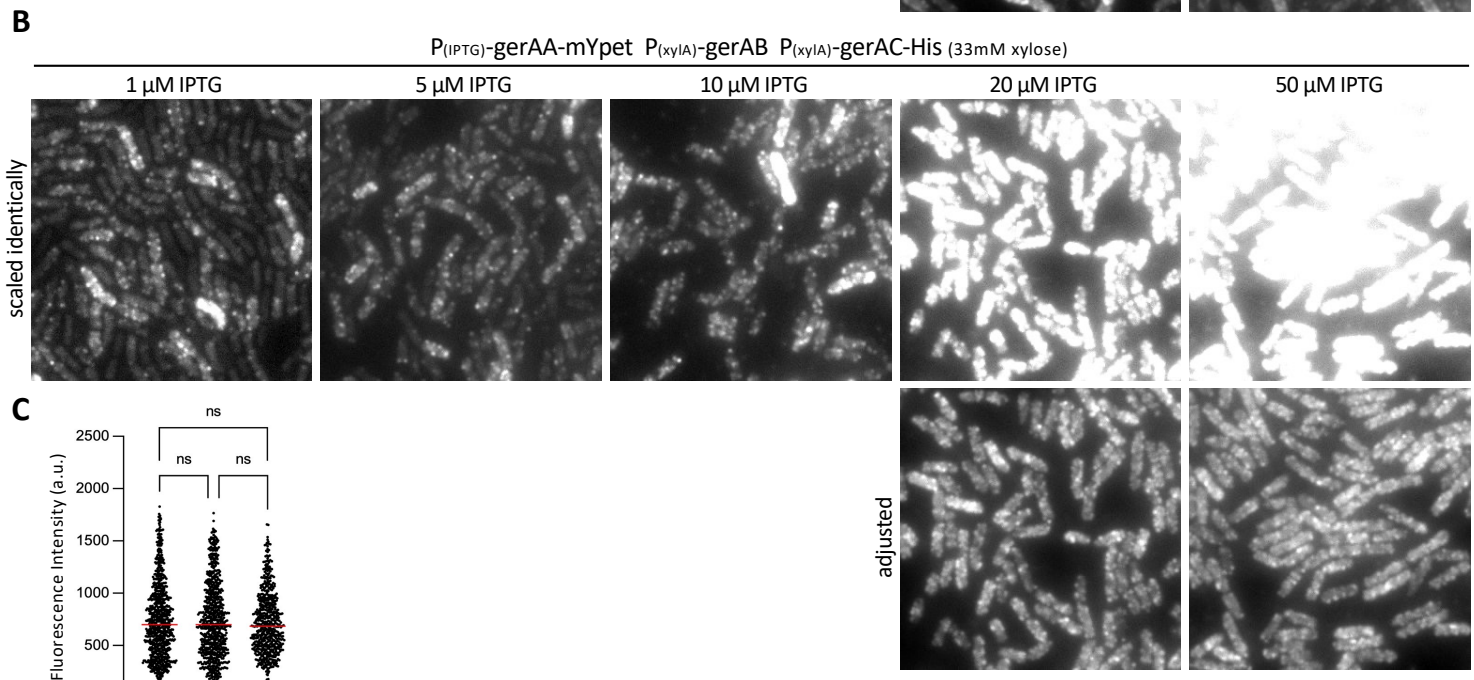

Figure S23. GerAA-mYpet fusions form discrete fluorescent foci with similar intensities when expressed at a different levels. Representative fluorescent images of vegetative cells expressing GerAA-mYpet in the presence of GerAB and GerAC-His. **(A)** GerAA-mYpet was expressed under the control of a xylose-regulated promoter (P_{xylA}) at the indicated concentrations of xylose. GerAB and GerAC-His were expressed under the control of an IPTG-regulated promoter with 1 mM IPTG. Scale bar, 5 µm. **(B)** GerAA-mYpet was expressed under the control of an IPTG-regulated promoter at the indicated concentrations of IPTG. GerAB and GerAC-His were expressed under the control of the xylose-regulated promoter $P_{(xylA)}$ with 33 mM xylose. The exposure time (500 ms) was the same for all conditions. The images at the top were scaled identically. The same images below were adjusted to best visualize the fluorescent foci. **(C)** Quantification of GerAA-mYpet foci intensities for the indicated strains and concentrations of inducers. The fluorescence intensities of foci from >500 cells from sparser fields of the strains in (A) and (B) were quantified using a custom spot-detection plugin in MicrobeJ. The red lines show the median fluorescence intensities. The differences in foci intensity between strains and conditions were not significant (ns). Representative data from one of four biological replicates are shown.

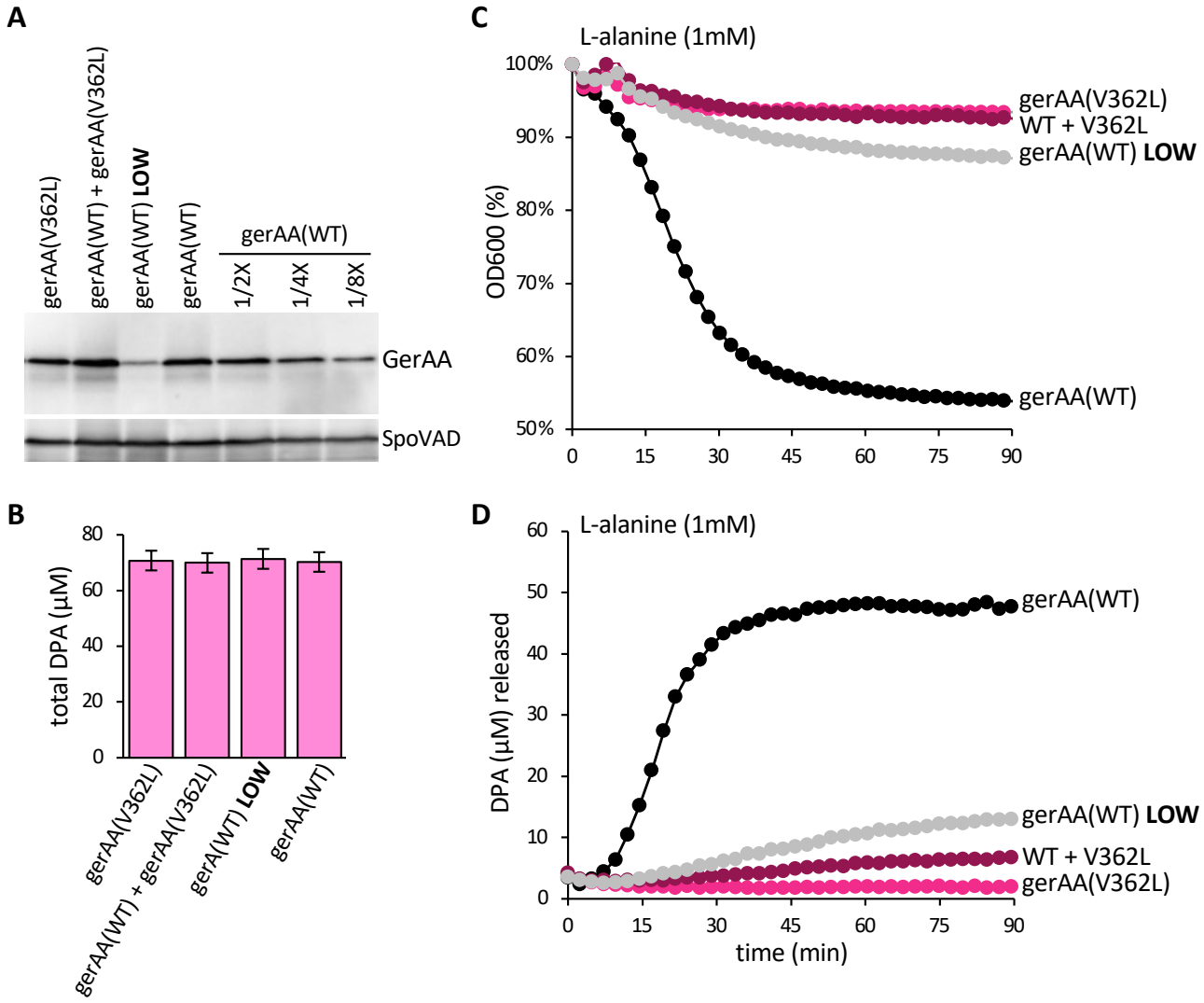

Figure S24. GerAA(V362L) is strongly dominant-negative. (A) Representative immunoblot monitoring GerAA levels in lysates from purified spores of the indicated strains. Spores harboring gerAA(WT) LOW contains a point mutation in the ribosome binding site, reducing the levels of wild-type GerAA by approximately 8-fold. Spore lysates with GerAA(WT) were diluted 2-, 4-, and 8-fold with spore lysates from a ΔgerAA strain to maintain equivalent amounts of total protein loaded. SpoVAD controls for loading. **(B)** Bar graph showing total DPA in purified spores from the indicated strains. **(C,D)** Purified spores from the indicated strains were mixed with 1 mM L-alanine and the optical density **(C)** and DPA release **(D)** were monitored over time. Spores with equivalent levels of GerAA(WT) and the channel-blocking mutant GerAA(V362L) were severely impaired in germination. DPA release and the drop in optical density in response to L-alanine in the merodiploid spores were more impaired than spores with the *gerAA* allele that produced >8-fold lower levels of wild-type GerAA. Representative data from one of two biological replicates are shown for (A) and one of three biological replicates for (B-D).

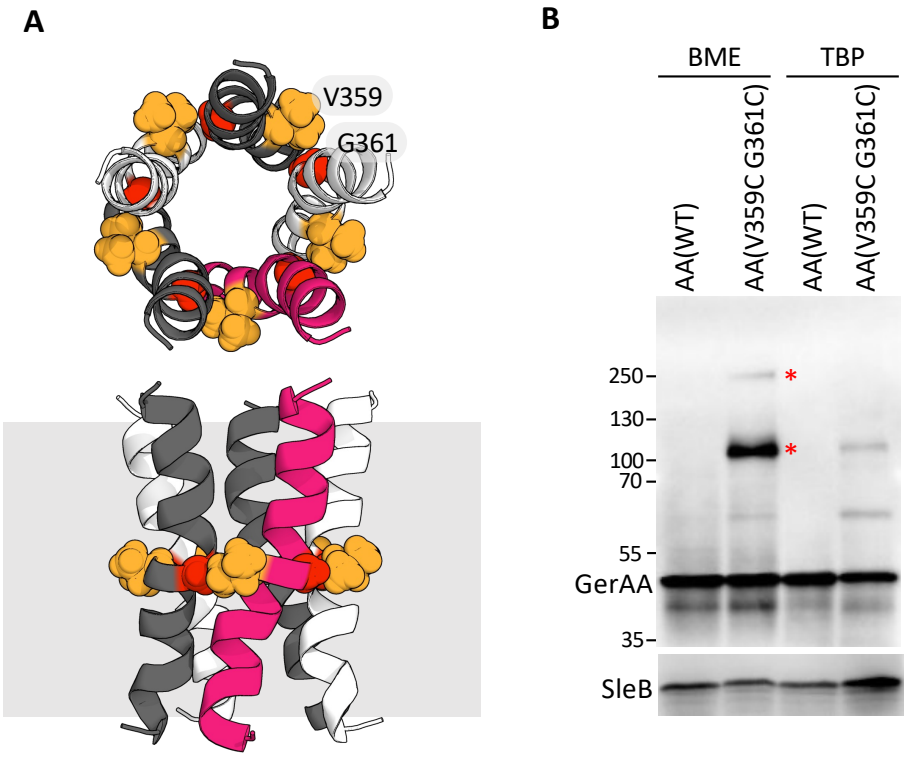

Figure S25. Cysteine-substituted GerAA proteins form disulfide species consistent with dimer and pentamer. (A) Top-down and side view of the channel in the GerAA pentamer model. Only TM3 from each GerAA protomer is shown. The two residues (V359, dark yellow and G361, red) that were changed to cysteine are highlighted. **(B)** Representative immunoblot from lysates of spores containing GerAA(WT) or GerAA(V359C, G361C). Lysates were split and incubated with ß-mercaptoethanol (BME) or tributyl phosphine (TBP). GerAA(V359C G361C) maintained disulfide species (red asterisks) with sizes of dimer and pentamer in the presence of BME but these species were largely lost in the presence of TBP. SleB controls for loading. Representative data from one of two biological replicates are shown.

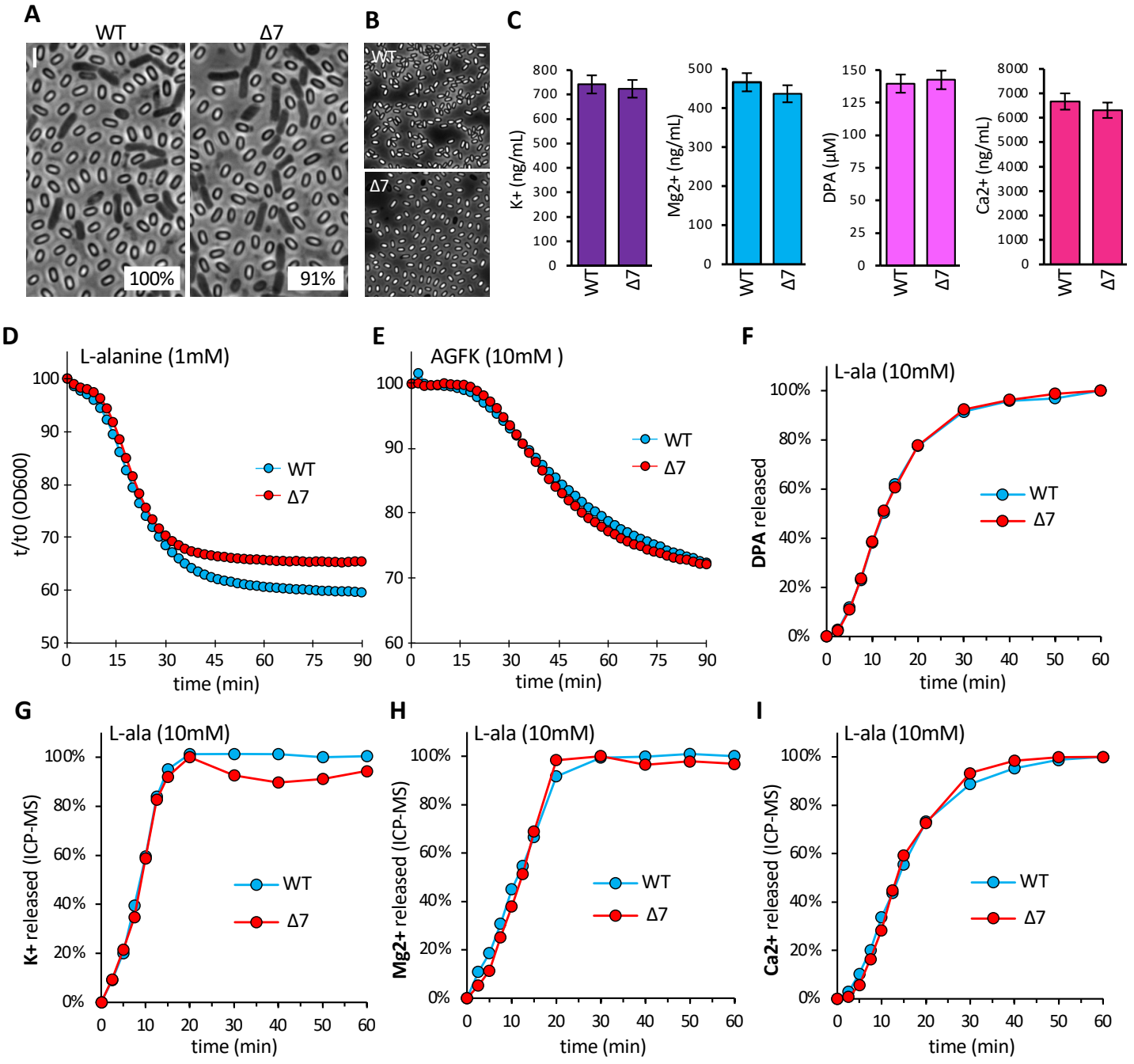

Figure S26. Spore germination in a mutant lacking seven putative ion transporters is similar to wild-type. Comparison of sporulation and germination in wild-type and a septuple mutant (Δ7) lacking seven putative ion transporters Δ*khtU* Δ*cpaA* Δ*nhaK* Δ*yugO* Δ*chaA* Δ*yugS* Δ*corA*. KhtU and CpaA are remote homologs of *B. cereus* GerN (Transporter Classification 2.A.37) that functions in germination in response to inosine in *B. cereus* (*33*). NhaK (TC 2.A.36), ChaA (TC 2.A.19), YugO (TC 1.A.1.13.4), CorA (TC 1.A.35) are members of distinct transporter families and YugS is a putative ion transporter (IPR044751). All seven proteins are expressed during sporulation (*61*) and/or are present in the spore inner membrane proteome (*62*). **(A)** Phase-contrast images of sporulated cultures of the indicated strains. The sporulation efficiencies are shown in the bottom right corner. Scale bar is 2 μm. **(B)** Images of the Histodenz-purified spores. **(C)** Levels of total K^+, Mg^{2+}, Ca^{2+}, and DPA in the wild-type and Δ7 purified spores. **(D-E)** Drop in optical densities over time after exposing the spores to L-alanine **(D)** or a mixture of L-asparagine, D-glucose, D-fructose, and K+ (AGFK) **(E)**. **(F-I)** After mixing the spores with 10 mM L-alanine (L-ala), germination exudates were collected at the indicated times and analyzed for DPA using $TbCl_3$ **(F)**, K^+ **(G),** Mg^{2+} **(H)**, and Ca^{2+} **(I)**, using ICP-MS. Representative data from one of three biological replicates are shown in each panel.

Table S1.

Strains	Genotype	Source	Figures
BDR2414	*Bacillus subtilis 168 (trpC2)*	(*39*)	S4, S12, S13, S15, S16, S17, S21, S22, S26
BDR4496	*ΔkhtU::lox72 ΔcpaA::lox72 ΔnhaK::lox72 ΔyugO::lox72 ΔchaA::lox72 ΔyugS::lox72 ΔcorA::lox72*	This study	S26
BAM841	*gerA+ ΔgerBB::lox72 ΔgerKB::lox72 ΔyfkT::lox72 ΔyndE::lox72*	(*58*)	1, S3
BAM860	*ΔgerAB::lox72 ΔgerBB::lox72 ΔgerKB::lox72 ΔyfkT::lox72 ΔyndE::lox72*		S3
BJA177a	*ΔgerA::cat ΔgerBB::lox72 ΔgerKB::lox72 ΔyfkT::lox72 ΔyndE::lox72, ycgO::gerAA(P326S)-gerAB-gerAC (spec)*	(*9*)	
BJA186a	*yhdG::erm sspE-lacZΩ (cat)*	This study	
BJA229	*yhdG::PgerA-gerAA(P326S)(tet)*	This study	S11
BJA230	*yhdG::PgerA-gerAA(P326S)(tet) sspE-lacZΩ (cat)*	This study	
BJA276	*yhdG::PgerA-gerAA(tet)*	This study	2, S11
BJA277	*yhdG::PgerA-gerAA(tet) sspE-lacZΩ (cat)*	This study	
BJA498	*yhdG::PgerA-gerAA(L348A)(tet)*	This study	S11
BJA500	*yhdG::PgerA-gerAA(T355M)(tet)*	This study	S11
BJA501	*yhdG::PgerA-gerAA(V362A)(tet)*	This study	2, S11
BJA508	*yhdG::PgerA-gerAA(P326S)(tet) ΔsleB::erm*	This study	S11
BJA509	*yhdG::PgerA-gerAA(tet) ΔsleB::erm*	This study	S11
BJA510	*yhdG::PgerA-gerAA(L348A)(tet) ΔsleB::erm*	This study	S11
BJA512	*yhdG::PgerA-gerAA(T355M)(tet) ΔsleB::erm*	This study	S11
BJA513	*yhdG::PgerA-gerAA(V362A)(tet) ΔsleB::erm*	This study	S11
BLA219	*ΔgerA::lox72 ΔgerBB::lox72 ΔgerKB::lox72 ΔyfkT::lox72 ΔyndE::lox72 lacA::PgerA-gerAC(erm) ycgO::PgerA-gerAB(spec) yhdG::PgerA-gerAA(tet)*	(*10*)	2, S12, S13, S24
BLA321	*ΔgerA::lox72 ΔgerBB::lox72 ΔgerKB::lox72 ΔyfkT::lox72 ΔyndE::lox72 lacA::PgerA-gerAC-his6(phleo) ycgO::PgerA-gerAB(spec) yhdG::PgerA-gerAA(tet)*	(*10*)	2, S13
BLA420	*ΔgerBB::lox72 ΔgerKB::lox72 ΔyfkT::lox72 ΔyndE::lox72 ΔgerA::lox72 lacA::Pveg-gerAC-His6(phleo) ycgO::Pveg-gerAB(spec)yhdG::Phy-gerAA(C100S)(erm)*	This study	3
BLA450	*ΔgerBB::lox72 ΔgerKB::lox72 ΔyfkT::lox72 ΔyndE::lox72 ΔgerA::lox72 lacA::Pveg-gerAC-His6(phleo) ycgO::Pveg-gerAB(spec) yhdG::Phy-gerAA(C100S, V359C, G361C)(erm)*	This study	3
BLA451	*ΔgerBB::lox72 ΔgerKB::lox72 ΔyfkT::lox72 ΔyndE::lox72 ΔgerA::lox72 lacA::Pveg-gerAC-His6(phleo) ycgO::Pveg-gerAB(spec) yhdG::Phy-gerAA(C100S, V359C)(erm)*	This study	3
BLA452	*ΔgerBB::lox72 ΔgerKB::lox72 ΔyfkT::lox72 ΔyndE::lox72 ΔgerA::lox72 lacA::Pveg-gerAC-His6(phleo) ycgO::Pveg-gerAB(spec) yhdG::Phy-gerAA(C100S, G361C)(erm)*	This study	3
BLA453	*ΔgerBB::lox72 ΔgerKB::lox72 ΔyfkT::lox72 ΔyndE::lox72 ΔgerA::lox72 yhdG::Phy-gerAA(C100S, V359C, G361C)(erm)*	This study	3
BLA438	*ΔgerBB::lox72 ΔgerKB::lox72 ΔyfkT::lox72 ΔyndE::lox72 ΔgerA::lox72 lacA::PgerA-gerAC(erm) ycgO::PgerA-gerAB(spec) yhdG::PgerA-gerAA(C100S, V359C, G361C)(tet) ΔcotE::phleo ΔgerE::kan*	This study	3, S25
BLA463	*ΔgerBB::lox72 ΔgerKB::lox72 ΔyfkT::lox72 ΔyndE::lox72 ΔgerA::lox72 lacA::PgerA-gerAC(erm) ycgO::PgerA-gerAB(spec) yhdG::PgerA-gerAA(C100S)(tet) ΔcotE::phleo ΔgerE::kan*	This study	3, S25
BYG1051	*ΔgerA::lox72 ΔgerBB::lox72 ΔgerKB::lox72 ΔyfkT::lox72 ΔyndE::lox72 yvbJ::Phy-gerAC-his6(Cm) ycgO::Phy-gerAB(spec) yhdG::Pxyl-gerAA-gfp(phleo)*	This study	3, S22
BYG1104	*ΔgerA::lox72 ΔgerBB::lox72 ΔgerKB::lox72 ΔyfkT::lox72 ΔyndE::lox72 lacA::PgerA-gerAC(erm) ycgO::PgerA-gerAB(spec) yhdG::Kan*	This study	S12, S13

BYG1116	*ΔgerA::lox72 ΔgerBB::lox72 ΔgerKB::lox72 ΔyfkT::lox72 ΔyndE::lox72 lacA::PgerA-gerAC(erm) ycgO::PgerA-gerAB(spec) yhdG::PgerA-gerAA(Q366L)(tet)*	This study	S12, S13
BYG1117	*ΔgerA::lox72 ΔgerBB::lox72 ΔgerKB::lox72 ΔyfkT::lox72 ΔyndE::lox72 ycgO::Phy-gerAB(spec) yhdG::Pxyl-gerAA-gfp(phleo)*	This study	S22
BYG1118	*ΔgerA::lox72 ΔgerBB::lox72 ΔgerKB::lox72 ΔyfkT::lox72 ΔyndE::lox72 yvbJ::Phy-gerAC-His6(Cm) yhdG::Pxyl-gerAA-gfp(phleo)*	This study	S22
BYG1126	*ΔgerA::lox72 ΔgerBB::lox72 ΔgerKB::lox72 ΔyfkT::lox72 ΔyndE::lox72 lacA::PgerA-gerAC(erm) ycgO::PgerA-gerAB(spec) yhdG::PgerA-gerAA(V362L)(tet)*	This study	2, S12, S13
BYG1127	*ΔgerA::lox72 ΔgerBB::lox72 ΔgerKB::lox72 ΔyfkT::lox72 ΔyndE::lox72 lacA::PgerA-gerAC(erm) ycgO::PgerA-gerAB(spec) yhdG::PgerA-gerAA(Q354L)(tet)*	This study	S12, S13
BYG1128	*ΔgerA::lox72 ΔgerBB::lox72 ΔgerKB::lox72 ΔyfkT::lox72 ΔyndE::lox72 lacA::PgerA-gerAC(erm) ycgO::PgerA-gerAB(spec) yhdG::PgerA-gerAA-gfp(tet)*	This study	2, S13
BYG1129	*ΔgerA::lox72 ΔgerBB::lox72 ΔgerKB::lox72 ΔyfkT::lox72 ΔyndE::lox72 lacA::PgerA-gerAC(erm) ycgO::PgerA-gerAB(spec) yhdG::PgerA-gerAA(V362A)(tet)*	This study	2
BYG1145	*ΔgerA::lox72 ΔgerBB::lox72 ΔgerKB::lox72 ΔyfkT::lox72 ΔyndE::lox72 yhdG::Pxyl-gerAA-gfp(phleo)*	This study	3, S22
BYG1146	*ΔgerA::lox72 ΔgerBB::lox72 ΔgerKB::lox72 ΔyfkT::lox72 ΔyndE::lox72 lacA::Pveg-gerAC-His6(phleo) ycgO::Pveg-gerAB(spec) yhdG::Phy-gerAA(L348A)(erm)*	This study	S16
BYG1147	*ΔgerA::lox72 ΔgerBB::lox72 ΔgerKB::lox72 ΔyfkT::lox72 ΔyndE::lox72 lacA::Pveg-gerAC-His6(phleo) ycgO::Pveg-gerAB(spec) yhdG::Phy-gerAA(T355M)(erm)*	This study	S16
BYG1148	*ΔgerA::lox72 ΔgerBB::lox72 ΔgerKB::lox72 ΔyfkT::lox72 ΔyndE::lox72 ycgO::Phy-gerAB(spec) yhdG::Pxyl-gerAA-gfp(phleo)*	This study	3
BYG1149	*ΔgerA::lox72 ΔgerBB::lox72 ΔgerKB::lox72 ΔyfkT::lox72 ΔyndE::lox72 yvbJ::Phy-gerAC-His6(Cm) yhdG::Pxyl-gerAA-gfp(phleo)*	This study	3
BYG1161	*ΔgerA::lox72 ΔgerBB::lox72 ΔgerKB::lox72 ΔyfkT::lox72 ΔyndE::lox72 yvbJ::Phy-gerAC-His6(Cm) ycgO::Phy-gerAB(spec) yhdG::Pxyl-gerAA-ProC(phleo) lacA::Pxyl-gerAA-FLAG(erm)*	This study	3
BYG1164	*ΔgerA::lox72 ΔgerBB::lox72 ΔgerKB::lox72 ΔyfkT::lox72 ΔyndE::lox72 lacA::PgerA-gerAC(erm) ycgO::PgerA-gerAB(spec) yhdG::PgerA-gerAA(V362L)-gfp(tet)*	This study	2, S13
BYG1165	*ΔgerA::lox72 ΔgerBB::lox72 ΔgerKB::lox72 ΔyfkT::lox72 ΔyndE::lox72 lacA::PgerA-gerAC(erm) ycgO::PgerA-gerAB(spec) yhdG::PgerA-gerAA(Q354L)-gfp(tet)*	This study	S13
BYG1166	*ΔgerA::lox72 ΔgerBB::lox72 ΔgerKB::lox72 ΔyfkT::lox72 ΔyndE::lox72 lacA::PgerA-gerAC(erm) ycgO::PgerA-gerAB(spec) yhdG::PgerA-gerAA(Q366L)-gfp(tet)*	This study	S13
BYG1179	*ΔgerA::lox72 ΔgerBB::lox72 ΔgerKB::lox72 ΔyfkT::lox72 ΔyndE::lox72 yvbJ::Phy-gerAC-His6(cat) ycgO::Phy-gerAB(spec) yhdG::Pxyl-gerAA-mYpet(phleo)*	This study	S23
BYG1188	*ΔgerA::lox72 ΔgerBB::lox72 ΔgerKB::lox72 ΔyfkT::lox72 ΔyndE::lox72 lacA::PgerA-gerAC(erm) ycgO::PgerA-gerAB(spec) yvbJ::PgerA-gerAA(V362L)(cat) yhdG::kan*	This study	S24
BYG1196	*ΔgerA::lox72 ΔgerBB::lox72 ΔgerKB::lox72 ΔyfkT::lox72 ΔyndE::lox72 lacA::PgerA-gerAC(erm) ycgO::PgerA-gerAB(spec) yvbJ::PgerA-gerAA(V362L)(cat) yhdG::PgerA-gerAA(tet)*	This study	S24
BYG1198	*ΔgerA::lox72 ΔgerBB::lox72 ΔgerKB::lox72 ΔyfkT::lox72 ΔyndE::lox72 lacA::Pveg-gerAC-His6(phleo) ycgO::Pveg-gerAB(spec) yhdG::Phy-gerAA(V362A)-gfp(erm)*	This study	S21
BYG1211	*ΔgerA::lox72 ΔgerBB::lox72 ΔgerKB::lox72 ΔyfkT::lox72 ΔyndE::lox72 yvbJ::Phy-gerAC-His6(cat) ycgO::Phy-gerAB(spec) yhdG::Pxyl-gerAA(phleo) lacA::Pxyl-gerAA-FLAG(erm)*	This study	3
BYG1212	*ΔgerA::lox72 ΔgerBB::lox72 ΔgerKB::lox72 ΔyfkT::lox72 ΔyndE::lox72 yhdG::Pxyl-gerAA-ProC(phleo) lacA::Pxyl-gerAA-FLAG(erm)*	This study	3

BYG1232	*yhdG::PgerA-gerAA(L358A)(tet)*	This study	S11
BYG1234	*yhdG::PgerA-gerAA(L358A)(tet) ΔsleB::lox72*	This study	S11
BYG1291	*ΔgerA::lox72 ΔgerBB::lox72 ΔgerKB::lox72 ΔyfkT::lox72 ΔyndE::lox72 lacA::PgerA-gerAC(erm) ycgO::PgerA-gerAB(spec) yhdG::PgerA-(weak RBS)-gerAA(tet)*	This study	S24
BYG1301	*ΔgerA::lox72 ΔgerBB::lox72 ΔgerKB::lox72 ΔyfkT::lox72 ΔyndE::lox72 lacA::Pveg-gerAC-His6(phleo) ycgO::Pveg-gerAB(G25A)(spec) yhdG::Phy-gerAA(erm)*	This study	3, S18
BYG1304	*ΔgerA::lox72 ΔgerBB::lox72 ΔgerKB::lox72 ΔyfkT::lox72 ΔyndE::lox72 lacA::Pveg-gerAC-His6(phleo) ycgO::Pveg-gerAB(spec) yhdG::Phy-gerAA(V362L)(erm) yvbJ::Pveg-BFP*	This study	S19
BYG1305	*ΔgerA::lox72 ΔgerBB::lox72 ΔgerKB::lox72 ΔyfkT::lox72 ΔyndE::lox72 lacA::Pveg-gerAC-His6(phleo) ycgO::Pveg-gerAB(G25A)(spec) yhdG::Phy-gerAA(erm) yvbJ::Pveg-BFP*	This study	S20
BYG1306	*ΔgerA::lox72 ΔgerBB::lox72 ΔgerKB::lox72 ΔyfkT::lox72 ΔyndE::lox72 lacA::Pveg-gerAC-His6(phleo) ycgO::Pveg-gerAB(spec) yhdG::Phy-gerAA(erm) yvbJ::Pveg-gfp*	This study	S19, S20
BYG1325	*ΔgerA::lox72 ΔgerBB::lox72 ΔgerKB::lox72 ΔyfkT::lox72 ΔyndE::lox72 lacA::Pveg-gerAC-His6(phleo) ycgO::Pveg-gerAB(spec) yhdG::Phy-gerAA-FLAG(erm)*	This study	S21
BYG1326	*ΔgerA::lox72 ΔgerBB::lox72 ΔgerKB::lox72 ΔyfkT::lox72 ΔyndE::lox72 lacA::Pveg-gerAC-His6(phleo) ycgO::Pveg-gerAB(spec) yhdG::Phy-gerAA(V362A)-FLAG(erm)*	This study	S21
BYG1327	*ΔgerA::lox72 ΔgerBB::lox72 ΔgerKB::lox72 ΔyfkT::lox72 ΔyndE::lox72 yvbJ::Phy-gerAC-His6(cat) ycgO::Phy-gerAB(spec) yhdG::Pxyl-gerAA(V362L)-mYpet(phleo)*	This study	S19
BYG1341	*ΔgerA::lox72 ΔgerBB::lox72 ΔgerKB::lox72 ΔyfkT::lox72 ΔyndE::lox72 yvbJ::Phy-gerAC-His6(cat) ycgO::Phy-gerAB(G25A)(spec) yhdG::Pxyl-gerAA-mYpet(phleo)*	This study	S20
BYG144	*ΔspoVA::tet yhdG::PsspB-spoVA1(Bc) (spec)*	This study	1, S2, S3, S4
BYG147	*ΔspoVA::tet ycgO::PsspB-spoVA2(Bc) (kan)*	This study	1, S2, S3, S4
BYG166	*ΔspoVA::tet yhdG::PsspB-spoVA (spec)*	This study	1, S2, S3, S4
BYG277	*ΔspoVA::tet ycgO::PsspB-spoVA(Cdif) (kan)*	This study	1, S2, S3, S4
BYG383	*ΔgerAB::lox72 ΔgerBB::lox72 ΔgerKB::lox72 ΔyfkT::lox72 ΔyndE::lox72 yhdG::PsspB-gerUA-gerUC-gerUB-gerVB(Bm) (spec)*	This study	1, S3
BYG452	*ΔgerAB::lox72 ΔspoVA::tet*	(*6*)	S4
BYG73	*ΔspoVA::tet*	(*6*)	S4
BYG779	*ΔgerA::lox72 ΔgerBB::lox72 ΔgerKB::lox72 ΔyfkT::lox72 ΔyndE::lox72 lacA::PgerA-gerAC-His6(phleo) ycgO::PgerA-gerAB(spec) yhdG::kan*	This study	2, S13
BYG783	*ΔgerA::cat ΔspoVA::tet ycgO::PsspB-spoVA(C. dif) (kan)*	This study	S4
BYG789	*ΔgerA::cat ΔspoVA::tet yhdG::PsspB-spoVA (spec)*	This study	S4
BYG790	*ΔgerA::cat ΔspoVA::tet yhdG::PsspB-spoVA1(Bc) (spec)*	This study	S4
BYG793	*ΔgerA::cat*	This study	S4
BYG797	*ΔgerA::cat ΔspoVA::tet ycgO::PsspB-spoVA2(Bc) (kan)*	This study	S4
BYG818	*ΔgerA::lox72 ΔgerBB::lox72 ΔgerKB::lox72 ΔyfkT::lox72 ΔyndE::lox72 lacA::PgerA-gerAC-His6(phleo) ycgO::PgerA-gerAB(spec) yhdG::PgerA-gerAA(V362L)(tet)*	This study	2, S13
BYG819	*ΔgerA::lox72 ΔgerBB::lox72 ΔgerKB::lox72 ΔyfkT::lox72 ΔyndE::lox72 lacA::PgerA-gerAC-His6(phleo) ycgO::PgerA-gerAB(spec) yhdG::PgerA-gerAA(Q354L)(tet)*	This study	S13
BYG825	*ΔgerA::lox72 ΔgerBB::lox72 ΔgerKB::lox72 ΔyfkT::lox72 ΔyndE::lox72 lacA::PgerA-gerAC-His6(phleo) ycgO::PgerA-gerAB(spec) yhdG::PgerA-gerAA(Q366L)(tet)*	This study	S13
BYG838	*ΔgerA::lox72 ΔgerBB::lox72 ΔgerKB::lox72 ΔyfkT::lox72 ΔyndE::lox72 lacA::Pveg-gerAC-His6(phleo) ycgO::Pveg-gerAB(spec) yhdG::Pspank-gerAA(erm)*	This study	S15
BYG839	*ΔgerA::lox72 ΔgerBB::lox72 ΔgerKB::lox72 ΔyfkT::lox72 ΔyndE::lox72 lacA::Pveg-gerAC-His6(phleo) ycgO::Pveg-gerAB(spec) yhdG::Pspank-gerAA(V362A)(erm)*	This study	S15

BYG841	*ΔgerA::lox72 ΔgerBB::lox72 ΔgerKB::lox72 ΔyfkT::lox72 ΔyndE::lox72 lacA::Pveg-gerAC-His6(phleo) ycgO::Pveg-gerAB(spec) yhdG::Phy-gerAA(erm)*	This study	3, S16, S17, S18, S21
BYG842	*ΔgerA::lox72 ΔgerBB::lox72 ΔgerKB::lox72 ΔyfkT::lox72 ΔyndE::lox72 lacA::Pveg-gerAC-His6(phleo) ycgO::Pveg-gerAB(spec) yhdG::Phy-gerAA(V362A)(erm)*	This study	3, S16, S17, S21
BYG843	*ΔgerA::lox72 ΔgerBB::lox72 ΔgerKB::lox72 ΔyfkT::lox72 ΔyndE::lox72 lacA::Pveg-gerAC-His6(phleo) ycgO::Pveg-gerAB(spec) yhdG::Phy-gerAA(V362L)(erm)*	This study	3, S18
BYG849	*ΔgerA::lox72 ΔgerBB::lox72 ΔgerKB::lox72 ΔyfkT::lox72 ΔyndE::lox72 yhdG::Phy-gerAA(V362A)(erm)*	This study	3, S17
BYG862	*ΔgerA::lox72 ΔgerBB::lox72 ΔgerKB::lox72 ΔyfkT::lox72 ΔyndE::lox72 ycgO::Pveg-gerAB(spec) yhdG::Phy-gerAA(V362A)(erm)*	This study	3
BYG863	*ΔgerA::lox72 ΔgerBB::lox72 ΔgerKB::lox72 ΔyfkT::lox72 ΔyndE::lox72 lacA::Pveg-gerAC-His6(phleo) yhdG::Phy-gerAA(V362A)(erm)*	This study	3
BYG891	*ΔgerA::lox72 ΔgerBB::lox72 ΔgerKB::lox72 ΔyfkT::lox72 ΔyndE::lox72 lacA::Pveg-gerAC-His6(phleo) ycgO::Pveg-gerAB(spec) yhdG::Phy-gerAA(L358A)(erm)*	This study	S16
BYG893	*ΔgerA::lox72 ΔgerBB::lox72 ΔgerKB::lox72 ΔyfkT::lox72 ΔyndE::lox72 lacA::Pveg-gerAC-His6(phleo) ycgO::Pveg-gerAB(spec) yhdG::Phy-gerAA-ProC(erm)*	This study	S21
BYG894	*ΔgerA::lox72 ΔgerBB::lox72 ΔgerKB::lox72 ΔyfkT::lox72 ΔyndE::lox72 lacA::Pveg-gerAC-His6(phleo) ycgO::Pveg-gerAB(spec) yhdG::Phy-gerAA-gfp(erm)*	This study	S21
BYG900	*ΔgerA::lox72 ΔgerBB::lox72 ΔgerKB::lox72 ΔyfkT::lox72 ΔyndE::lox72 lacA::Pveg-gerAC-His6(phleo) ycgO::Pveg-gerAB(spec) yhdG::Phy-gerAA(V362A)-ProC(erm)*	This study	S21
BYG1466	*ΔgerA::lox72 ΔgerBB::lox72 ΔgerKB::lox72 ΔyfkT::lox72 ΔyndE::lox72 yvbJ::Pxyl-gerAC(cat) ycgO::Pxyl-gerAB(spec) yhdG::Pspank-gerAA-mYpet(erm)*	This study	S23
B. cereus			
569 UM20.1	wild-type 10876 (*trp-1* Str^R)	Anne Moir	2, S14
BDR4445	*gerQΩpFR69-gerQA(I363A)(erm)*	This study	2, S14

Table S1. Strains used in this study.

Table S2.

Plasmid	Genotype	Source
pDR183	*lacA::erm (amp)*	laboratory stock
pDR244	*cre (spec) (amp)*	laboratory stock
pWX318	*mYpet (cat) (amp)*	laboratory stock
pER083	*sacA::Pveg-BFP(phleo) (amp)*	laboratory stock
pER117	*sacA::Pveg-gfp(phleo) (amp)*	laboratory stock
pCB006	*yvbJ::cat (amp)*	laboratory stock
pCB033	*yhdG::spec (amp)*	laboratory stock
pCB057	*yhdG::Pspank (erm) (amp)*	laboratory stock
pCB058	*yhdG::Pspank (spec) (amp)*	laboratory stock
pCB096	*ycgO::Pxyl (spec) (amp)*	laboratory stock
pCB100	*yhdG::Phy (erm) (amp)*	laboratory stock
pCB109	*yhdG::Pxyl (phleo) (amp)*	laboratory stock
pCB124	*yvbJ::Phypespank (hy) (cat) (amp)*	laboratory stock
pCB130	*yvbJ::Pxyl (Cm) (amp)*	laboratory stock
pLA13	*ycgO::PgerA-gerAB(spec) (amp)*	(*10*)
pLA29	*ycgO::PgerA-gerAA (spec) (amp)*	(*10*)
pLA39	*yhdG::PgerA-gerAA(tet) (amp)*	(*10*)
pLA131	*lacA::PgerA-gerAC-his6(phleo) (amp)*	(*10*)
pLA155	*ycgO::Pveg-gerAB(spec)(amp)*	(*10*)
pLA137	*yhdG::PgerA-gerAA(C100S)(tet) (amp)*	(*10*)
pLA178	*yhdG::Phy-gerAA(C100S)(erm) (amp)*	This study
pLA191	*yhdG::PgerA-(RBSgerAB)-gerAA(C100S, V359C, G361C)(tet) (amp)*	This study
pLA201	*yhdG::Phy-gerAA(C100S, V359C, G361C)(erm) (amp)*	This study
pLA202	*yhdG::Phy-gerAA(C100S, V359C)(erm) (amp)*	This study
pLA203	*yhdG::Phy-gerAA(C100S, G361C)(erm) (amp)*	This study
pFR69	*pMiniMAD-Pveg-mCherry–gerQA(I363A)(erm) (amp)*	This study
pJA047	*yhdG::PgerA-gerAA(P326S) (tet)*	This study
pJA060	*yhdG::PgerA (spec)*	This study
pYG63	*yhdG::PsspB-spoVA(spec) (amp)*	This study
pYG53	*yhdG::PsspB-spoVA1(Bc)(spec) (amp)*	This study
pYG56	*ycgO::PsspB-spoVA2(Bc)(kan) (amp)*	This study
pYG95	*ycgO::PsspB-spoVA(Cdif)(kan) (amp)*	This study
pYG129	*yhdG::PsspB-gerUA-gerUC-gerUB-gerVB(spec) (amp)*	This study
pYG275	*yhdG::PgerA-gerAA(V362A)(tet) (amp)*	This study
pYG243	*yhdG::PgerA-gerAA(V362L)(tet) (amp)*	This study
pYG244	*yhdG::PgerA-gerAA(Q366L)(tet) (amp)*	This study
pYG245	*yhdG::PgerA-gerAA(Q354L)(tet) (amp)*	This study
pYG248	*yhdG::PgerA-gerAA(L358A)(tet) (amp)*	This study
pYG262	*yhdG::PgerA-gerAA-gfp(tet) (amp)*	This study
pYG253	*yhdG::PgerA-gerAA(V362L)-gfp(tet) (amp)*	This study
pYG254	*yhdG::PgerA-gerAA(Q366L)-gfp(tet) (amp)*	This study
pYG255	*yhdG::PgerA-gerAA(Q354L)-gfp(tet) (amp)*	This study
pYG263	*yhdG::Pspank-gerAA(erm) (amp)*	This study
pYG264	*yhdG::Pspank-gerAA(V362A)(erm) (amp)*	This study
pYG265	*yhdG::Phy-gerAA(erm) (amp)*	This study
pYG266	*yhdG::Phy-gerAA(V362A)(erm) (amp)*	This study
pYG268	*yhdG::Phy-gerAA(V362L)(erm) (amp)*	This study
pYG304	*ycgO::Phy-gerAB(spec) (amp)*	This study
pYG305	*yvbJ::Phy-gerAC-His6(cat) (amp)*	This study
pYG316	*yhdG::Pxyl-gerAA-proC(phleo) (amp)*	This study
pYG383	*lacA::Pxyl-gerAA-FLAG(erm) (amp)*	This study
pYG372	*yhdG::Pxyl-gerAA(phleo) (amp)*	This study
pYG313	*yhdG::Pxyl-gerAA-gfp(phleo) (amp)*	This study
pYG359	*yhdG::Pxyl-gerAA-mYpet(phleo) (amp)*	This study

pYG344	*yhdG::Phy-gerAA(L348A)(erm) (amp)*	This study
pYG345	*yhdG::Phy-gerAA(T355M)(erm) (amp)*	This study
pYG282	*yhdG::Phy-gerAA(L358A)(erm) (amp)*	This study
pYG365	*ycgO::Pveg-gerAB(G25A)(spec) (amp)*	This study
pYG278	*yhdG::Phy-gerAA-proC(erm) (amp)*	This study
pYG298	*yhdG::Phy-gerAA(V362A)-proC(erm) (amp)*	This study
pYG427	*yhdG::Phy-gerAA-FLAG(erm) (amp)*	This study
pYG428	*yhdG::Phy-gerAA(V362A)-FLAG(erm) (amp)*	This study
pYG276	*yhdG::Phy-gerAA-gfp(erm) (amp)*	This study
pYG366	*yhdG::Phy-gerAA(V362A)-gfp(erm) (amp)*	This study
pYG363	*yvbJ::PgerA-gerAA(V362L)(cat) (amp)*	This study
pYG409	*yhdG::PgerA-(weak RBS)-gerAA(tet) (amp)*	This study
pYG422	*yvbJ::Pveg-BFP(kan) (amp)*	This study
pYG423	*yvbJ::Pveg-gfp(kan) (amp)*	This study
pYG440	*yhdG::Pxyl-gerAA(V362L)-gfp(phleo) (amp)*	This study
pYG441	*yhdG::Pxyl-gerAA(V362L)-mYpet(phleo) (amp)*	This study
pYG442	*ycgO::Phy-gerAB(G25A)(spec) (amp)*	This study
pYG460	*yhdG::Pspank-gerAA-mYpet(erm) (amp)*	This study
pYG469	*ycgO::Pxyl-gerAB(spec) (amp)*	This study
pYG470	*yvbJ::Pxyl-gerAC(cat) (amp)*	This study

Table S2. Plasmids used in this study.

Table S3.

oligos	sequence	use
oCB59	GCGACTAGTaagatggtgatcaatgatggaacaaacgatttatattaaaatgcgc	pYG53
oLA112	ggcGGATCCagccgtcaggcgtattagcc	pYG363
oLA197	aaatacaatgcttGCGgccggacttttaaca	pYG365, pYG442
oLA41	GCCGAATTCgctgttcaaatgatctaatgagctgttc	pYG363
oYG110	ctggcggaagcggaggatccAAGGGAGAAGAGTTGTTTACGGGT	pYG262
oYG117	caagcgGAATTCGACTAGCTTAGCCTAAACGGCTAAG	pYG53, pYG56, pYG63, pYG95
oYG118	ctggACTAGTTTTTTATTTAGTATGGTTGGGTTAACT	pYG53, pYG56, pYG63, pYG95
oYG119	ctggCTCGAGCCTTCCATACACAATATCTACTCTAAGTG	pYG53
oYG120	ctggCTCGAGccctgcttatgtatcttcAACATCATAAC	pYG56
oYG122	cagcgACTAGTacaTAAGGAGGaactactATGACTGTAATTACGAAACTAAAGCAAAC	pYG56
oYG148	gcgACTAGTaagatggtgatcaatgATGGAACGACGAATATTTATCCGGCT	pYG63
oYG149	ctggCTCGAGTTATGAATTGGTAGGCTGCCTTAAG	pYG63
oYG255	cagcgACTAGTacaTAAGGAGGaactactatggataaaaattataaaaaatatgtagacc	pYG95
oYG256	ctggCTCGAGttatggttttgcttttggagtaaatac	pYG95
oYG259	CTCGAGatGCTAGCatGGATCCCCCT	pYG129
oYG260	TGAGGTCACCTCTTATCCACTAGTTTTTTATTTAGTATGGTTGGGTTAACTGGA	pYG129
oYG292	GAATTCGACATCAAGAGCGGGAAGGGAGATTTG	pYG422, pYG423
oYG293	CTCGAGatGCTAGCatGGATCCcagc	pYG422, pYG423
oYG324	ACTAGTGGATAAGAGGTGACCTCAatgccttcgtttttttaaagatcgaaaatc	pYG129
oYG341	GATCCatGCTAGCatCTCGAGgttatcctctctgtttctttctgtttttc	pYG129
oYG352	ggatcctccgcttccgccagagcctccAGTTTCAGTGGAGTCTGTTTTTG	pYG262, pYG359
oYG534	CTACTTATCATCATCATCCTTATAGTCggatcctccgcttccgccagagc	pYG383
oYG569	acgatcggcctcgttgggggcCtagtcatcggacaggctgctg	pYG243, pYG253, pYG268, pYG440, pYG441
oYG570	cagcagcctgtccgatgactaGgcccccaacgaggccgatcgt	pYG243, pYG253, pYG268, pYG440, pYG441
oYG571	tgggggcgtagtcatcggacTggctgctgtagaagcgaatc	pYG244, pYG254
oYG572	gattcgcttctacagcagccAgtccgatgactacgccccca	pYG244, pYG254
oYG573	gactccccaatccgctcggacTgacgatcggcctcgttgg	pYG245, pYG255
oYG574	ccaacgaggccgatcgtcAgtccgagcggattggggagtc	pYG245, pYG255
oYG579	gctcggacagacgatcggcGCcgttgggggcgtagtcatcgga	pYG248, pYG282
oYG580	tccgatgactacgcccccaacgGCgccgatcgtctgtccgagc	pYG248, pYG282
oYG589	GGATCCTTCTGCTCCCTCGCTCAGTAC	pYG262
oYG590	AGCGAGGGAGCAGAAGGATCCTTaggtgctACTAGTAGAACCACCGCCT	pYG262
oYG596	acgatcggcctcgttgggggcGCagtcatcggacaggctgctg	oYG275, pYG264, pYG266, pYG298, pYG366, pYG428

oYG597	cagcagcctgtccgatgactGCgcccccaacgaggccgatcgt	oYG275, pYG264, pYG266, pYG298, pYG366, pYG428
oYG600	GTGAGCGGATAACAATTAAGCTTaaccaaaagaggtgaataatccaatggaac	pYG263, pYG265, pYG276
oYG601	GCTAGCatCTGCAGttACTAGTagccgtcaggcgtattagccttagtg	pYG263, pYG265
oYG614	aGCTAGCatCTGCAGttACTAGTTTaggtgctACTAGTAGAACCACCGCCT	pYG276
oYG617	ATGAGCCGCGGATCTACTTGGTCTTCACTAGTggatcctccgcttccgccagagc	pYG278
oYG618	GCgaGCTAGCatCTGCAGttATCACTTCCCATCAATGAGCCGCGGATCTACTTGGTC	pYG278
oYG619	GtAATTGTGAGCGGATAACAATTAaaccaaaagaggtgaataatccaatggaac	pYG278, pYG427
oYG650	GtAATTGTGAGCGGATAACAATTAaaccaaaagaggtgaataatccaaatgagc	pYG304
oYG651	TGCgaGCTAGCatCTGCAGttAtcattttgttgtaatcctcctcttgagagc	pYG304
oYG652	GtAATTGTGAGCGGATAACAATTAgctctcaagaggaggattacaacaaaatg	pYG305
oYG653	TGCgaGCTAGCatCTGCAGttAtcaatggtgatggtgatggtggctgcctttgtttgc	pYG305
oYG658	cataacctgaagAATTgGATCCatCTTaggtgctACTAGTAGAACCACCGCCT	pYG313
oYG659	gaaataaaatgcatctgtatttgaatgAaaccaaaagaggtgaataatccaatggaac	pYG313, pYG316, pYG372
oYG667	taacctgaagAATTgGATCCatCTCACTTCCCATCAATGAGCCGCGGATCTACTTGGTC	pYG316
oYG684	ctcgagtagtcgacatgaattcatGAGCT	pYG383
oYG685	CatgaattcatgtcgactactcgagCGTGCCATGTCACTATTGCTTCAGA	pYG383
oYG699	tgctaagggaagccggactgcgaGCccccaatccgctcggacaga	pYG344
oYG700	tctgtccgagcggattggggGCtcgcagtccggcttcccttagca	pYG344
oYG701	actccccaatccgctcggacagaTgatcggcctcgttgggggcgt	pYG345
oYG702	acgcccccaacgaggccgatcAtctgtccgagcggattggggagt	pYG345
oYG721	GACTATAAGGATGATGATGATAAGTAGAACGAAATGATACACCAATCAGTGCA	pYG383
oYG737	GGATCcAATTcttcaggttatgaccatctgtgccag	pYG359
oYG738	tctggcggaagcggaggatccTCAAAAGGCGAAGAGCTGTTTACCGGAG	pYG359
oYG739	gtcataacctgaagAATTgGATCCTTACTTGTAAAGTTCATTCATCCCTTCTGT	pYG359
oYG745	taacctgaagAATTgGATCCatCttaagtttcagtggagtctgtttttggct	pYG372
oYG788	ctactaaggttttACTAGTaaccaaaaTaggtgaataatccaatggaaca	pYG409
oYG789	tgttccattggattattcacctAttttggttACTAGTaaaaccttagtag	pYG409
oYG812	TCCCGCTCTTGATGTCGAATTCtCttgaaaacctgcataggagagctatg	pYG422, pYG423
oYG813	tgGGATCCatGCTAGCatCTCGAGGATCCTTAATTCAGTTTGTGACCCAG	pYG422
oYG814	tgGGATCCatGCTAGCatCTCGAGccttatttgtatagttcatccatgcca	pYG423
oYG821	GCgaGCTAGCatCTGCAGttACTACTTATCATCATCATCCTTATAGTCgga	pYG427
oYG832	TGCgaGCTAGCatCTGCAGttATTACTTGTAAAGTTCATTCATCCCTTCTGT	pYG460
oYG868	GTGGAATTGTGAGCGGATAACAATTAaaccaaaagaggtgaataatccaatggaac	pYG460
oYG883	gaaataaaatgcatctgtatttgaatgAgctctcaagaggaggattacaacaaaatg	pYG470
oYG885	gaaataaaatgcatctgtatttgaatgAaaccaaaagaggtgaataatccaaatgagc	pYG469
oYG886	CCATTCGCCAGGGGGATCCatCtcattttgttgtaatcctcctcttgagagc	pYG469
oYG887	CTATTGCCGTATGGGATCCatCCTATTTGTTTGCGCCTTTCGTTCCGAAG	pYG470

oJM28	TTCTGCTCCCTCGCTCAG	*kan/phleo* cassette (isothermal assembly)
oJM29	CAGGGAGCACTGGTCAAC	*kan/phleo* cassette (isothermal assembly)
oLA323	CGATTCTCAACGGCAATTCAGCTGTGTTTATCAACG	pLA137, pLA178
oLA384	TCGGACAGACGATCGGCCTCTGTGGGTGTGTAGTCATCGGACAGGCTGC	pLA191, pLA201
oLA408	GACGATCGGCCTCTGTGGGGGCGTAGTCATC	pLA202
oLA409	CGATCGGCCTCGTTGGGTGTGTAGTCATCGGACAGG	pLA203
oLA412	GACAGAGAGCGTTACATGGAGCTGG	*cotE::phleo* (isothermal assembly)
oLA413	TCCCGGGCATTGACATTTCCG	*cotE::phleo* (isothermal assembly)
oLA414	CTGAGCGAGGGAGCAGAAGCCATTCCGGCATGCCTCCTTGTTC	*cotE::phleo* (isothermal assembly)
oLA415	GTTGACCAGTGCTCCCTGTAAAAAAGGGACTAGGGGAGACAGTACCC	*cotE::phleo* (isothermal assembly)
oLA416	GGCGCATGTTCAATGGTTATAAACGG	*gerE::kan* (isothermal assembly)
oLA417	GGTTTTAACAATCTCGTCTGCTGTTTTGTCG	*gerE::kan* (isothermal assembly)
oLA418	CTGAGCGAGGGAGCAGAATGCAAGTATTGTAACCCTCCTTGCTAAGGTGAG	*gerE::kan* (isothermal assembly)
oLA419	GTTGACCAGTGCTCCCTGTAATCCTTGCCGGTATTCCTTCTTTTGGAAGG	*gerE::kan* (isothermal assembly)
oFR399	cgccaagcttgcatgcctgcaggcctttctttagaaccaaaagaaag	pFR69
oFR400	taccgatgcttgtccaatcacagccaccacctactataccgacagttaa	pFR69
oFR401	actgtcggtatagtaggtggtgctgtgattggacaagcatcggtagaa	pFR69
oFR402	atggacgaattatacaaataagtcccagtgcctcttttataccacg	pFR69
oJA105	ggcgaacagggaaaacgtgccgttctctccgatatttgaagccctgctgatg	pJA047
oJA106	catcagcagggcttcaaatatcggagagaacggcacgttttccctgttcgcc	pJA047
oJA117	aaatctcgctctgatcagac	Sanger sequencing oligo for mutagenized *gerAA*
oJA148	tgcaaatacaatgcttgggg	Sanger sequencing oligo for mutagenized *gerAA*
oJA176	ggactggtttttgctcagac	Amplification of *yhdG::gerAA* locus for Sanger sequencing
oJA177	gtggctgttaatcggcttgg	Amplification of *yhdG::gerAA* locus for Sanger sequencing
oJA178	ACAGGAAAAGATaacctctactaaggttttACTAG	Amplification of *gerAA* using error prone PCR for library creation using pJA060
oJA179	GCGAGGGAGCAGAAGGATCC	Amplification of *gerAA* using error prone PCR for library creation using pJA060

Table S3. Oligonucleotides used in this study.

Data S1.
PDB of AlphaFold2 model of the GerAA/GerAB/GerAC trimer.

Data S2.
PDB of AlphaFold2 model of the GerAA pentamer.

Data S3.
PDB of AlphaFold2 model of the GerAC pentamer.

Data S4.
PDB of AlphaFold2 model of a dimer the GerAA/GerAB/GerAC trimer.

Data S5.
PDB of model of the GerAA/GerAB/GerAC pentamer manually built from the AlphaFold2 model of the dimer of trimers.

References and Notes

1. S. André, T. Vallaeys, S. Planchon, Spore-forming bacteria responsible for food spoilage. *Res. Microbiol.* **168**, 379–387 (2017). doi:10.1016/j.resmic.2016.10.003 Medline

2. M. Mallozzi, V. K. Viswanathan, G. Vedantam, Spore-forming Bacilli and Clostridia in human disease. *Future Microbiol.* **5**, 1109–1123 (2010). doi:10.2217/fmb.10.60 Medline

3. P. Setlow, Spore resistance properties. *Microbiol. Spectr.* **2**, 2.5.11 (2014). doi:10.1128/microbiolspec.TBS-0003-2012 Medline

4. A. Moir, G. Cooper, Spore germination. *Microbiol. Spectr.* **3**, microbiolspec.TBS-0014-2012 (2015). doi:10.1128/microbiolspec.TBS-0014-2012 Medline

5. P. Setlow, S. Wang, Y. Q. Li, Germination of spores of the orders Bacillales and Clostridiales. *Annu. Rev. Microbiol.* **71**, 459–477 (2017). doi:10.1146/annurev-micro-090816-093558 Medline

6. Y. Gao, R. D. C. Barajas-Ornelas, J. D. Amon, F. H. Ramírez-Guadiana, A. Alon, K. P. Brock, D. S. Marks, A. C. Kruse, D. Z. Rudner, The SpoVA membrane complex is required for dipicolinic acid import during sporulation and export during germination. *Genes Dev.* **36**, 634–646 (2022). doi:10.1101/gad.349488.122 Medline

7. V. R. Vepachedu, P. Setlow, Role of SpoVA proteins in release of dipicolinic acid during germination of *Bacillus subtilis* spores triggered by dodecylamine or lysozyme. *J. Bacteriol.* **189**, 1565–1572 (2007). doi:10.1128/JB.01613-06 Medline

8. D. Paredes-Sabja, P. Setlow, M. R. Sarker, Germination of spores of Bacillales and Clostridiales species: Mechanisms and proteins involved. *Trends Microbiol.* **19**, 85–94 (2011). doi:10.1016/j.tim.2010.10.004 Medline

9. J. D. Amon, L. Artzi, D. Z. Rudner, Genetic evidence for signal transduction within the *Bacillus subtilis* GerA Germinant receptor. *J. Bacteriol.* **204**, e0047021 (2022). doi:10.1128/jb.00470-21 Medline

10. L. Artzi, A. Alon, K. P. Brock, A. G. Green, A. Tam, F. H. Ramírez-Guadiana, D. Marks, A. Kruse, D. Z. Rudner, Dormant spores sense amino acids through the B subunits of their germination receptors. *Nat. Commun.* **12**, 6842 (2021). doi:10.1038/s41467-021-27235-2 Medline

11. J. Trowsdale, D. A. Smith, Isolation, characterization, and mapping of *Bacillus subtilis* 168 germination mutants. *J. Bacteriol.* **123**, 83–95 (1975). doi:10.1128/jb.123.1.83-95.1975 Medline

12. M. B. Francis, C. A. Allen, R. Shrestha, J. A. Sorg, Bile acid recognition by the Clostridium difficile germinant receptor, CspC, is important for establishing infection. *PLOS Pathog.* **9**, e1003356 (2013). doi:10.1371/journal.ppat.1003356 Medline

13. G. Christie, C. R. Lowe, Role of chromosomal and plasmid-borne receptor homologues in the response of Bacillus megaterium QM B1551 spores to germinants. *J. Bacteriol.* **189**, 4375–4383 (2007). doi:10.1128/JB.00110-07 Medline

14. Y. Chen, B. Barat, W. K. Ray, R. F. Helm, S. B. Melville, D. L. Popham, Membrane proteomes and ion transporters in Bacillus anthracis and *Bacillus subtilis* dormant and

germinating spores. *J. Bacteriol.* **201**, e0062-18 (2019). doi:10.1128/JB.00662-18 Medline

15. B. M. Swerdlow, B. Setlow, P. Setlow, Levels of H+ and other monovalent cations in dormant and germinating spores of Bacillus megaterium. *J. Bacteriol.* **148**, 20–29 (1981). doi:10.1128/jb.148.1.20-29.1981 Medline

16. R. B. Bass, P. Strop, M. Barclay, D. C. Rees, Crystal structure of *Escherichia coli* MscS, a voltage-modulated and mechanosensitive channel. *Science* **298**, 1582–1587 (2002). doi:10.1126/science.1077945 Medline

17. R. Evans *et al*., Protein complex prediction with AlphaFold-Multimer. *bioRxiv*, 2021.2010.2004.463034 (2022).

18. J. Jumper, R. Evans, A. Pritzel, T. Green, M. Figurnov, O. Ronneberger, K. Tunyasuvunakool, R. Bates, A. Žídek, A. Potapenko, A. Bridgland, C. Meyer, S. A. A. Kohl, A. J. Ballard, A. Cowie, B. Romera-Paredes, S. Nikolov, R. Jain, J. Adler, T. Back, S. Petersen, D. Reiman, E. Clancy, M. Zielinski, M. Steinegger, M. Pacholska, T. Berghammer, S. Bodenstein, D. Silver, O. Vinyals, A. W. Senior, K. Kavukcuoglu, P. Kohli, D. Hassabis, Highly accurate protein structure prediction with AlphaFold. *Nature* **596**, 583–589 (2021). doi:10.1038/s41586-021-03819-2 Medline

19. M. Mirdita, K. Schütze, Y. Moriwaki, L. Heo, S. Ovchinnikov, M. Steinegger, ColabFold: Making protein folding accessible to all. *Nat. Methods* **19**, 679–682 (2022). doi:10.1038/s41592-022-01488-1 Medline

20. T. A. Hopf, A. G. Green, B. Schubert, S. Mersmann, C. P. I. Schärfe, J. B. Ingraham, A. Toth-Petroczy, K. Brock, A. J. Riesselman, P. Palmedo, C. Kang, R. Sheridan, E. J. Draizen, C. Dallago, C. Sander, D. S. Marks, The EVcouplings Python framework for coevolutionary sequence analysis. *Bioinformatics* **35**, 1582–1584 (2019). doi:10.1093/bioinformatics/bty862 Medline

21. Á. Nemecz, M. S. Prevost, A. Menny, P. J. Corringer, Emerging molecular mechanisms of signal transduction in pentameric ligand-gated ion channels. *Neuron* **90**, 452–470 (2016). doi:10.1016/j.neuron.2016.03.032 Medline

22. S. Uysal, V. Vásquez, V. Tereshko, K. Esaki, F. A. Fellouse, S. S. Sidhu, S. Koide, E. Perozo, A. Kossiakoff, Crystal structure of full-length KcsA in its closed conformation. *Proc. Natl. Acad. Sci. U.S.A.* **106**, 6644–6649 (2009). doi:10.1073/pnas.0810663106 Medline

23. N. Unwin, Refined structure of the nicotinic acetylcholine receptor at 4A resolution. *J. Mol. Biol.* **346**, 967–989 (2005). doi:10.1016/j.jmb.2004.12.031 Medline

24. S. Zhu, C. M. Noviello, J. Teng, R. M. Walsh Jr., J. J. Kim, R. E. Hibbs, Structure of a human synaptic $GABA_A$ receptor. *Nature* **559**, 67–72 (2018). doi:10.1038/s41586-018-0255-3 Medline

25. W. Mongkolthanaruk, G. R. Cooper, J. S. Mawer, R. N. Allan, A. Moir, Effect of amino acid substitutions in the GerAA protein on the function of the alanine-responsive germinant receptor of *Bacillus subtilis* spores. *J. Bacteriol.* **193**, 2268–2275 (2011). doi:10.1128/JB.01398-10 Medline

26. K. K. Griffiths, J. Zhang, A. E. Cowan, J. Yu, P. Setlow, Germination proteins in the inner membrane of dormant *Bacillus subtilis* spores colocalize in a discrete cluster. *Mol. Microbiol.* **81**, 1061–1077 (2011). doi:10.1111/j.1365-2958.2011.07753.x Medline

27. P. J. Barlass, C. W. Houston, M. O. Clements, A. Moir, Germination of *Bacillus cereus* spores in response to L-alanine and to inosine: The roles of gerL and gerQ operons. *Microbiology (Reading)* **148**, 2089–2095 (2002). doi:10.1099/00221287-148-7-2089 Medline

28. J. A. Maurer, D. E. Elmore, H. A. Lester, D. A. Dougherty, Comparing and contrasting *Escherichia coli* and Mycobacterium tuberculosis mechanosensitive channels (MscL). New gain of function mutations in the loop region. *J. Biol. Chem.* **275**, 22238–22244 (2000). doi:10.1074/jbc.M003056200 Medline

29. X. Ou, P. Blount, R. J. Hoffman, C. Kung, One face of a transmembrane helix is crucial in mechanosensitive channel gating. *Proc. Natl. Acad. Sci. U.S.A.* **95**, 11471–11475 (1998). doi:10.1073/pnas.95.19.11471 Medline

30. J. D. te Winkel, D. A. Gray, K. H. Seistrup, L. W. Hamoen, H. Strahl, Analysis of antimicrobial-triggered membrane depolarization using voltage sensitive dyes. *Front. Cell Dev. Biol.* **4**, 29 (2016). doi:10.3389/fcell.2016.00029 Medline

31. C. R. Woese, H. J. Morowitz, C. A. Hutchison 3rd, Analysis of action of L-alanine analogues in spore germination. *J. Bacteriol.* **76**, 578–588 (1958). doi:10.1128/jb.76.6.578-588.1958 Medline

32. T. L. Kirley, Inactivation of (Na+,K+)-ATPase by beta-mercaptoethanol. Differential sensitivity to reduction of the three beta subunit disulfide bonds. *J. Biol. Chem.* **265**, 4227–4232 (1990). doi:10.1016/S0021-9258(19)39551-1 Medline

33. P. D. Thackray, J. Behravan, T. W. Southworth, A. Moir, GerN, an antiporter homologue important in germination of Bacillus cereus endospores. *J. Bacteriol.* **183**, 476–482 (2001). doi:10.1128/JB.183.2.476-482.2001 Medline

34. A. Senior, A. Moir, The *Bacillus cereus* GerN and GerT protein homologs have distinct roles in spore germination and outgrowth, respectively. *J. Bacteriol.* **190**, 6148–6152 (2008). doi:10.1128/JB.00789-08 Medline

35. K. Kikuchi, L. Galera-Laporta, C. Weatherwax, J. Y. Lam, E. C. Moon, E. A. Theodorakis, J. Garcia-Ojalvo, G. M. Süel, Electrochemical potential enables dormant spores to integrate environmental signals. *Science* **378**, 43–49 (2022). doi:10.1126/science.abl7484 Medline

36. S. Wang, J. R. Faeder, P. Setlow, Y. Q. Li, Memory of germinant stimuli in bacterial spores. *mBio* **6**, e01859–e15 (2015). doi:10.1128/mBio.01859-15 Medline

37. P. Zhang, J. Liang, X. Yi, P. Setlow, Y. Q. Li, Monitoring of commitment, blocking, and continuation of nutrient germination of individual *Bacillus subtilis* spores. *J. Bacteriol.* **196**, 2443–2454 (2014). doi:10.1128/JB.01687-14 Medline

38. M. J. Wilson, P. E. Carlson, B. K. Janes, P. C. Hanna, Membrane topology of the Bacillus anthracis GerH germinant receptor proteins. *J. Bacteriol.* **194**, 1369–1377 (2012). doi:10.1128/JB.06538-11 Medline

39. D. R. Zeigler, Z. Prágai, S. Rodriguez, B. Chevreux, A. Muffler, T. Albert, R. Bai, M. Wyss, J. B. Perkins, The origins of 168, W23, and other *Bacillus subtilis* legacy strains. *J. Bacteriol.* **190**, 6983–6995 (2008). doi:10.1128/JB.00722-08 Medline

40. P. Schaeffer, J. Millet, J. P. Aubert, Catabolic repression of bacterial sporulation. *Proc. Natl. Acad. Sci. U.S.A.* **54**, 704–711 (1965). doi:10.1073/pnas.54.3.704 Medline

41. B. M. Koo, G. Kritikos, J. D. Farelli, H. Todor, K. Tong, H. Kimsey, I. Wapinski, M. Galardini, A. Cabal, J. M. Peters, A.-B. Hachmann, D. Z. Rudner, K. N. Allen, A. Typas, C. A. Gross, Construction and analysis of two genome-scale deletion libraries for *Bacillus subtilis*. *Cell Syst.* **4**, 291–305.e7 (2017). doi:10.1016/j.cels.2016.12.013 Medline

42. A. J. Meeske, L.-T. Sham, H. Kimsey, B.-M. Koo, C. A. Gross, T. G. Bernhardt, D. Z. Rudner, MurJ and a novel lipid II flippase are required for cell wall biogenesis in *Bacillus subtilis*. *Proc. Natl. Acad. Sci. U.S.A.* **112**, 6437–6442 (2015). doi:10.1073/pnas.1504967112 Medline

43. L. Pravda, D. Sehnal, D. Toušek, V. Navrátilová, V. Bazgier, K. Berka, R. Svobodová Vareková, J. Koča, M. Otyepka, MOLEonline: A web-based tool for analyzing channels, tunnels and pores (2018 update). *Nucleic Acids Res.* **46** (W1), W368–W373 (2018). doi:10.1093/nar/gky309 Medline

44. T. A. Hopf, L. J. Colwell, R. Sheridan, B. Rost, C. Sander, D. S. Marks, Three-dimensional structures of membrane proteins from genomic sequencing. *Cell* **149**, 1607–1621 (2012). doi:10.1016/j.cell.2012.04.012 Medline

45. D. S. Marks, L. J. Colwell, R. Sheridan, T. A. Hopf, A. Pagnani, R. Zecchina, C. Sander, Protein 3D structure computed from evolutionary sequence variation. *PLOS ONE* **6**, e28766 (2011). doi:10.1371/journal.pone.0028766 Medline

46. L. S. Johnson, S. R. Eddy, E. Portugaly, Hidden Markov model speed heuristic and iterative HMM search procedure. *BMC Bioinformatics* **11**, 431 (2010). doi:10.1186/1471-2105-11-431 Medline

47. A. Ducret, E. M. Quardokus, Y. V. Brun, MicrobeJ, a tool for high throughput bacterial cell detection and quantitative analysis. *Nat. Microbiol.* **1**, 16077 (2016). doi:10.1038/nmicrobiol.2016.77 Medline

48. A. Ramirez-Peralta, P. Zhang, Y. Q. Li, P. Setlow, Effects of sporulation conditions on the germination and germination protein levels of *Bacillus subtilis* spores. *Appl. Environ. Microbiol.* **78**, 2689–2697 (2012). doi:10.1128/AEM.07908-11 Medline

49. K. A. Stewart, X. Yi, S. Ghosh, P. Setlow, Germination protein levels and rates of germination of spores of *Bacillus subtilis* with overexpressed or deleted genes encoding germination proteins. *J. Bacteriol.* **194**, 3156–3164 (2012). doi:10.1128/JB.00405-12 Medline

50. V. R. Vepachedu, P. Setlow, Localization of SpoVAD to the inner membrane of spores of *Bacillus subtilis*. *J. Bacteriol.* **187**, 5677–5682 (2005). doi:10.1128/JB.187.16.5677-5682.2005 Medline

51. D. Z. Rudner, R. Losick, A sporulation membrane protein tethers the pro-sigmaK processing enzyme to its inhibitor and dictates its subcellular localization. *Genes Dev.* **16**, 1007–1018 (2002). doi:10.1101/gad.977702 Medline

52. M. Fujita, Temporal and selective association of multiple sigma factors with RNA polymerase during sporulation in *Bacillus subtilis*. *Genes Cells* **5**, 79–88 (2000). doi:10.1046/j.1365-2443.2000.00307.x Medline

53. X. Wang, O. W. Tang, E. P. Riley, D. Z. Rudner, The SMC condensin complex is required for origin segregation in *Bacillus subtilis*. *Curr. Biol.* **24**, 287–292 (2014). doi:10.1016/j.cub.2013.11.050 Medline

54. H. Szurmant, T. Fukushima, J. A. Hoch, The essential YycFG two-component system of *Bacillus subtilis*. *Methods Enzymol.* **422**, 396–417 (2007). doi:10.1016/S0076-6879(06)22020-2 Medline

55. C. B. Bernhards, D. L. Popham, Role of YpeB in cortex hydrolysis during germination of Bacillus anthracis spores. *J. Bacteriol.* **196**, 3399–3409 (2014). doi:10.1128/JB.01899-14 Medline

56. P. A. Levin, I. G. Kurtser, A. D. Grossman, Identification and characterization of a negative regulator of FtsZ ring formation in *Bacillus subtilis*. *Proc. Natl. Acad. Sci. U.S.A.* **96**, 9642–9647 (1999). doi:10.1073/pnas.96.17.9642 Medline

57. S. Ghosh, B. Setlow, P. G. Wahome, A. E. Cowan, M. Plomp, A. J. Malkin, P. Setlow, Characterization of spores of *Bacillus subtilis* that lack most coat layers. *J. Bacteriol.* **190**, 6741–6748 (2008). doi:10.1128/JB.00896-08 Medline

58. F. H. Ramírez-Guadiana, A. J. Meeske, X. Wang, C. D. A. Rodrigues, D. Z. Rudner, The *Bacillus subtilis* germinant receptor GerA triggers premature germination in response to morphological defects during sporulation. *Mol. Microbiol.* **105**, 689–704 (2017). doi:10.1111/mmi.13728 Medline

59. Y. Li, P. Catta, K.-A. V. Stewart, M. Dufner, P. Setlow, B. Hao, Structure-based functional studies of the effects of amino acid substitutions in GerBC, the C subunit of the *Bacillus subtilis* GerB spore germinant receptor. *J. Bacteriol.* **193**, 4143–4152 (2011). doi:10.1128/JB.05247-11 Medline

60. Y. Li, K. Jin, A. Perez-Valdespino, K. Federkiewicz, A. Davis, M. W. Maciejewski, P. Setlow, B. Hao, Structural and functional analyses of the N-terminal domain of the A subunit of a *Bacillus megaterium* spore germinant receptor. *Proc. Natl. Acad. Sci. U.S.A.* **116**, 11470–11479 (2019). doi:10.1073/pnas.1903675116 Medline

61. A. Gharpure, J. Teng, Y. Zhuang, C. M. Noviello, R. M. Walsh Jr., R. Cabuco, R. J. Howard, N. T. Zaveri, E. Lindahl, R. E. Hibbs, Agonist selectivity and ion permeation in the α3β4 ganglionic nicotinic receptor. *Neuron* **104**, 501–511.e6 (2019). doi:10.1016/j.neuron.2019.07.030 Medline

62. P. Nicolas, U. Mäder, E. Dervyn, T. Rochat, A. Leduc, N. Pigeonneau, E. Bidnenko, E. Marchadier, M. Hoebeke, S. Aymerich, D. Becher, P. Bisicchia, E. Botella, O. Delumeau, G. Doherty, E. L. Denham, M. J. Fogg, V. Fromion, A. Goelzer, A. Hansen, E. Härtig, C. R. Harwood, G. Homuth, H. Jarmer, M. Jules, E. Klipp, L. Le Chat, F. Lecointe, P. Lewis, W. Liebermeister, A. March, R. A. T. Mars, P. Nannapaneni, D.

Noone, S. Pohl, B. Rinn, F. Rügheimer, P. K. Sappa, F. Samson, M. Schaffer, B. Schwikowski, L. Steil, J. Stülke, T. Wiegert, K. M. Devine, A. J. Wilkinson, J. M. van Dijl, M. Hecker, U. Völker, P. Bessières, P. Noirot, Condition-dependent transcriptome reveals high-level regulatory architecture in *Bacillus subtilis*. *Science* **335**, 1103–1106 (2012). doi:10.1126/science.1206848 Medline

63. L. Zheng, W. Abhyankar, N. Ouwerling, H. L. Dekker, H. van Veen, N. N. van der Wel, W. Roseboom, L. J. de Koning, S. Brul, C. G. de Koster, *Bacillus subtilis* spore inner membrane proteome. *J. Proteome Res.* **15**, 585–594 (2016). doi:10.1021/acs.jproteome.5b00976 Medline